Design, Development and Evaluation of Nanoformulation for Brain Targeting and Bioavailability enhancement of anti-viral drug

A Thesis submitted to Gujarat Technological University

for the Award of

Doctor of Philosophy

in

Pharmacy

by

Ms. Shweta H. Gupta

[Enrollment No. : 119997290052]

under supervision of

Dr. Rajesh K.S.

GUJARAT TECHNOLOGICAL UNIVERSITY

AHMEDABAD

June - 2017

DECLARATION

I declare that the thesis entitled "**Design, Development and Evaluation of Nanoformulation for Brain Targeting and Bioavailability enhancement of anti-viral drug"** submitted by me for the degree of Doctor of Philosophy is the record of research work carried out by me during the period from July 2011 to July 2016 under the supervision of Dr. Rajesh K.S. and Dr. Abdelwahab Omri and this has not formed the basis for the award of any degree, diploma, associateship, fellowship, titles in this or any other University or other institution of higher learning.

I further declare that the material obtained from other sources has been duly acknowledged in the thesis. I shall be solely responsible for any plagiarism or other irregularities, if noticed in the thesis.

Signature of the Research Scholar: …….…… Date: ….……

Name of Research Scholar: Ms. Shweta H. Gupta

Place : Vadodara, Gujarat, India.

CERTIFICATE

I certify that the work incorporated in the thesis "**Design, Development and Evaluation of Nanoformulation for Brain Targeting and Bioavailability enhancement of anti-viral drug"** submitted by Ms. Shweta Gupta was carried out by the candidate under my supervision/guidance. To the best of my knowledge: (i) the candidate has not submitted the same research work to any other institution for any degree/diploma, Associateship, Fellowship or other similar titles (ii) the thesis submitted is a record of original research work done by the Research Scholar during the period of study under my supervision, and (iii) the thesis represents independent research work on the part of the Research Scholar.

Signature of Supervisor: …… Date: ……

Name of Supervisor: …….

Place: ……..……

Originality Report Certificate

It is certified that PhD Thesis titled "**Design, Development and Evaluation of Nanoformulation for Brain Targeting and Bioavailability enhancement of anti-viral drug"** by **Ms. Shweta Gupta** has been examined by us. We undertake the following:

a. Thesis has significant new work / knowledge as compared already published or are under consideration to be published elsewhere. No sentence, equation, diagram, table, paragraph or section has been copied verbatim from previous work unless it is placed under quotation marks and duly referenced.

b. The work presented is original and own work of the author (i.e. there is no plagiarism). No ideas, processes, results or words of others have been presented as Author own work.

c. There is no fabrication of data or results which have been compiled / analysed.

d. There is no falsification by manipulating research materials, equipment or processes, or changing or omitting data or results such that the research is not accurately represented in the research record.

e. The thesis has been checked using "**turnitin**" (copy of originality report attached) and found within limits as per GTU Plagiarism Policy and instructions issued from time to time (i.e. permitted similarity index <=25%).

Signature of the Research Scholar : …… Date: ….……

Name of Research Scholar: …….

Place : ……..……

Signature of Supervisor: …… Date: ……

Name of Supervisor: ……..……

Place: ……

Thesis-sg

ORIGINALITY REPORT

%9	%8	%7	%7
SIMILARITY INDEX	INTERNET SOURCES	PUBLICATIONS	STUDENT PAPERS

PRIMARY SOURCES

1	www.ncbi.nlm.nih.gov Internet Source	%2
2	Submitted to Institute of Technology, Nirma University Student Paper	%2
3	Submitted to The Hong Kong Polytechnic University Student Paper	%1
4	Advances in Delivery Science and Technology, 2015. Publication	%1
5	www.gmpua.com Internet Source	%1
6	Wong, H.L.. "Nanotechnology applications for improved delivery of antiretroviral drugs to the brain", Advanced Drug Delivery Reviews, 20100318 Publication	%1
7	gnu.inflibnet.ac.in Internet Source	%1

Internet Source

%1

EXCLUDE QUOTES	ON	EXCLUDE MATCHES	< 1%
EXCLUDE BIBLIOGRAPHY	ON		

PhD THESIS Non-Exclusive License to

GUJARAT TECHNOLOGICAL UNIVERSITY

In consideration of being a PhD Research Scholar at GTU and in the interests of the facilitation of research at GTU and elsewhere, I, Shweta H. Gupta (Enrollment No. : 119997290052) hereby grant a non-exclusive, royalty free and perpetual license to GTU on the following terms:

a) GTU is permitted to archive, reproduce and distribute my thesis, in whole or in part, and/or my abstract, in whole or in part (referred to collectively as the "Work") anywhere in the world, for non-commercial purposes, in all forms of media;

b) GTU is permitted to authorize, sub-lease, sub-contract or procure any of the acts mentioned in paragraph (a);

c) GTU is authorized to submit the Work at any National / International Library, under the authority of their "Thesis Non-Exclusive License";

d) The Universal Copyright Notice (©) shall appear on all copies made under the authority of this license;

e) I undertake to submit my thesis, through my University, to any Library and Archives. Any abstract submitted with the thesis will be considered to form part of the thesis.

f) I represent that my thesis is my original work, does not infringe any rights of others, including privacy rights, and that I have the right to make the grant conferred by this non-exclusive license.

g) If third party copyrighted material was included in my thesis for which, under the terms of the Copyright Act, written permission from the copyright owners is required, I have obtained such permission from the copyright owners to do the acts mentioned in paragraph (a) above for the full term of copyright protection.

h) I retain copyright ownership and moral rights in my thesis, and may deal with the copyright in my thesis, in any way consistent with rights granted by me to my University in this non-exclusive license.

i) I further promise to inform any person to whom I may hereafter assign or license my copyright in my thesis of the rights granted by me to my University in this non exclusive

license.

j) I am aware of and agree to accept the conditions and regulations of PhD including all policy matters related to authorship and plagiarism.

Signature of the Research Scholar:……..……

Name of Research Scholar:……

Date:…… Place: ……

Signature of Supervisor:……

Name of Supervisor:……..

Date:…….. Place:

Seal:

Thesis Approval Form

The viva-voce of the PhD Thesis submitted by Ms. Shweta H. Gupta (Enrollment No. 119997290052) entitled "**Design, Development and Evaluation of Nanoformulation for Brain Targeting and Bioavailability enhancement of anti-viral drug"** was conducted on …….....…… (day and date) at Gujarat Technological University.

(Please tick any one of the following option)

☐ The performance of the candidate was satisfactory. We recommend that he/she be awarded the PhD degree.

☐ Any further modifications in research work recommended by the panel after 3 months from the date of first viva-voce upon request of the Supervisor or request of Independent Research Scholar after which viva-voce can be re-conducted by the same panel again.

(briefly specify the modifications suggested by the panel)

☐ The performance of the candidate was unsatisfactory. We recommend that he/she should not be awarded the PhD degree.

(The panel must give justifications for rejecting the research work)

---------- ----------

Name and Signature of Supervisor with Seal 1) (External Examiner 1) Name and Signature

---------- ----------

2) (External Examiner 2) Name and Signature 3) (External Examiner 3) Name and Signature

ABSTRACT

HIV infections causing AIDS is one of the most life-threatening infections and is the sixth leading cause of death. The non-nucleoside reverse transcriptase inhibitors, used for the treatment of HIV infections are reported to have low bioavailability pertaining to high first pass metabolism, high protein binding and enzymatic metabolism. They also show low permeability across blood brain barrier. The central nervous system is reported to be the most important HIV reservoir site. In the present study, solid lipid nanoparticles of efavirenz were prepared with the objective to provide increased permeability and protection to drug by biocompatible lipidic content and nano-scale size, and thus to develop formulation having potential for enhanced bioavailability and brain targeting. Solid lipid nanoparticles (SLN) were prepared by high pressure homogenization technique using a systematic approach of design of experiments and evaluated for particle size, polydispersity index (PDI), zeta potential and entrapment efficiency. Particles of average size 108.5 nm having PDI of 0.172 with 64.9% entrapment efficiency were produced. Zeta potential was found to be -21.2 mV and the formulation was found stable. Transmission electron microscopic evaluation and the histopathological studies respectively indicated spherical shape and non-irritant nature of the formulated solid lipid nanoparticles. The optimized SLN were incorporated in thermo-sensitive *in-situ* gelling system. The efavirenz SLN based gel was evaluated for various parameters like gelation temperature, pH, viscosity, transmittance, mucoadhesive strength, spreadability, *in-vitro* and *ex-vivo* release studies. The release of drug was found to best fit in the Zero order release kinetics ($R^2 = 0.9873$), indicating concentration independent diffusion controlled release. The *in-vivo* pharmacokinetic studies revealed increased concentration of the drug in brain, when administered through intranasal route indicating its potential for an attempt towards complete eradication of HIV and cure of HIV-infected patients.

Keywords: Efavirenz (EFV), SLN, High pressure homogenization, DoE, *In-situ* gel, Nose-to-brain, Brain targeting

ACKNOWLEDGEMENT

Thank you, God, for little things that often come our way-
the things we take for granted and don't mention when we pray,

Thank You, God for the "miracles", we are much too blind to see,
A hand reached out to help us, in the time of sudden need.

Thank u God for fulfilling my needs in a very special way!!!

I offer flowers of gratitude to the almighty God for the benediction and grace & for being the source of strength throughout my life.

Every achievement is a result of committed activities that too when headed & guided by worthy and knowledgeable persons. Clear paths or hazy roads I always remember the supports I got from the people whose names I feel privileged to mention here. It is with a sense of pride and pleasure that, I humbly look back to acknowledge, those who have been a source of encouragement in my entire endeavour.

At the outset I feel that I may not have reached this stage without the blessings, love & care of my well wishers, loving parents, beloved bhaiya, supportive husband and in-laws, didi-jiju & my other relatives. I also acknowledge Gujarat Technological University for giving me the opportunity to proceed with the research work and do the PhD.

With a deep sense of respect and gratitude, I would like to express my sincere thanks to my esteemed guide, ***Dr. Rajesh K.S.****, Principal & Professor in Pharmaceutics, ISF college of Pharmacy, Moga, Punjab for giving me the opportunity to work in the field of nanotechnology. Without his perpetual encouragement, constructive guidance, advice and support throughout my journey of the doctoral research, I would never have succeeded in accomplishing the work.*

My sincere gratitude to my co-guide, ***Dr. Abdel Omri****, Professor, Laurentia University, Canada for showing his willingness to act as my international co-guide and providing his valuable insights, prompt, timely and helpful guidance throughout as well as for the unmatched support rendered at the time of publication of the articles too.*

With great reverence, I take this opportunity to express my debt of gratitude to the DPC (Doctoral Progress committee) members, ***Dr. A.N. Misra,*** *Professor, Faculty of Pharmacy, M.S. University of Baroda and* ***Dr. N.P. Chotai,*** *Professor, A.R. College of Pharmacy, Vallabh Vidyanagar for their critical review, guidance and support for the work.*

*I wish to express my heartiest thanks to **Dr. Devanshu Patel** and other members of the Managing trustee of Parul University, **Dr. Abhay Dharamsi**, Dean and Principal, Faculty of Pharmacy, **Dr. Sulekha Bhadra**, Head of the Pharmaceutics Dept, **Dr. Lalit Lata Jha**, **Mr. Javid Mansuri**, **Mrs. Archana Navale**, **Mr. Anand Pithadia**, **Mr. Ashish Patel, Mr. Akhil Nagar, Dr. Gajanan Shinde, Mr. Surjya Narayan Mandal, Dr. Falguni Tandel, Ms. Monica, Ms. Rashmita** and all others at Parul University for providing me the infrastructural and other direct or indirect support for the successful completion of research work. It would be remiss on my part if I don't acknowledge the help and support of all my friends and colleagues for their wonderful company, unending inspirations, motivations, constant encouragement, technical assistance throughout the research work.*

I am also thankful to SICART (Sophisticated Instrumentation Centre for Applied Research and Testing) , Insta Analytical Labs and Chandrakant's histopathological laboratory for providing me the technical and infrastructural support for carrying out the TEM analysis, HPLC method development & validation and histopathological studies respectively.

*I am immensely thankful to **M/s Sun Pharma Ltd.,** Sikkim, India for providing the gift sample of drug, Paradise Healthcare, Vadodara for providing the internal standard, Sigma Aldrich for the excipients and PASM hospital for providing the plasma samples required for the study.*

*I would like to bid special thanks appreciation to Mr. Shobharam Jamre, Librarian, Mr. Primesh Patel, Stores in-charge, **Vasavabhai,** Ms. Priyanka Patel, Mrs. Anandiben, Mr. Praveenbhai, Simon kaka, **Govindbhai** and to all office and laboratory staff of the Faculty of Pharmacy, Parul University for their kind co-operation and assistance during the journey to this stage.*

I would also like to put in record my thanks to Honorable Vice Chancellor Prof. (Dr.) Navin Sheth), Ex-Vice-Chancellor Dr. Akshai Aggarwal, I/C Registrar, Mr. J.C.Lilani, Research Coordinator, Ms. Mona Chaurasiya, Mr. Dhaval Gohil and other Staff Members of Ph.D section for their co-operative assistance and support.

.

I express my sincere thanks and apology to all those who have contributed to the success of this work & helped me in whatsoever manner during this work & whose name I might have missed inadvertently or those who are like countless stars in numerous galaxies.

Thanks to one & all…

Date : …. June, 2017

Place : Baroda

Shweta Gupta

Dedicated to my Beloved Family Members & The Supreme God…

Table of Contents

List of Abbreviation

Abbreviations	Full form
ABC	ATP-binding cassette
AIDS	Acquired Immuno-deficiency Syndrome
AMT	Adsorptive-mediated transcytosis
ANOVA	Analysis of Variance
ARR	Amount remaining to release
BBB	Blood Brain Barrier
BCRP	Breast Cancer Resistance Protein
BCS	Biopharmaceutical Classification System
BCSFB	Brain Cerebro-Spinal Fluid Barrier
CCD	Charge coupled device
CD4	Cluster of differentiation 4
CDC	Centre for Disease Control and Prevention
CFR	Code of Federal Regulations
CNS	Central Nervous System
CP	Cetyl Palmitate
CPCSEA	Committee for the Purpose of Control and Supervision of Experiments on Animals
CQA	Critical Quality Attributes
CSF	Cerebro-Spinal Fluid
Da	Dalton
DLS	Dynamic light scattering
DNA	Deoxyribonucleic acid
DoE	Design of Experiment
Ds	Double-stranded
EFV	Efavirenz
FDA	Food and Drug Administration

FT-IR	Fourier Transform Infrared
GDS	Glyceryl distearate
GIT	Gastro- Intestinal Tract
GMS	Glycerymonostearate
GPS	Glyceryl palmitostearate
GRAS	Generally Regarded As Safe
GRAS	Generally regarded as safe
GTP	Glyceryl tripalmitate (Tripalmitin)
HAART	High Activity Antiretroviral Therapy
HAD	HIV Associated Dementia
HED	Human equivalent dose
HIV	Human Immuno-deficiency Virus
HIVE	HIV Encephalitis
HPH	High pressure homogenization
HPLC	High Performance Liquid Chromatography
IAEC	Institutional Animal Ethics Committee
ICH	International Council for Harmonisation
IUPAC	International Union of Pure and Applied Chemistry
IV	Intra-venous
LOD	Limit of Detection
LOQ	Limit of Quantification
MDR	Mild Neurocognitive Disorder
MRP	Multidrug Resistance-associated Proteins (MRP)
NMT	Not more than
NNRTI	Non-nucleoside reverse transcriptase inhibitor
PAA	Polyacrylic Acid
PASM	Parul Arogya Seva Mandal
PBS	Phosphate-buffered Saline
PDI	Poly dispersity index

PDS	Plain drug suspension
PEO	Poly (ethylene oxide)
p-gp	p-glycoprotein
PPO	Poly (propylene oxide)
PS	Particle size
QTPP	Quality Target Product Profile
RH	Relative humidity
RMT	Receptor - mediated transcytosis
RNA	Ribonucleic Acid
RPM	Rotations per minute
RSD	Relative standard deviation
RT	Room Temperature
SD	Standard deviation
SLN	Solid Lipid Nanoparticles
Ss	Single –stranded
TDF	Tenofovir disoproxil fumarate
TEM	Transmission electron microscopy
UV	Ultra-violet

List of Symbols

Symbol	Meaning
μg	Microgram
gm	Gram
mg	Milligram
Ng	Nanogram
Cm	Centimeter
Nm	Nanometer
F	Mucoadhesive force (dynes / cm^2)
λ_{max}	Maximum wavelength
G	acceleration due to gravity (cm/s^2)
°C	Degree Celcius
^0F	Degree Fahrenheit
K	Kelvin
mV	Millivolts
R	Linear correlation coefficient
T	Time
%	Percent
Q	Amount of drug released
K_0	Zero order release constant
K_1	First order release constant
K_h	Higuchi square root of time release constant
$Q\infty$	Total drug released after infinite time
Λ	Diffusion exponents that characterizes the mechanism of drug release
Pka	Degree of ionization
Psi	Pounds per square inch

List of Figures

List of Tables

List of Appendices

CHAPTER 1
Introduction

Poorly soluble drugs are highly prevalent in the pharmaceutical field leading to low bioavailability. In drug discovery, the number of drug candidates having low solubility has increased, and 70% of new drug candidates have shown poor aqueous solubility in recent years [1]. These drugs pose a major challenge to the formulation scientists in order to increase the bioavailability and develop a targeted drug delivery system [2]. Drug delivery to brain is even more challenging due to the presence of blood brain barrier (BBB) and brain cerebrospinal fluid barrier (BCSFB) [3, 4].

Viral infections are extremely widespread and are of various types like common cold, influenza, rabies, measles, chickenpox, small pox, herpes, AIDS, mumps, measles, rubella, viral hepatitis, viral meningitis, viral pneumonia, etc [5,6]. The most life - threatening infection is of HIV causing AIDS. According to the World Health Organization, approximately 35 million people worldwide are living with HIV/ AIDS including 3.2 million children of less than 15 years age and an estimated 2.1 million individuals worldwide are newly infected with HIV every year [7]. AIDS is the sixth leading cause of death among people aged 25 - 44 in the United States [8].

1.1 Definition of the problem

From the literature review on the subject related to HIV/AIDS and their available therapies, the challenges associated with the current therapies were identified, and from the review emerged the research problem to be addressed.

Current therapies for HIV infections with antiretroviral drugs is effective in reducing plasma viral levels, but are ineffective in eradicating the virus from other sites like CNS due to their

inability to reach and accumulate in these cellular and anatomical reservoirs where virus potentially harbours. The CNS is the most important HIV reservoir site [9]. Due to the restricted entry of anti-HIV drugs, the brain is thought to form a viral sanctuary site. This not only results in virological resistance, but also is often associated with the development of complications such as progressive deterioration in mental function, symptoms of motor abnormalities, mild neurocognitive disorder (MDR), HIV associated dementia (HAD), HIV encephalitis (HIVE) and even death in many cases [4, 9, 10].

Efavirenz (EFV) is a non-nucleoside reverse transcriptase inhibitor (NNRTI) of choice and is recommended as a first line antiretroviral drug used in the high activity antiretroviral therapy (HAART) for the infections of human immunodeficiency virus [11]. Efavirenz is a highly lipophilic drug of BCS (Biopharmaceutical Classification System) class II having water solubility of 9.2 µg/ml (pH 8.7) at 25°C and 4.6 as the log P value [12]. Because of low water solubility of the drug, extensive first pass metabolism, metabolism by enzymes, high protein binding, efflux mechanisms, low bioavailability (40-45%) of the drug has been reported [13-17].

1.2 Aim of the research work

The aim of the present investigations were to design and develop nanoparticles of anti-viral drug, efavirenz to deliver it to the brain in order to increase their bioavailability at the reservoir site of HIV, perform the evaluation studies and compare the formulation with the existing one.

1.3 Objectives and scope of work

The overall objectives of the research are summarized as:

- To select the right material, process and optimization design for preparation of solid lipid nanoparticles.
- To provide lipid protection to the drug.

- To avoid extensive first pass metabolism of the drug.
- To select proper route of administration.
- To target the drug to the brain.
- To estimate the drug concentration in brain and plasma post-administration of formulation and comparison with existing formulation.

Scope of the research work:

By developing the effective delivery system for the existing drug which can effectively diffuse in cellular and tissue compartments where the virus harbors (reservoir site of HIV) is a potential way in an attempt for completely cure the HIV-infected patients. After clinical trials and fulfillment of other regulatory requirements, the developed formulation may prove to be a boon to the society at large for the complete treatment of the highly-dreaded disease of AIDS.

1.4 Rationale of the research work

1.4.1 Selection of anti-viral drug

1.4.1.1. Challenges associated with the anti-viral drugs including efavirenz:

- **Low Oral Bioavailability**

The anti-viral drugs including efavirenz are reported to have low oral bioavailability because of the following mentioned reasons [9, 18-20].

- Extensive first pass metabolism
- Low solubility
- High protein binding
- Powerful metabolizing enzymes
- Low permeability across the blood-brain-barrier
- Drug efflux due to multidrug resistant efflux proteins (MRP) such as p-glycoprotein (p-gp) [21].

- **Variable bioavailability**

The bioavailability is often reported to be variable (60–90%) depending on their site of absorption [9, 20].

- **Long-term Drug Therapy**

The therapy requires a long time of at least 5 years to eliminate the latent viral reservoir completely [9].

- **Resistance due to genetic mutations**

The therapy should remain uninterrupted to prevent the development of resistance where compliance issues become problematic many a times [9, 22, 23].

1.4.2 The need for the present investigation:

The insufficient delivery of anti-viral agents to the CNS leads to low and sustained viral replication within the CNS even during prolonged therapy which hinders the complete cure of the infection leading to therapeutic failure of antiretroviral drug therapy [9, 10].

.

Thus, developing drugs or the effective drug delivery systems for the existing drugs that can effectively diffuse in various cellular and tissue compartments where the virus harbors and reach to CNS is a potential way to completely cure the HIV-infected patients. Therefore, developing novel approaches that are targeted at enhancing the brain delivery of anti-viral drugs are required.

1.4.3 Selection of Nano-formulation

Novel developments emerging in the field of polymer science, lipid formulations and nanotechnology provide an option by which the obstacles of limited brain entry can be surmounted [24]. Examples of drug delivery systems having potential for targeting the brain include nano-formulations such as nanoparticles, polymeric micelles, liposomes, dendrimers, etc [9, 24-26].

1.4.3.1 Solid Lipid Nanoparticles

Solid lipid nanoparticles (SLN) are colloidal dispersions or particulates in the size range of 100–500 nm composed of biocompatible lipid matrix that are physiologically well tolerated when administered *in-vivo* [27]. The lipidic nanoparticles are promising nano-formulations owing to their prevalence over other formulations in terms of toxicity, production feasibility and scalability which are widely documented in the literature [24, 28, 29, 30]. SLN are gaining increased attention during recent years because of various advantages over other colloidal drug delivery systems.

❖ **Potential Advantages of SLN**

Various potential advantages of solid lipid nanoparticles may be summarized as [24, 28, 31]

- Biocompatibility of physiological lipids
- Potential for increased permeability due to small size as well as lipid and surfactant contents and hence, enhanced bioavailability
- Increased protection and stability to the encapsulated drug in biological fluids as compared to other colloidal systems, such as liposomes or micelles
- Possibility for passive or ligand-mediated targeting, CNS delivery
- High drug loading capacity
- Suitable for different routes of administration (oral, parenteral, dermal, nasal, ocular, etc.)
- Possibility of controlled drug release
- Less variability in release mechanisms and their kinetics
- Ease of large scale production and sterilization

1.4.4 Selection of Nasal route of drug delivery

Intranasal delivery of anti-retroviral drugs has been proposed as a potential strategy to overcome the poor penetration of the drugs into the brain and to target HIV that harbour in the CNS [4,32].

❖ **Advantages of the nasal route of drug delivery**

The potential advantages of nasal route of drug delivery may be summarized as [13, 33, 34, 35]

- Non-invasiveness
- By pass the BBB, direct transport to CNS
- Avoidance of first pass metabolism and drug degradation
- Improved bioavailability
- Lower dose/ reduced side effects
- Reduce blood borne exposure risks of HIV
- Improved convenience and compliance

1.5 Hypothesis

It was hypothesized that the solid lipid nanoparticles of EFV would enhance the delivery of EFV to brain and plasma because of

- Better absorption due to the small size of the particles
- Improved permeability of the drug due to lipid and surfactant content
- Lipid protections of drug from enzymatic degradation
- Targeted delivery of the drug to brain (reservoir site of HIV)
- Reduced dose and reduced toxicity due to targeted delivery (direct nose to brain delivery)
- Avoidance of first-pass metabolism
- Avoidance of enzymatic degradation of drug in gastro- intestinal tract (GIT)
- Prevention from being effluxed out due to the presence of pluronics, thus facilitating its CNS delivery [24, 36]

1.6 Proposed plan of work

In the present investigation, an attempt was made to design and formulate solid lipid nanoparticles of the anti-viral drug, efavirenz to increase their bioavailability and

overcome the challenges associated with the drug. The nanoparticles of efavirenz were also proposed to target the drug to brain and increase its bioavailability in brain when administered through intranasal route. The work may be categorized as follows:

- Literature review
- Selection / Development of the analytical method(s) for analyzing EFV in the formulation and for determining the drug release profile.
- Preformulation studies including selection of various components, technique, etc.
- Formulation, optimization & characterization of SLN of EFV.
- Formulation, optimization and characterization of EFV loaded SLN *in-situ* gelling system to increase the residence time.
- *In-vitro* diffusion studies of the developed formulations.
- *Ex-vivo* absorption studies on freshly excised goat nasal mucosa.
- Histopathological studies
- *In-vivo* studies for estimation of drug in brain and plasma on intranasal administration of the developed formulation.
- Stability studies as per ICH guidelines.

1.7 Outline of Thesis

The report on the present research work has been divided into major five chapters of the thesis. The first chapter of introduction includes brief background, definition of the problem, aim, objectives, rationale, hypothesis, proposed plan of work and significant contributions by the present work. Chapter 2 presents literature review on various aspects related with the work including the description about disease, disease causing virus, available therapies, challenges associated with them, approaches to overcome them, selected formulation, selected route of administration, targeted delivery to desired site and brief profile of the components used in the final formulation. Chapter 3 deals with the description of experimental work performed for the investigations including analytical method development, validation, formulation development, optimization and their

evaluation; while chapter 4 includes results obtained with the experiments performed and detailed discussions on them. Chapter 5 on summary and conclusions finally presents the summary of the work and concludes the thesis.

1.8 References

1. Kawabata Y, Wada K, Nakatani M, Yamada S, Onoue S., (2011). Formulation design for poorly water-soluble drugs based on biopharmaceutics classification system: Basic approaches and practical applications. *Int J Pharm*; 420(1):1-10.
2. Kawakami K., (2012). Modification of physicochemical characteristics of active pharmaceutical ingredients and application of supersaturatable dosage forms for improving bioavailability of poorly absorbed drugs. *Adv Drug Deliv Rev*. ;64(6):480-495.
3. Wong HL, Wu XY, Bendayan R., (2012). Nanotechnological advances for the delivery of CNS therapeutics. *Adv Drug Deliv Rev*. ;64(7):686-700.
4. Cundy KC, Lynch G, Lee WA., (1997). Bioavailability and metabolism of cidofovir following topical administration to rabbits**.** Antiviral Research ;35(2):113-122.
5. List of Viral Diseases. [Online]. Available: http://doctors-hospitals-medical-cape-town-south-africa.blaauwberg.net/details.php?id=768. [Accessed 25 June 2016]
6. Infectitious viral diseases. [Online]. Available: usa.gov/search?affiliate=ri.gov&query=viral&sitelimit=health.ri.gov [Accessed 12 November 2015]
7. Global HIV/AIDS Overview. [Online]. Available: https://www.aids.gov/federal-resources/around-the-world/global-aids-overview/. [Accessed 12 November, 2015]
8. WHO | HIV/AIDS. [Online]. Available: http://www.who.int/gho/hiv/en/. [Accessed 12 November, 2015.
9. Rao KS, Ghorpade A, Labhasetwar V., (2009). Targeting anti-HIV drugs to the CNS.

Expert Opin Drug Deliv.;6(8):771-784.

10. Hasegawa T, Kawaguchi T., (2002). Delivery of Anti-Viral Nucleoside Analogues to the Central Nervous System. *Curr Med Chem -Anti-Infective Agents*;1(1):55-63.
11. Corbau R, Mori J, Phillips C, et al., (2010). Lersivirine, a nonnucleoside reverse transcriptase inhibitor with activity against drug-resistant human immunodeficiency virus type 1. *Antimicrob Agents Chemother*;54(10):4451-4463.
12. DrugBank: Efavirenz. [Online]. Available: http://www.drugbank.ca/drugs/DB00625. [Accessed 12 November, 2015]
13. Mistry A, Stolnik S, Illum L., (2009). Nanoparticles for direct nose-to-brain delivery of drugs;379:146-157.
14. Kaur IP, Bhandari R, Bhandari S, Kakkar V., (2008). Potential of solid lipid nanoparticles in brain targeting. *J Control Release*;127(2):97-109.
15. Das NJ, Amiji MM, Bahia MF, Sarmento B., (2010). Nanotechnology-based systems for the treatment and prevention of HIV/AIDS. *Adv Drug Deliv Rev*.;62(4-5):458-477.
16. Gupta U, Jain NK., (2010). Non-polymeric nano-carriers in HIV/AIDS drug delivery and targeting. *Adv Drug Deliv Rev*.;62(4-5):478-490.
17. WHO. Safety of Efavirenz. 2010. [Online]. Available: http://www.who.int/hiv/topics/treatment/efavirenz_safety_review.pdf. [Accessed 12 November, 2015]
18. Bocedi A, Notaril S NP., (2004). Binding of anti- HIV drugs to human serum albumin. *Drug Metab Dispos*.:606-609.
19. Peroni RN, Di Gennaro SS, Hocht C, et al., (2011). Efavirenz is a substrate and in turn modulates the expression of the efflux transporter ABCG2/BCRP in the gastrointestinal tract of the rat. *Biochem Pharmacol*.;82(9):1227-1233.
20. Lembo D, Cavalli R., (2010). Nanoparticulate delivery systems for antiviral drugs. *Antivir Chem Chemother*.;21(2):53-70.
21. Varatharajan L, A TS., (2009). The transport of anti-HIV drugs across blood–CNS interfaces: Summary of current knowledge and recommendations for further research. *Antiviral Res*.;82(2):A99-A109.

22. Soto-Ramirez LE, Rodriguez-Diaz R, Harris DR, Hazra R., (2010). HIV drug resistance-associated mutations in antiretroviral na??ve HIV-1-infected Latin American children. *Adv Virol*.;2010.
23. Rausch DM, Stover ES., (2001). Neuroscience research in AIDS. *Prog Neuro-Psychopharmacology Biol Psychiatry*.;25(1):231-257.
24. Mallipeddi R, Rohan LC., (2010). Progress in antiretroviral drug delivery using nanotechnology. *Int J Nanomedicine*. (1):533-547.
25. Date A., Destache CJ., (2013). A review of nanotechnological approaches for the prophylaxis of HIV/AIDS. *Biomaterials*.;34(26):6202-6228.
26. Kreuter J., (2014). Drug delivery to the central nervous system by polymeric nanoparticles: What do we know? *Adv Drug Deliv Rev*.;71:2-14.
27. Attama A, Momoh MA, (2012). Builders PF. Lipid Nanoparticulate Drug Delivery Systems: A Revolution in Dosage Form Design and Development. *Recent Adv Nov Drug Carr Syst*. 107-140.
28. Mehnert W, Mäder K., (2012). Solid lipid nanoparticles. *Adv Drug Deliv Rev*. ;64:83-101.
29. Blasi P, Giovagnoli S, Schoubben A, Ricci M, Rossi C., (2007). Solid lipid nanoparticles for targeted brain drug delivery. *Adv Drug Deliv Rev*.;59(6):454-477.
30. Füredi P, Kovács K, Ludányi K, Antal I, Klebovich I., (2016). Development and characterization of voriconazole loaded nanoparticles for parenteral delivery. *Int J Pharm*. ;510(1):159-163.
31. Blasi P, Giovagnoli S, Schoubben A, et al., (2011). Lipid nanoparticles for brain targeting I. Formulation optimization. *Int J Pharm*.;419(1-2):287-295.
32. Nowacek AS, McMillan J, Miller R, Anderson A, Rabinow B, Gendelman HE., (2010). Nanoformulated antiretroviral drug combinations extend drug release and antiretroviral responses in HIV-1-infected macrophages: Implications for NeuroAIDS therapeutics. *J Neuroimmune Pharmacol*.;5(4):592-601.
33. Galligioni V, Scagliarini A, Lorenzini L, et al. Nose-to-brain delivery of ribavirin (RBV) for the treatment of viral encephalitis. :4.

34. Singh AK SA and MN., (2012). Nasal cavity: A promising platform for drug delivery and research approaches from nasal to brain targeting. *J drug del ther*.;2(3):22-33.
35. Karavasili C, Fatouros DG., (2016). Smart materials: In situ gel-forming systems for nasal delivery. *Drug Discov Today*.; 21(1):157-166.
36. Lun H, Chattopadhyay N, Yu X, Bendayan R., (2010). Nanotechnology applications for improved delivery of antiretroviral drugs to the brain. *Adv Drug Deliv Rev*. ;62(4-5):503-517.

CHAPTER 2
Literature Review

2.1 Overview

This review mainly includes the review on the viruses including human immuno-deficiency virus (HIV), viral infections, acquired immune-deficiency syndrome (AIDS), anti-viral drugs, challenges associated with the therapy with anti-viral drugs, approaches to overcome them, potential of nano-formulations specifically solid lipid nanoparticles, *in-situ* gelling system, anatomy and physiology CNS and brain to understand the brain targeting approaches, nasal route of drug delivery for brain targeting and bioavailability enhancement. The chapter also includes the profile of drug and the excipients used for the formulation.

2.2 Virus

Viruses are small infective agents characterized by a lack of independent metabolism and the inability to replicate outside the living host cells. Viruses can infect all types of life forms, from animals and plants to microorganisms [1].

2.2.1 Structure of virus

Viruses are small obligate intracellular parasites, which by definition contain either a RNA or DNA genome surrounded by a protective protein coat (capsid). Capsid is composed with identical units, which are called capsomeres. The capsid is symmetrical and varied from simple helical form to highly complex structures. The coat plus the nucleic acid core is termed nucleocapsid. Some viruses have, in addition, a lipoprotein envelop, which may contain antigenic viral glycoproteins, as well as host phospholipids acquired when the virus nucleocapsid buds through the nuclear membrane or plasma membrane of the host

cell. Certain viruses also contain enzymes that initiate their replication in host cell. The whole infective particle is termed as virion. Genome may be double or single stranded depending on the type of virus [2,3]. A schematic diagram of the components of a virus particle (virion) is shown in Figure 2.1

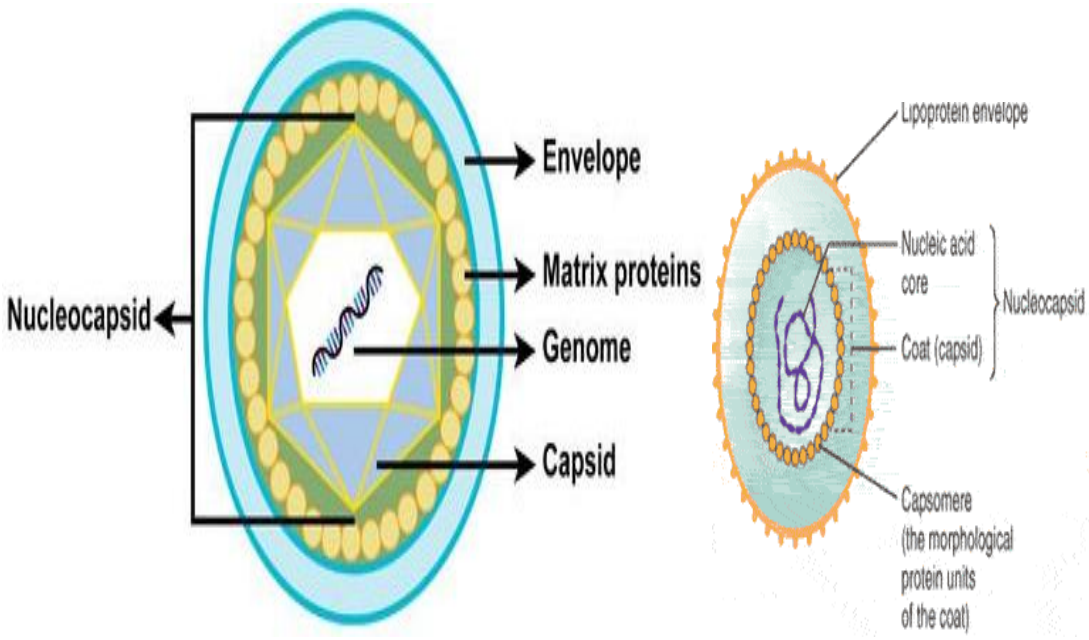

FIGURE 2.1: Structure of virus

2.2.2 Types of viruses

The genetic material in all types of cells is double-stranded DNA, but some viruses use RNA or single-stranded DNA to carry genetic information.

As per Baltimore classification system, there are seven groups based on genetic contents and replication strategies of viruses[4]. The seven groups of viruses with examples are summarized in Table 2.1.

TABLE 2.1: Types of viruses with examples

Group/ Class	Viruses	Examples	Envelop
I	dsDNA	Herpes virus Poxvirus Adenovirus Papillomavirus	Yes Yes No No
II	ssDNA	Adeno-associated virus	No
II	dsRNA	Reovirus	No
IV	(+)ssRNA	Togavirus Poliovirus Foot-and-mouth disease virus Hepatitis A virus Hepatitis C virus	Yes No No No Yes
V	(-)ssRNA	Influenza virus	Yes
VI	RNA reverse transcribing	HIV Retroviruses	Yes
VII	DNA reverse transcribing	Hepatitis	Yes

Ds = double strand, ss = single strand, (+) RNA is the one which can function as mRNA for the synthesis of proteins. (-) RNA cannot function as mRNA

2.2.2.1 Retrovirus

Virus that carries reverse transcription is called retrovirus. It is a single-stranded positive-sense RNA virus with a DNA intermediate. These viruses can

convert their RNA into DNA copy. This process is catalyzed by reverse transcriptase enzyme. Then this DNA is integrated covalently into the host genome using integrase enzymes, which is coded by reverse transcriptase. They are integrated into the host genome directly and the virus thereafter replicates as a part of host cell's DNA. The reverse transcription is much faster than the normal transcription process and it is not much accurate. Retroviruses can cause HIV and number of cancers in animals [5-7].

2.2.2.2 Differences between virus and retroviruse

Differences between virus and retrovirus is described in Table 2.2 [2, 8].

TABLE 2.2: Differences between virus and Retrovirus

Virus	Retrovirus
Includes a group of retrovirus	A group of viruses with special characteristics
Virus contains DNA or RNA as genetic material	Retrovirus contains only RNA
If the virus has DNA, it inserts DNA into the host cell, and it is integrated directly into the host genome at the lytic phase.	Retrovirus has RNA as its genetic material and needs to convert RNA to DNA before inserted into the host genome
In most viruses, DNA is transcribed into RNA, and then RNA is translated into protein.	The RNA is reverse-transcribed into DNA, which is integrated into the host cell's genome (called provirus), and then undergoes the usual transcription and translational processes to express the genes carried by the virus.
Viruses have transcription process	Retroviruses have reverse transcription process.
Mostly the second generation is similar to first generation genetically since the virus	The second generation of the retrovirus may be different from the first generation

has normal transcription process which is accurate than the reverse transcription.	because of the inaccuracy of the revere transcription process.
The treatments for infections caused by normal virus are easier.	Because of the vast genetic change in second generation of retroviruses, treatments for diseases caused by them are difficult.

2.2.3 Human Immunodeficiency Virus (HIV)

HIV is a member of the genus *Lentivirus*, (a subgroup of retrovirus) part of the family *Retroviridae* that causes HIV infection and over time acquired immunodeficiency syndrome (AIDS). There are two types of HIV: HIV-1 and HIV-2. HIV-1 is the virus that was initially discovered and is more virulent, more infective, than HIV-2 and is the cause of the majority of HIV infections globally. The HIV-2 is found less infective and has relatively poor capacity for transmission compared to HIV-1. HIV-2 is largely confined to west Africa [9].

2.2.3.1 Structure of HIV

HIV is different in structure from other retroviruses. The anatomy of HIV is shown in Figure 2.2. It is roughly spherical with a diameter of about 120 nm, around 60 times smaller than a red blood cell [10]. The viral core contains the viral capsule protein p24 which surrounds two single strands of HIV RNA and the enzymes needed for HIV replication, such as reverse transcriptase, protease, ribonuclease, and integrase; out of the nine virus genes, there are three, namely gag, pol and env, which contain the information needed to make structural proteins for new virus particles [3].

A matrix composed of the viral protein p17 surrounds the capsid ensuring the integrity of the virion particle. This is, in turn, surrounded by the viral envelope, that is composed of the lipid bilayer. Different proteins are embedded in the viral envelop, forming “spikes” consisting of the outer glycoprotein (gp)120 and the transmembrane gp41 [11]. The lipid

membrane is borrowed from the host cell during the budding process (formation of new particles). Gp120 is needed to attach the host cell and gp41 is critical for the cell fusion process.

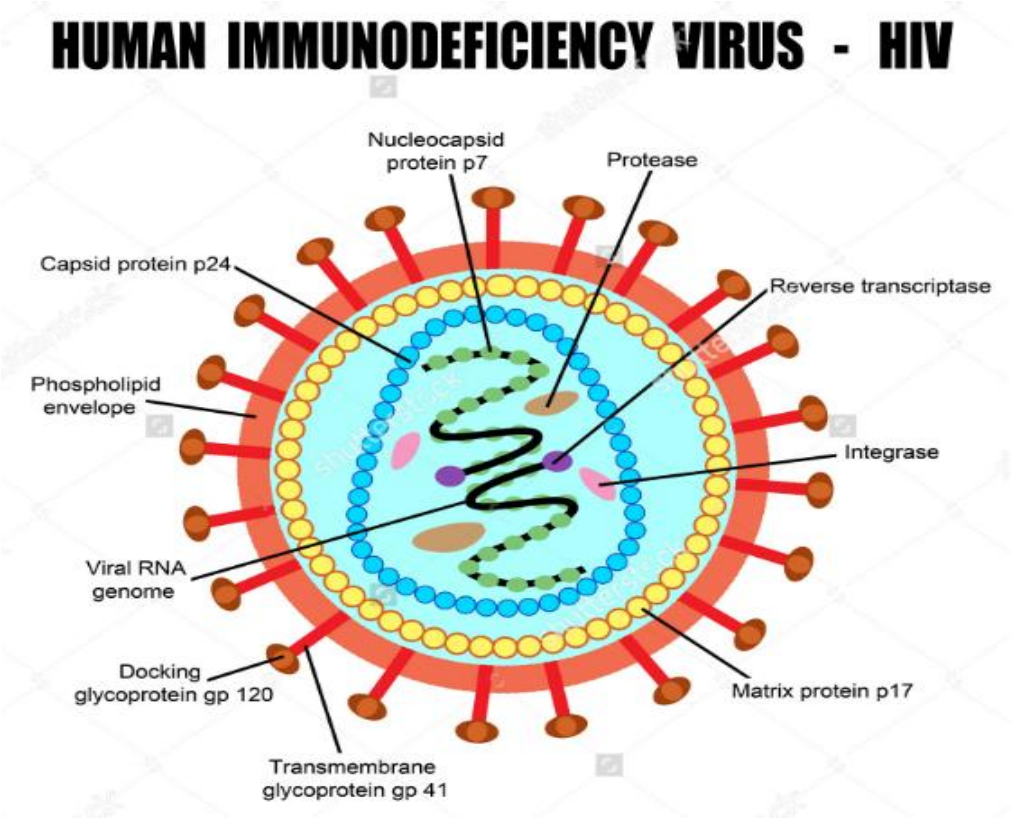

FIGURE 2.2: Anatomy of human immunodeficiency virus (HIV)

HIV infects mainly the CD4+ lymphocytes (T cells), but also to a lesser degree monocytes, macrophages and dendritic cells (these cells are also CD4+cells). Once infected, the cell turns into an HIV-replicating cell and loses its function in the human immune system [12].

2.3 Viral Infections

Viral infections are extremely widespread. Viruses can affect any part of the body or body system, and can cause infections such common cold, influenza, rabies, measles, chickenpox, small pox, herpes, AIDS, mumps, measles, rubella, viral hepatitis, viral meningitis, viral pneumonia, etc. The most life - threatening infection is of HIV causing AIDS [13, 14].

Viral infections come with a variety of symptoms ranging from mild to severe. Symptoms may vary depending on what part of the body is affected, type of viruses, age, and overall health of the affected person. The symptoms of viral infections can include fever, coughing, sneezing, headache, diarrhoea, vomiting or general weakness to more severe symptoms like personality changes, seizures, paralysis of the limbs, loss of sensation, sleepiness that can progress into a coma or death [15].

2.3.1 Types of viral infections

The most common viral infections are of following types:

- **Respiratory infections:** Infections of the nose, throat, upper airways, and lungs. The most common respiratory infections are sore throat, sinusitis, common cold, influenza, pneumonia, bronchiolitis.

- **Gastrointestinal tract infections:** Infections of the gastrointestinal tract, such as gastroenteritis (commonly caused by viruses such as noroviruses and rotaviruses).

- **Liver infections:** These infections cause hepatitis.

- **Nervous system infections:** Some viruses, such as the rabies virus and the West Nile virus, infect the brain, causing encephalitis. Others infect the layers of tissue that cover the brain and spinal cord (meninges), causing meningitis or polio.

- **Skin infections:** Viral infections that affect only the skin which sometimes result in warts or other blemishes. Many viruses that affect other parts of the body, such as chickenpox, also cause a rash.

- **Infections of various body systems:** Some viruses typically affect many body systems. Such viruses include enteroviruses and cytomegaloviruses.

- **Infections causing immune deficiency**: Infections by viruses such as HIV finally resulting in acquired immunodeficiency syndrome (AIDS).

2.3.2 Acquired immune deficiency syndrome (AIDS)

AIDS is a spectrum of conditions caused by infection with the human immunodeficiency virus (HIV). Following initial infection, a person may not notice any major symptoms. As the infection progresses, it interferes more with the immune system, increasing the risk of common infections like tuberculosis, as well as other opportunistic infections, and tumors that rarely affect people who have working immune systems [16]. HIV is spread primarily by unprotected sex , contaminated blood transfusions, hypodermic needles, and from mother to child during pregnancy, delivery, or breastfeeding [17].

According to the World Health Organization approximately 35 million people worldwide are living with HIV/AIDS 35 including 3.2 million children of less than 15 years age and an estimated 2.1 million individuals worldwide are newly infected with HIV every year [18]. AIDS is the sixth leading cause of death among people aged 25 - 44 in the United States [19].

2.3.2.1 Current therapies for AIDS

There are presently many antiretroviral drugs that have been approved by FDA (Food and Drug Administration) for use in the treatment of human immunodeficiency virus (HIV). Currently, many antiretrovirals are being evaluated for the prevention of HIV infections in clinic. The approved antiviral drugs for HIV infections are summarized in Table 2.3 [2, 20, 21]. As shown, the majority of antiviral drugs are administered orally, although some are delivered via parenteral (subcutaneous, intravenous and intravitreal) or topical routes. New drug delivery systems and strategies are needed to facilitate a functional cure and/or enable HIV eradication. Achieving efficacious drug concentrations in HIV reservoir sites using targeting approaches and reducing cellular efflux and metabolism to prolong effective drug concentrations in target cells remain significant drug delivery challenges [22].

TABLE 2.3: Approved antiviral drugs for HIV infections

Drug class and name Route	**Route of administration**	**Drug class and name Route**	**Route of administration**
Nucleoside reverse transcriptase inhibitors		**Protease inhibitors**	
Abacavir	Oral	Amprenavir	Oral
Didanosine	Oral	Atazanavir	Oral
Emtricitabine	Oral	Darunavir	Oral
Lamivudine	Oral	Fosamprenavir (a prodrug of amprenavir)	Oral
Stavudine	Oral	Indinavir	Oral
Zalcitabine	Oral	Lopinavir	Oral
Zidovudine	Oral	Nelfinavir	Oral
Nucleotide reverse transcriptase inhibitors		Ritonavir	Oral
Tenofovir disoproxil fumarate	Oral	Saquinavir	Oral
Non-nucleoside reverse transcriptase inhibitors		Tipranavir	Oral
Delavirdine	Oral	**Fusion/entry inhibitors**	
Efavirenz	Oral	Enfuvirtide (T-20)	Subcutaneous
Etravirine	Oral	Maraviroc	Oral
Nevirapine	Oral	**Integrase inhibitors**	
Rilpivirine	Oral	Raltegravir	Oral
Pharmacokinetic Enhancers		Dolutegravir	Oral
Cobicistat	Oral	Elvitegravir	Oral

2.3.2.2 HAART: Combination therapy

HAART (Highly Active Anti-Retroviral Therapy) combines three or more drugs from at least two different classes to suppress the replication process of the virus in at least two different ways. Using this method the replication process is slowed down and the rate at which drug resistance can develop is vastly reduced because HIV finds it more difficult to overcome this combined attack.

These current therapies for HIV infections with antiretroviral drugs is effective in reducing plasma viral levels, but are ineffective in eradicating the virus from other sites like CNS due to their inability to reach and accumulate in these cellular and anatomical reservoirs where virus potentially harbours. The CNS is reported to be the most important HIV reservoir site [23, 24]. HIV is known to invade the central nervous system (CNS) early in the course of the infection and primarily targets brain mononuclear macrophages, perivascular macrophages and microglia [25]. Important brain structures such as microglia, macrophages and possibly neurons, play a major role in viral persistence in the CNS [26]. Due to the restricted entry of anti-HIV drugs, the brain is thought to form a viral sanctuary site. This not only results in virological resistance, but also is often associated with the development of complications such as progressive deterioration in mental function, symptoms of motor abnormalities, mild neurocognitive disorder (MDR), HIV associated dementia (HAD), HIV encephalitis (HIVE) and even death in many cases [23, 26, 27].

2.4 CENTRAL NERVOUS SYSTEM (CNS)

The central nervous system (CNS) is the part of the nervous system consisting of the brain and spinal cord. Retina and the optic nerve (2^{nd} cranial nerve), as well as the olfactory nerves (1st) and olfactory epithelium are considered as parts of the CNS, synapsing directly on brain tissue without intermediate ganglia [28]. The olfactory epithelium is the only central nervous tissue in direct contact with the environment, which opens up for therapeutic treatments [29].

2.4.1 BRAIN

The brain makes up the largest portion of the central nervous system, and is often the main structure referred to when speaking of the nervous system. The brain is the major functional unit of the central nervous system and a highly protected organ from the periphery by two major barriers, the blood–brain barrier (BBB) and the blood–cerebrospinal fluid barrier (BCSFB). The anatomy of the brain is shown in Figure

2.3. The brain is located in the head, usually close to the primary sensory organs for such senses as vision, hearing, balance, taste and smell. The brain is the most complex organ in a vertebrate's body. In a typical human, the cerebral cortex (the largest part) is estimated to contain 15–33 billion neurons [30], each connected by synapses to several thousand neurons. These neurons communicate with one another by means of long protoplasmic fibers called axons, which carry trains of signal pulses called action potentials to distant parts of the brain or body targeting specific recipient cells. Microglia is a type of glial cell located throughout the brain and spinal cord [31]. Microglia account for 10–15% of all cells found within the brain. As the resident macrophage cells, they act as the first and main form of active immune defense in the central nervous system (CNS) [32]. Microglia (and other glia including astrocytes) are distributed in large non-overlapping regions throughout the CNS [33].

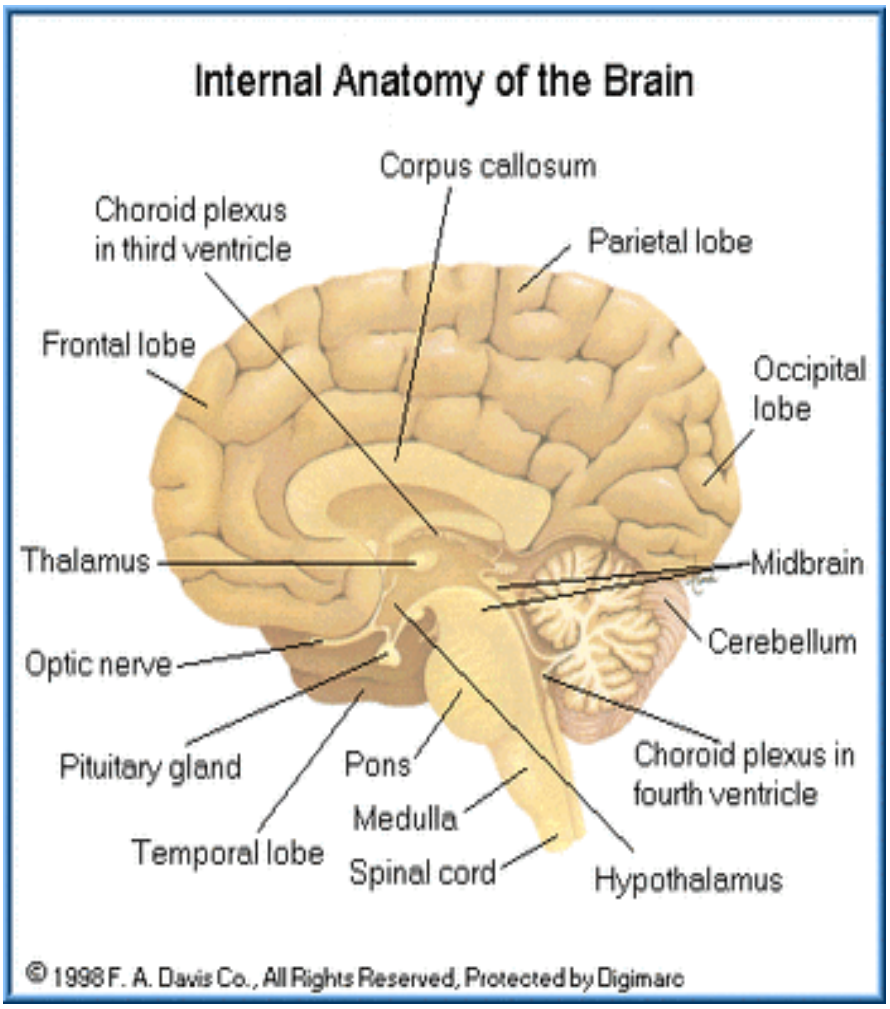

FIGURE 2.3: Anatomy of the brain

2.5 Brain Targeting

2.5.1 Blood –brain barrier and Blood-cerebrospinal fluid barrier

Blood–brain barrier (BBB) is a highly dynamic neuroprotective barrier, constituted by the endothelial cells of the capillaries in the brain. The BBB presents the main obstacle for entrance of large or hydrophilic molecules, microorganisms or the nanoparticles into the brain [34]. The blood–cerebrospinal fluid barrier (BCSFB) is composed of choroid plexus epithelial cells and also plays a role in the permeability of nutrients and xenobiotics. The restricted and highly controlled access to the brain is present due to mainly following three types of barriers [35, 36].

- Physical barrier: BBB displays the largest surface area (approximately 20 m^2) with presence of relatively impermeable endothelial cells with tight junctions which prevent paracellular transport, no fenestration exists in the endothelium and there is reduced rate of pinocytosis from the luminal side. The barrier due to BCSFB exists due to a monolayer of polarized epithelial cells surrounding the fenestrated capillaries that are joined together by tight junctional proteins [36].

- Transport/ Biological barrier: Expression and function of several receptors, ion channels and influx/efflux transport protein which controls transcellular transport. In particular, ATP-binding cassette (ABC) membrane-associated transporters such as P-glycoprotein (P-gp), Multidrug Resistance-associated Proteins (MRPs) and Breast Cancer Resistance Protein (BCRP, ABCG2) play a significant role in restricting the permeability of several pharmacological agents including anti-cancer and anti-HIV agents. The most extensively characterized transporter protein at the BBB is P-gp [36].

- Metabolic barrier/ Chemical barrier: Metabolizing enzymes may prevent transcellular transport. Complex drug interactions may also occur with these transport and enzyme systems which ultimately may result in therapeutic failure and/or toxicity.

2.5.2 Transport routes across the blood-brain barrier:

Various transport routes by which solute molecules move across the BBB are as follows (shown in Figure 2.4) [37].

- Paracellular aqueous pathway - Small water-soluble molecules diffuse through this pathway to a small extent.

- Transcellular lipophilic pathway - Small lipid soluble molecules like alcohol, steroid hormones, etc. penetrate transcellularly by dissolving in their lipid plasma membrane.

- Transport proteins / Carrier-mediated transport – It involves binding of a solute such as glucose or amino acids to a protein transporter on one side of the membrane resulting in a conformational change of the protein and transport of the substance to the other side of the membrane (from high to low concentration) or facilitated by energy provided by ATP for movement against concentration gradient.

- Efflux pumps - Responsible for extruding drugs from the brain.

- Receptor - mediated transcytosis (RMT): It is highly specific transport mechanism for uptake of macromolecules presented on the luminal side of the brain endothelia cells and delivering them to the brain with the receptor recycled back to the luminal membrane .RMT is an important transport pathway for endogenous peptides such as insulin, insulin - like growth factor and transferrin.

- Adsorptive transcytosis /Adsorptive-mediated transcytosis (AMT)/ Pinocytosis route – This type of transport is triggered by an electrostatic interaction between a positively charged substance, usually the charged moiety of a peptide, and the negatively charged plasma membrane surface (i.e. heparin sulphate proteoglycans).

- Cell mediated transcytosis : This is a considerably recently identified route of drug transport across the BBB and is a well established mechanism for some pathogens such as Cryptococcus neoformans and HIV entry into the brain, known as " Trojan horse" model [38]. This transport route relies on immune cells such as monocytes or macrophages to

cross the intact BBB. It can be used virtually for any type of molecules or materials as well as particulate carrier systems [39].

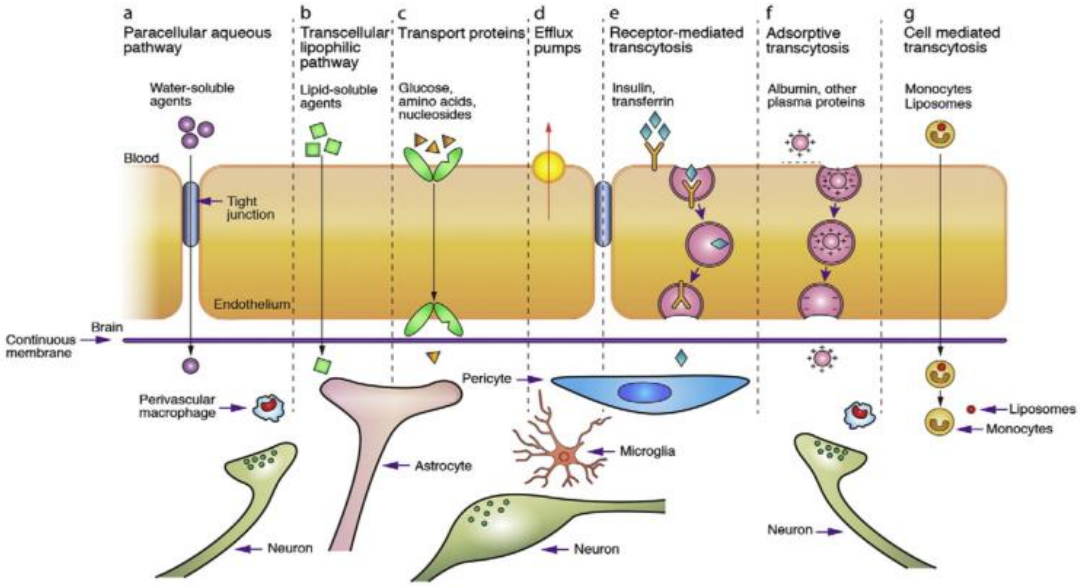

FIGURE 2.4: Transport route across blood-brain

Varatharajan et. al. summarised the existing knowledge on the transport of anti-HIV drugs across the blood–brain barrier and the choroid plexus. There are recommendations for future research as well [40].

2.5.3 Approaches for transporting drugs across the blood-brain barrier:

There are various approaches proposed and/ or adopted for effective delivery of drugs to the brain. Each of these strategies have some strengths and some limitations. These strategies could involve [25, 26]

2.5.3.1 Drug modification approach

It involves coupling drugs to molecules that have the ability to penetrate the tight vasculature or chemically modifying the functional groups of drugs to form “prodrugs” with more favourable lipophilicity for improved BBB passage. These prodrugs can be hydrolysed and release the parent drug on gaining access to endothelial cells [41]. Since the prodrug is officially considered to be a distinct chemical entity, the method requires substantially more drug purification steps, screening test and clinical studies, which usually lead to increase of cost [42].

2.5.3.2 Disruption of BBB:

- **Hyper-osmotic opening of the BBB:** A hypertonic solution of mannitol or urea can be infused to shrink the capillary endothelial cells by inducing water efflux which subsequently opens the tight junction network momentarily. As a result, the paracellular flow can be considerably increased allowing more efficient BBB passage by drug compounds. This strategy has been found to increase the BBB permeability to some extent. However, it induced seizures in experimental animals as well as chronic neuropathological changes making it to be a risky procedure, especially for long-term therapy [43].

- **By chemical agent :** Cytotoxic agents (like alkylating agents - etoposide and cisplatin), vasoactive agents (bradykinin, peptidase inhibitors, angiotensin II) may disrupt tight junctions and create openings between the endothelial cells [44]. However, most of these compounds are toxic, long-term use of this strategy for brain delivery of drugs is not appropriate.

- **Low-frequency ultrasound / Thermal shock approach:** BBB can be disrupted via mechanisms such as by using low-frequency ultrasound (260 Hz) or thermal shock. Presumably, the disruption by this method occurs due to interaction between ultrasonic waves, microbubbles and the brain microvasculature [45]. However, there are several concerns regarding the safety of this strategy [46]. More work is required to establish the optimal conditions for extensive use of this method.

2.5.3.3 Inhibition of transporters:

A number of chemical entities have been developed in the past decade having capability of blocking specific transporters. Multiple fold increase in the brain accumulation of drug is reported to be observed in animals treated with P-gp blocker/ MRP inhibitor. These blockers, unlikely to be CNS-specific, may lead to elevated risks of drug toxicity and unpredictable drug-drug interactions.

2.5.3.4 Active targeting strategies:

Nano-formulations can cross the BBB via receptor-mediated transcytosis, but this process is found to be inefficient. The delivery of the drugs to CNS is reported to be significantly improved by modifying the systems with "targeting molecules" such as monoclonal antibodies, cell- penetrating peptides and/or receptor substrates [47, 48]. Direct conjugates or fusion proteins of drug and targeting ligand often have a drawback of loss of drug's activity especially when conjugated via a non-cleavable linker [35].

2.5.3.5 Nanotechnology/ Development of novel drug delivery systems/ Nanoformulations / Nanocarriers:

Various drugs are reported to be effectively delivered to the brain using drug nanocarriers [49-54]. Different nanocarriers include nanoparticles, nanoemulsions, liposomes, polymeric systems, micelles, dendrimer, niosomes nanogel, etc., which can further be modified with targeting moieties as well [36, 52, 55]. Mallipeddi et al. provided a summary of the application of various nanocarrier systems like polymeric, inorganic, solid lipid, liposomes, polymeric micelles, dendrimers, cyclodextrins and cell based nanoformulations to the delivery of anti-HIV drugs, specifically antiretrovirals [24].

2.5.3.6 Alternate route of drug delivery/ Nose-to-brain delivery: Various researchers have successfully investigated direct delivery of various drugs from nose to brain [51, 56, 57]. Kumar et al. prepared intranasal nanoemulsion based brain targeting drug delivery system of risperidone [58]. Patel et. al. prepared risperidone loaded solid lipid nanoparticles and studied the possibility of brain targeting by nose-to-brain delivery [59]. Rao et al., 2009 summarized about targeting anti-HIV drugs to the CNS [26]. They have also summarized the mechanisms of viral infection, neurodegeneration due to HIV infection, antiretroviral therapies, their limitations and various approaches to overcome the BBB to enhance CNS delivery of anti-HIV drugs. Seju et. al. prepared a nanoparticulate drug delivery system of olanzapine using poly(lactic-co-glycolic acid) (PLGA) for direct nose-to-brain delivery to provide brain targeting and sustained release [60].

2.6 SOLID LIPD NANOPARTICLES

Lipid - based nanocarriers have strong potential for delivery of drugs to the CNS. There are a wide range of physiological lipids and phospholipids available for lipid nanocarriers which are biocompatible and biodegradable. There are several classes of lipid - based nanocarriers available which includes liposomes, micro- or nano - emulsion and solid lipid nanoparticles [25, 61].

Solid lipid nanoparticles (SLN) are colloidal dispersions or particulates in the size range of 100–500 nm composed of biocompatible lipid matrix that are physiologically well tolerated when administered *in-vivo* [62]. SLN are gaining increased attention during recent years because of various advantages over other colloidal drug delivery systems.

2.6.1 Advantages of SLN [24, 63, 64]

- Biocompatibility of physiological lipids
- Potential for increased permeability due to small size as well as lipid and surfactant contents and hence, enhanced bioavailability
- Increased protection and stability to the encapsulated drug in biological fluids as compared to other colloidal systems, such as liposomes or micelles
- Possibility for passive or ligand-mediated targeting, CNS delivery
- High drug loading capacity
- Suitable for different routes of administration (oral, parenteral, dermal, nasal, ocular, etc.)
- Possibility of sustained/ controlled drug release
- Less variability in release mechanisms and their kinetics
- Ease of large scale production and sterilization

2.6.2 Solid Lipid Nanoparticles for Nose to Brain Delivery

Several investigations have been done by various researchers to study the delivery of different drugs for CNS disorders in solid lipid nanoparticles for delivery to CNS / brain

and have evidenced the existence of a direct nose-to-brain delivery route for nanoparticles administered to the nasal cavity [56, 57, 65, 66]. It has been observed that nano-sized drug delivery systems can enhance nose-to-brain delivery of drugs compared to equivalent drug solutions formulations. Protection of the drug from degradation and/or efflux back into the nasal cavity may partly be the reason for this effect of nanoparticles [67]. However, whether the drug from the nanoparticles is being released in the nasal cavity or the nanoparticles carrying the drug are transported via the olfactory system or the trigeminal nerves into the CNS where the drug is released is not certain.

2.7 Gelling system

A gel is a solid jelly – like material that can have properties ranging from soft and weak to hard and tough. Gels may be defined as a substantially dilute three-dimensional cross-linked system, which exhibits no flow when in the steady-state.

2.7.1 *In-situ* gels

In-situ forming gels are formulations, intended to be applied as solutions, sols, or suspensions, which undergo gelation after administration due to the physicochemical environment [68]. In other words, *in-situ* gels are polymeric solutions which can be administrated as liquid, but upon exposure to the physiological environments, undergo a phase transition to semisolid gel. The formation of gel may depend on factors like temperature, pH change, presence of ions, etc. The formulations in the liquid state are easy to be administered and on gelation after administration, increases the residence time and the drug gets released in a sustained and controlled manner, and thus the *in-situ* gels incorporate the benefits of both the state.

Mucoadhesion/ Bioadhesion indicate the attachment of a synthetic or biological macromolecule to a biological tissue resulting in formation of bond with epithelial cell and/or the mucus layer. Mucoadhesive *in-situ* gel formulations are reported to enhance the permeation characteristics of the drug through nasal route by increasing the residence time

[69]. The *in-situ* gel forming polymeric formulations offer several advantages like sustained and prolonged action in comparison to conventional drug delivery systems. Ravi et. al. developed thermo-sensitive nasal *in-situ* gel using poloxamers and mucoadhesive polymers and evaluated for sol-gel transition temperature, *in-vitro* and *in-vivo* release and transit time. Pharmacokinetic study in rabbits showed significant improvement in bioavailability of drug from intranasal gels than oral solution [70]. Different mechanisms may be used for triggering the *in-situ* gel formation for drug delivery.

2.7.1.1 In- situ gel formation based on physiological stimuli (temperature and/or pH)

a) Thermally triggered systems

The application of various polymers / biomaterials whose transitions from sol to gel is triggered by increase in temperature provides a most common and simple approach for *in-situ* gel formation. For sol to gel transition, the ideal critical temperature range is ambient and physiologic temperature, so that no external source of heat other than that of body is required for triggering gelation. Temperature-sensitive hydrogels may be classified as negatively thermo-sensitive, positively thermo-sensitive and thermally reversible gels. Negative temperature-sensitive hydrogels have a lower critical solution temperature (LCST) and contract upon heating above the LCST. Polymers having low critical solution temperature (LCST) has the ability to transition between ambient and physiologic temperature are thus frequently used for the purpose. A positive temperature sensitive hydrogel has an upper critical solution temperature (UCST), such a hydrogel which contracts upon cooling below the UCST. Polymer networks of poly(acrylic acid) (PAA) and polyacrylamide (PAAm) or poly(acrylamide-co-butyl methacrylate) have positive temperature dependence of swelling [71]**.** Different thermosensitive gelling agents include poloxamers, cellulose derivatives, xyloglucan, etc. The most commonly used thermo-reversible gels are those prepared from poloxamers [69, 72]. Other than poloxamers, hydroxypropyl methylcellulose (HPMC) and the polyvinyl pyrrolidone (PVP) are reported to have thermo-sensitive characteristics [73, 74].

(b) pH triggered systems:

The formation of gel may also be induced by physiological pH changes. All the pH-sensitive polymers contain acidic or basic groups that either accept or release protons in response to changes in environmental pH. Swelling of hydrogel increases as the external pH increases in the case of weakly acidic (anionic) groups, but decreases if polymer contains weakly basic (cationic) groups. The majority of anionic pH-sensitive polymers are based on polyacrylic acid (carbomer) or its derivatives [69].

2.7.1.2. In-situ gel formation based on chemical reactions

In-situ gel formation may take place due to chemical reactions involving precipitation of inorganic solids from supersaturated ionic solutions, enzymatic processes or photo-initiated polymerization processes. For example, gellan gum is an anionic polysaccharide that undergoes *in-situ* gelling in the presence of mono and divalent cations, including Na^+ K^+, Ca^{2+} and Mg^{2+}. Photo-polymerisation is reported to be used for *in-situ* gel formation of biomaterials. Acrylate or similar polymerizable functional groups like the methacrylated monomers photopolymerize quickly to form crosslinked networks, and the rate of polymerization is readily controlled by the photo initiation conditions like incident light intensity or initiator concentration [73].

2.8 Nose to brain drug delivery system

The direct anatomical connection between the nasal cavity and the brain/CNS opens a pathway to deliver many drugs into the CNS by circumventing the BBB. It provides the basis for the development of delivery systems for intranasal administration. In the past decades, the use of the nasal cavity as a route for drug delivery and targeting the brain/ CNS is becoming the area of great interest. Various investigations have been frequently done to study the delivery of drug to brain via intranasal administration [56, 57, 74-80]. Drugs have been shown to reach the CNS from the nasal cavity by direct transport across the olfactory and trigeminal neural pathways [81]. It is the only site in the human body

where the nervous system is in direct contact with the surrounding environment [82]. Intranasal route of drug delivery is demonstrated to be a simple, non-invasive, convenient, cost-effective, and a better option for direct transport of drug to target drugs to brain/CNS owing to its ability to not only circumvent the BBB but also avoid the hepatic first-pass effect.

2.8.1 Anatomy and physiology of nasal cavity

The external nose has a pyramidal shape, which may differ greatly depending on race. The main functions of nose are olfaction, regulation of humidity & temp of inhaled air and removal of microorganism or particulate matter from inhaled air. There are several types of external noses in world population out of which mainly 3 types of nostrils are commonly observed:

(i) Leptorrhine: long and narrow nostrils

(ii) Plalyrrhine : broad and flat nostrils

(iii) Mesorrhine : Intermediate nostrils

The external nasal anatomy can be classified into bony, cartilaginous, and soft tissue components. The soft tissue component of the nose is composed of skin, fibro-adipose tissue and muscles of facial expression, controlled by the facial nerve.

The nose is divided into two large irregular cavities formed by 14 bones connected to each other by a tough fibrous membrane. The nasal passage is about 12-14 cm long and about 5 cm high. The total surface area of both nasal cavities is about 160 cm^2 (96m^2 if the nasal epithelial microvilli are included), the total volume is about 15 ml. The surface area of the olfactory region is 8 cm^2 (0.3 m^2 including microvilli). The volume which can be administered per nostril is 15 µl [29].

Nasal cavity is divided into three regions:

1. Nasal vestibule
2. Olfactory region
3. Respiratory region

There are 6 arterial branches that serve the nasal cavity, making this region a very attractive route for drug administration. Many of the side effects seen following intranasal administration are caused by some of the 6 nerves that serve the nasal cavity. The 5th cranial nerve (trigeminal nerve) is responsible for sensing pain and irritation following nasal administration but the 7th cranial nerve (facial nerve) will respond to such irritation by stimulating glands and cause facial expressions in the subject. The first cranial nerve (olfactory nerve), however, is the target when direct absorption into the brain is the goal, since this is the only site in our body where the central nervous system is directly expressed on the mucosal surface. The nasal mucosa contains 7 cell types and 4 types of glands. Four types of cells and 2 types of glands are located in the respiratory region but 6 cell types and 2 types of glands are found in the olfactory region.

2.8.2 Olfactory region:

The olfactory region is located at the upper portion of the nasal cavities, just below the cribriform plate of the Ethmoid bone, which contains openings to allow the passage of neuronal bundles from the olfactory epithelium to the CNS [29, 67]. The olfactory epithelium predominantly contain three cell types - Olfactory neural cells, Sustentaculum (supporting) cells, and basal cell as shown in Figure 2.5 [67]. The nerves serving the olfactory region are called the first cranial nerves or the olfactory nerves. These are twenty special nerves [83]. They are connected to the olfactory bulb, an oval greyish mass which rests on the cribiform plate of the ethmoid bone. The olfactory nerves convey nerve impulses arising from the bipolar olfactory neurons in the olfactory mucosa and through the axons the impulse is brought to a synapse in the olfactory bulb.

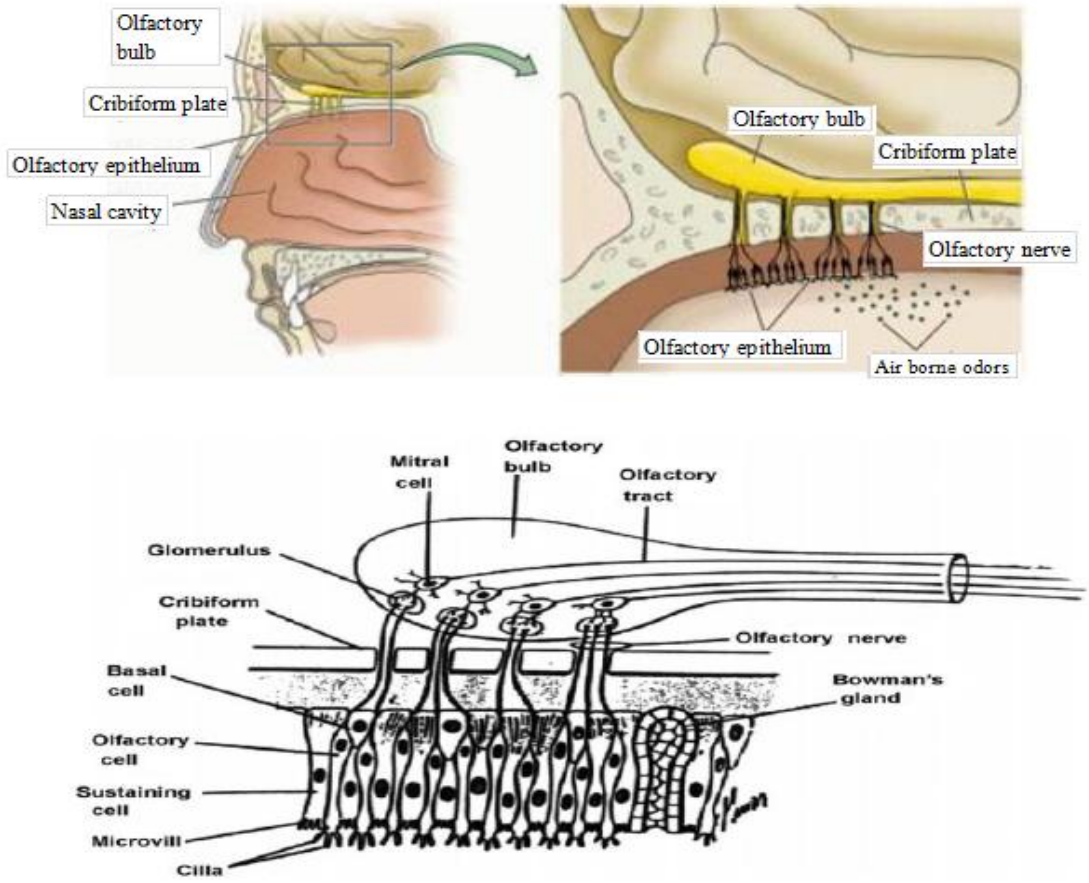

FIGURE 2.5 : Olfactory region showing the olfactory epithelium, bulb and tract [79]

2.8.3 Trigeminal nerve

Another set of nerves emanating from the nasal cavity is the maxillary branch of the trigeminal nerves, which are general sensory nerves. The trigeminal nerve is thought to be the largest of the cranial nerves and has three major branches namely - ophthalmic nerve, maxillary nerve and mandibular nerve having motor functions as well along with the sensory functions. Neurones from the ophthalmic and maxillary branches of the trigeminal nerve pass directly through the nasal mucosa and are thus important for nose-to-brain drug delivery [85].

The region which is responsible for the direct delivery of drugs from the nose to the brain is the olfactory region and the trigeminal nerve areas. Delivery from the nose to the central nervous system occurs within minutes along both the olfactory and trigeminal nerves [81].

2.8.4 Mechanism and Pathways for nose to brain delivery:

The small nanoparticles penetrate intranasally through the mucosal membrane by paracellular or transcellular route. The transcellular process is responsible for the transport of lipophilic drugs that show a rate dependency on their lipophilicity [86]. The close connection between the olfactory bulb and the cerebrospinal fluid (CSF) offers a potential route for nasally delivered drugs to the CSF, provided the drug is able to cross the nasal epithelium and the arachnoid membrane. Trigeminal pathways deliver a low molecular weight drug from the nose to the brain [81]. Both small and large molecules can pass rapidly from the nose into the brain along olfactory nerves and trigeminal nerve structures, without primarily passing via the CSF [87]. The reports indicate good bioavailability being achieved for molecules up to 1000 Da (without enhancers) and good availability extended to at least 6000 Da with enhancers [88]. Singh et.al. summarised the anatomical, histological and physiological overview of nose, nasal delivery, absorption enhancers, advantages, barriers related to nasal drug delivery, physicochemical, biological and formulation related factors affecting nasal drug delivery system. The research approaches on brain targeting through nasal cavity has also been highlighted [89].

2.8.5 Advantages of nasal route of drug delivery

- Non-invasiveness
- By pass the BBB, direct transport to CNS
- Avoidance of first pass metabolism and drug degradation
- Enhanced systemic absorption of drugs due to rich vasculature in nasal mucosa.
- Reduced enzymatic degradation of drugs.
- Improved bioavailability
- Lower dose/ reduced side effects
- Reduce blood borne exposure risks
- Improved convenience and compliance

2.8.6 Limitation of nasal route of drug delivery

- Only low molecular weight lipophilic, unionized drugs are favourably absorbed through this route of delivery
- The drug therapy may be hampered during the nasal congestion due to the allergy or infection
- The possibility of toxicity at the olfactory area and the trigeminal nerve.
- Drug residence time / Mucociliary clearance

2.8.7 Factors affecting nose-to-brain drug delivery

There are various factors which affect the permeation and delivery of drug from nose to brain including the physicochemical properties of the drug, nasal environment and the selected nasal drugs delivery system.

- Physicochemical properties of the drug [90]
    - Solubility
    - Lipophilicity / (Hydrophilic-lipophilic balance) HLB
    - Relative molecular weight
    - Degree of ionization (pKa)
- Nasal Environment
    - Blood Flow
    - Mucociliary Clearance
    - Nasal enzymes
    - Pathological conditions
    - Efflux transporter systems
- Formulation related factors
    - Viscocity
    - pH

2.9 DRUG PROFILE – EFAVIRENZ

Efavirenz is a non-nucleoside reverse transcriptase inhibitor (NNRTI), having the structure as shown in Figure 2.6 and is used as part of highly active antiretroviral therapy (HAART)

for the treatment of human immunodeficiency virus (HIV) type 1. Efavirenz is also used in combination with other antiretroviral agents as part of an expanded post-exposure prophylaxis regimen to prevent HIV transmission for those exposed to materials associated with a high risk for HIV transmission. For HIV infection that has not previously been treated, efavirenz and lamivudine in combination with zidovudine or tenofovir is the preferred NNRTI-based regimen. The detailed drug profile is given in Table 2.4.

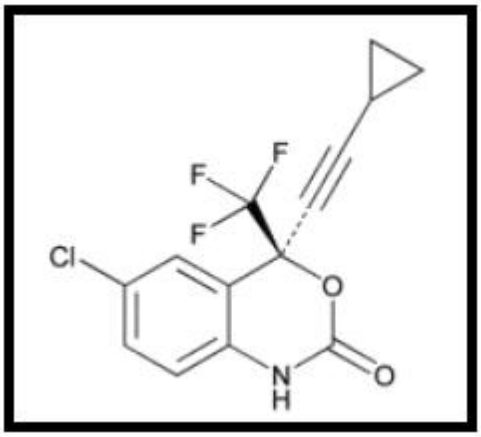

FIGURE 2.6: Structure of Efavirenz

TABLE 2.4: Drug Profile – Efavirenz [91]

Drug	Efavirenz
Chemical Formula	$C_{14}H_9ClF_3NO_2$ {(4S)-6-chloro-4-(cyclopropylethynyl)-1,4-dihydro-4-(triflouoromethyl)-2H-3,1-benzoxazin-2-one.
Description	NNRTI (Non – nucleoside reverse transcriptase inhibitor) used as part of HAART for the treatment of a human HIV -1
Drug Category	Antiviral agent (Non- nucleoside Reverse Transcriptase Inhibitor)
Indication	in combination treatment of HIV infection (AIDS)
Pharmacodynamics	Efavirenz (dideoxyinosine, ddI) is an oral non-nucleoside reverse transcriptase inhibitor (NNRTI). It is a synthetic purine derivative

	and, similar to zidovudine, zalcitabine, and stavudine. Efavirenz was originally approved specifically for the treatment of HIV infections in patients who failed therapy with zidovudine. Currently, the CDC recommends Efavirenz also as a part of a three-drug regimen that includes another nucleoside reverse transcriptase inhibitor (e.g., lamivudine, stavudine, and zidovudine) and a protease inhibitor or efavirenz when treating HIV infection.
Mechanism of action	Efavirenz inhibits the activity of viral RNA-directed DNA polymerase (i.e., reverse transcriptase). Antiviral activity of efavirenz is dependent on intracellular conversion to the active triphosphorylated form. The rate of efavirenz phosphorylation varies, depending on the cell type. It is believed that inhibition of reverse transcriptase interferes with the generation of DNA copies of viral RNA, which, in turn, are necessary for synthesis of new virions. Intracellular enzymes subsequently eliminate the HIV particle that previously had been uncoated, and left unprotected, during entry into the host cell.
BCS class	II
Average mol. Weight	315.675
Melting point	139 - 141 ^{0}C
Water solubility	9.2 µg/mL (pH 8.7) at 25°C
Log P	4.6
pKa	10.2
Protein binding	99.5-99.75%
Absorption	40-45%
Half life	40-55 hrs
Dose	50-600 mg

Cmax	4.0±1.7 µg/ ml [92]
CSF:Plasma ratio	0.69% (range 0.26 - 1.19%) [92]
Therapeutic range of efavirenz	1000 – 4000ng / dose [93]
Marketed Products	Efavir, Stocrin, Sustiva (600 mg tab, 200, 100, 50 mg cap), (Bristol-Myers Sqibb, Ranbaxy Lab Ltd., Aspen Pharmacare, etc.)

2.10 EXCIPIENT'S PROFILE

2.10.1 TRIPALMITIN

Tripalmitin is a triglyceide derived from the fatty acid palmitic acid. A triglyceride is an ester derived from glycerol and three fatty acids which are the main constituents of body fat in humans and animals, as well as vegetable fat. The detailed profile about Triplamitin is given in Table 2.5.

TABLE 2.5 : Description about Tripalmitin

Product name	Tripalmitin
IUPAC Name	1,2,3-Propanetriyl trihexadecanoate
Appearance	White powder
Chemical formula	$C_3H_5(OOC_{16}H_{31})_3$ or $C_{51}H_{98}O_6$
Synonyms	Palmitin, Glycerol tripalmitate, Glycerin tripalmitate, Glyceryl triplamitate, Palmitic triglyceride, Tripalmitoyl glycerol,

Structure	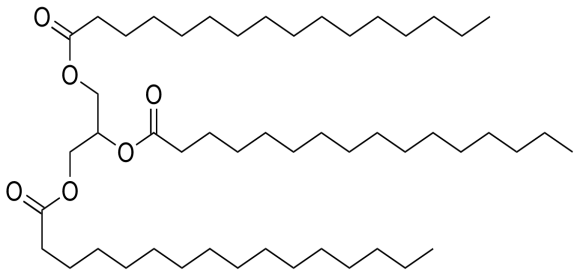
Molar mass	807.34 g mol^{-1}
Density	0.8752 g/cm^3 (70^0C)
Melting point	44.7–67.4 ^{0}C (112.5–153.3^{0}F, 317.8-340.5 K
Refractive Index	1.4381
Boiling point	315 ^{0}C (599^{0}F, 588 K) at 760 mm Hg
Solubility in water	Insoluble
Solubility	Soluble in diethyl ether, benzene, chloroform
Regulatory status	GRAS listed. Accepted for use as a food additive in Europe. Included in the FDA Inactive Ingredients Guide (capsules and tablets). Included in the Canadian List of Acceptable Non-medicinal Ingredients.

Tripalmitin SLN have been observed to organize into the stable β-form when different surfactants were used for SLN preparation [94].

2.10.2 POLOXAMERS

Poloxamers are nonionic triblock copolymers composed of a central hydrophobic chain of polyoxypropylene (poly (propylene oxide)) flanked by two hydrophilic chains of polyoxyethylene (poly (ethylene oxide)) [PEO-PPO-PEO] having the general structure as shown in Figure 2.7.

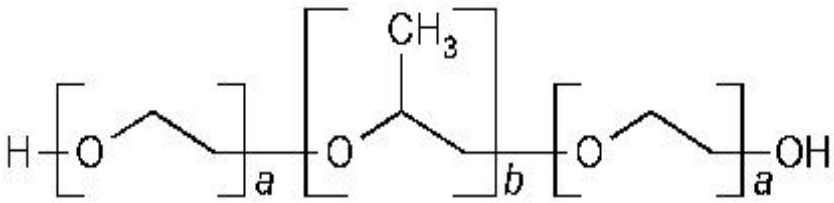

FIGURE 2.7: Structure of Poloxamer

Many different poloxamers exist depending on the lengths of the polymer blocks that have slightly different properties. These copolymers are commonly named with the letter "P" (for poloxamer) followed by three digits: the first two digits x 100 give the approximate molecular mass of the polyoxypropylene core, and the last digit x 10 gives the percentage polyoxyethylene content. The generic poloxamers are available with the trade name Pluronic. The coding of these Pluronics starts with a letter to define its physical form at room temperature (L = liquid, P = paste, F = flake (solid)) followed by two or three digits, The first digit (two digits in a three-digit number) in the numerical designation, multiplied by 300, indicates the approximate molecular weight of the hydrophobe; and the last digit x 10 gives the percentage polyoxyethylene content.

Pluronics are fluid at low temperature, but form thermo-reversible gel when the temperature is increased as a consequence of disorder-order transition in micelle packing which makes these polymers suitable for in-situ gelation [74].

2.10.2.1 Poloxamer 188

The detailed profile about poloxamer 188 is given in Table 2.6.

TABLE 2.6 : Description about Poloxamer 188

Product Name	Poloxamer 188
Trade name	Pluronic F68
Appearance	White or almost white, waxy powder, microbeads, or flakes

Chemical Formula	$HO(C_2H_4O)_a(C_3H_6O)_b(C_2H_4O)_aH$ {a=80, b=27}
Molecular weight	7680 to 9510 g/mole
Synonyms	Pluronic F68, Polyethylene-polypropylene glycol, Polyoxyethylene-Polyoxypropylene block copolymer, Poly(Ethylene oxide-co-Polypropylene oxide), Block, Block Copolymer of Ethylene Oxide and Propylene Oxide
Melting point	52-57ºC
HLB value	29
Flowability	Free flowing
Solubility	Freely soluble in ethanol and water
Functional Category	Dispersing agent, emulsifying and co-emulsifying agent, solubilizing agent, tablet lubricant, wetting agent
Stability and Storage condition:	Poloxamers are stable materials. Aqueous solutions are stable in the presence of acids, alkalis, and metal ions. The bulk material should be stored in airtight containers in a cool, dry place.
Incompatibility:	Depending on the relative concentrations, poloxamer 188 is incompatible with phenols and parabens
Safety	Poloxamers are used in a variety of oral, parenteral, and topical pharmaceutical formulations and are generally regarded as nontoxic and nonirritant materials. Poloxamers are reported to be nonirritating and non-sensitizing when applied in 5% w/v and 10% w/v concentration to the eyes, gums, and skin.
Regulatory Status:	GRAS listed. Accepted for use as a food additive in Europe. Included in the FDA Inactive Ingredients Guide Included in the Canadian List of Acceptable Non-medicinal Ingredients.

2.10.2.2 Poloxamer 407

The detailed profile [69] about poloxamer 407 is given in Table 2.7.

TABLE 2.7: Description about Poloxamer 407

Product Name	Poloxamer 407
Trade name	Pluronic F 127 / Synperonic PE/F 127
Appearance	White Solid (Granular solid, Coarse particle)
Chemical Formula	$HO(C_2H_4O)_a(C_3H_6O)_b(C_2H_4O)_aH$ { a = 101 and b = 56.}
Molecular weight	9840 - 14600 g/mole
Synonyms	Pluronic F127, Polyethylene-polypropylene glycol, Polyoxyethylene-Polyoxypropylene Block Copolymer, Poly(Ethylene oxide-co-Polypropylene oxide), Block, Block Copolymer of Ethylene Oxide and Propylene Oxide, Ethylene oxide/Polypropylene oxide copolymer; Methyl-oxirane polymer with oxirane
Melting point	56°C
HLB value	22 (at 22^0C)
Flowability	Good
Solubility	Freely soluble in water, in alcohol, and in isopropyl alcohol. Soluble in cold water. Solubility in Water: 175g/L (23^0C)
Functional Category	Surfactant, emulsifying and co-emulsifying agent, cleaning, thermoreversible *in-situ* gel forming system
Pharmaceutical applications	IV, inhalation, oral solution, suspension, ophthalmic or topical formulations. Poloxamers are reported to increase the absorption of liquid paraffin and other fat-soluble substances.
Stability and Storage condition:	Poloxamers are stable materials. To be stored in air-tight containers in a cool, dry, well-ventilated area, away from

	heat.
Incompatibility:	Poloxamers have been reported to be incompatible with hydroxybenzoates and phenols.
Safety	Poloxamers are used in a variety of oral, parenteral, and topical pharmaceutical formulations and are generally regarded as non-toxic and non-irritant materials. Poloxamers to be nonirritating and nonsensitizing when applied in 5% w/v and 10% w/v concentration to the eyes, gums, and skin.
Regulatory Status:	GRAS listed. Accepted for use as a food additive in Europe. Included in the FDA Inactive Ingredients Guide. Included in the Canadian List of Acceptable Non-medicinal Ingredients.

2.10.3 CARBOPOL

Carbomers are cross-linked poly (acrylic acid) of high molecular weight, commercially available as Carbopol®. The acrylic acid monomer unit in carbomer polymers is shown in Figure 2.8. Different carbomer codes (910, 934, 940, 941 and 934P) are an indication of molecular weight and the specific components of the polymer.

Carbopol® 934 is a synthetic polymer composed of 62% of carboxyl groups with a high molecular weight formed by repeating units of acrylic acid, cross-linked with either allyl ether of sucrose or allyl ethers of pentaerythritol. In an aqueous solution at neutral pH, it acts is an anionic polymer, i.e. they aquire a negative charge by losing protons from their side chains. This makes the carbomers polyelectrolytes with the ability to absorb and retain water and swell to many times their original volume. They are extremely efficient rheology modifier capable of providing high viscosity and form sparkling clear water or hydroalcoholic gels and creams. Carbopol offers the advantage of exhibiting excellent

mucoadhesive properties when compared with other polymers (e.g. cellulose derivatives and polyvinyl alcohol) [95].

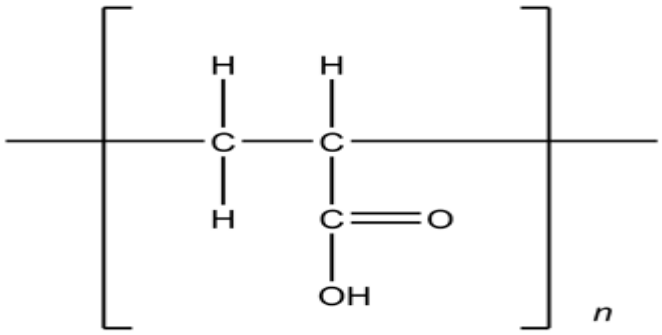

FIGURE 2.8: Acrylic acid monomer unit in carbomer polymers

The detailed profile about carbopol 934P is given in Table 2.8.

TABLE 2.8: Description about Carbopol 934

Product Name	Carbomer
Trade name	Carbopol 934
Description	A high molecular weight polymer of acrylic acid cross-linked with allyl ethers of sucrose.
Appearance	white coloured, fluffy, hygroscopic powder
Synonyms	Acritamer, acrylic acid polymer, Carbopol, carboxy polymethylene, polyacrylic acid, PAA carboxyvinyl polymer, Pemulen, Ultrez.
Melting point	260°C
Density	1.76–2.08 g/cm^3
Viscocity	30,500-39,400cp (0.5% aqueous dispersion at neutral pH)
Solubility	Soluble in water, in ethanol (95%) and glycerin
Functional Category	Bioadhesive, emulsifying agent, release-modifying agent, suspending agent, tablet binder, viscosity-increasing agent.
Stability and Storage	Carbomers are stable, hygroscopic materials that may be

condition:	heated at temperatures below 104°C for up to 2 hours without affecting their thickening efficiency. Exposure to excessive temperatures may result in discoloration and reduced stability. Carbomer powder should be stored in an airtight, corrosion-resistant container in a cool, dry place. The use of glass, plastic, or resin-lined containers is recommended for the storage of formulations containing carbomer.
Incompatibility:	Carbomers are discolored by resorcinol and are incompatible with phenol, cationic polymers, strong acids, and high levels of electrolytes. Certain antimicrobial adjuvants should also be avoided or used at low level.
Safety	No evidence of hypersensitivity reactions in humans has been reported when used topically.
Pharmaceutical Applications	Mainly used in liquid or semisolid pharmaceutical formulations as suspending, viscosity-enhancing agents or emulsifying agents. Formulations include creams, gels, and ointments for use in topical ophthalmic, rectal preparations. Also used as dry or wet binders and as a rate controlling excipient. Carbomer resins have also been investigated in the preparation of sustained release matrix beads. Carbomers are also used in cosmetics. **Use Concentration (%):** ▪ Emulsifying agent 0.1–0.5 ▪ Gelling agent 0.5–2.0 ▪ Suspending agent 0.5–1.0 ▪ Tablet binder 5.0–10.0

Regulatory Acceptance	Included in the FDA Inactive Ingredients Guide (oral suspensions, tablets; ophthalmic, rectal, and topical preparations transdermal preparations, vaginal suppositories).

2.11 References

1. Michael J Pelczar, ECS Chan NRK. *Microbiology*., (1993). 5th ed. Tata Mc Graw Hill Publishing company Ltd.,New Delhi.
2. H.P. Rang, M.M.Dale, J.M. Ritter PKM. Pharmacology. In: *Pharmacology*. 5th ed. Churchill Livingstone; 2003:654-665.
3. Gelderblom HR. (1996). Structure and Classification of Viruses. In: Baron S, Medical Microbiology. 4th ed. Galveston (TX): University of Texas Medical Branch at Galveston.
4. Hynes M. Baltimore Classification of Viruses. *Mol Biol Webb*. 2015:1.
5. Retroviruses. [Online]. Available:http://retrovirology.biomedcentral.com/ [Accessed 12 November, 2015]
6. Thakur DS, Behera CK, Patidar A, Kumar P, Kumar P, Lal C., (2010). Anti-HIV agents: A step towards future. *Int J Pharm Sci Rev Res*.;3(2):10-18.
7. Gupta U, Jain NK., (2010). Non-polymeric nano-carriers in HIV/AIDS drug delivery and targeting. *Adv Drug Deliv Rev*.;62(4-5):478-490.
8. Virus vs Retrovirus. [Online]. Available: http://www.differencebetween.com/difference-between-retrovirus-and-vs-virus/. [Accessed 25 June 2016]
9. Gupta U, Jain NK., (2010). Non-polymeric nano-carriers in HIV/AIDS drug delivery and targeting. *Adv Drug Deliv Rev*.;62(4-5):478-490.
10. Fisher, Bruce; Harvey, Richard P.; Champe PC. (2007). In: *Lippincott's Illustrated Reviews: Microbiology (Lippincott's Illustrated Reviews Series)*:3.
11. Chan DC, Fass D, Berger JM, Kim PS. , (1997) Core structure of gp41 from the HIV

envelope glycoprotein. *Cell*.;89(2):263-273.

12. Foxall RB, Soares RS, Albuquerque AS, Cortesao CS, Victorino RMM, Sousa AE., (2008). Increased frequency of CD25dimCD4+ T-cells in HIV-2 infection, a naturally occurring attenuated form of HIV-1. *Clin Immunol*.;127(2):158-167.
13. List of Viral Diseases. [Online]. Available: http://doctors-hospitals-medical-cape-town-south-africa.blaauwberg.net/details.php?id=768. [Accessed 25 June 2016]
14. Top 10 Deadliest Diseases in the world. [Online]. Available: https://www.microhealthllc.com/top-10-deadliest-diseases-in-the-world/ [Accessed 25 June 2016]
15. Overview of viral infections. [Online]. Available: http://www.merckmanuals.com/home/infections/viral-infections/overview-of-viral-infections. [Accessed 25 June 2016]
16. Alexander Krämer, Mirjam Kretzschmar KK., (2010). *Modern Infectious Disease Epidemiology Concepts, Methods, Mathematical Models, and Public Health*. New York: Springer.
17. William N. Rom SBM., (2007). *Environmental and Occupational Medicine*. 4th ed. Lippincott Williams & Wilkins.
18. Global HIV/AIDS Overview. https://www.aids.gov/federal-resources/around-the-world/global-aids-overview/. Accessed November 12, 2015.
19. WHO | HIV/AIDS. [Online]. Available: http://www.who.int/gho/hiv/en/. [Accessed November 12, 2015]
20. Lembo D, Cavalli R., (2010). Nanoparticulate delivery systems for antiviral drugs. *Antivir Chem Chemother*.;21(2):53-70.
21. FDA. FDA approved -HIV-Medicines. 2016. [Online]. Available: https://aidsinfo.nih.gov/education-materials/fact-sheets/21/58/fda-approved-hiv-medicines.[Accessed November 11, 2016].
22. Nelson AG, Zhang X, Ganapathi U, et al., (2015). Drug delivery strategies and systems for HIV/AIDS pre-exposure prophylaxis and treatment. *J Control*

Release.;219(2015):669-680.

23. Hasegawa T, Kawaguchi T., (2002). Delivery of Anti-Viral Nucleoside Analogues to the Central Nervous System. *Curr Med Chem -Anti-Infective Agents*;1(1):55-63. 23.
24. Mallipeddi R, Rohan LC., (2010). Progress in antiretroviral drug delivery using nanotechnology. *Int J Nanomedicine*.;5(1):533-547.
25. Lun H, Chattopadhyay N, Yu X, Bendayan R., (2010). Nanotechnology applications for improved delivery of antiretroviral drugs to the brain. *Adv Drug Deliv Rev*. ;62(4-5):503-517.
26. Rao KS, Ghorpade A, Labhasetwar V.,(2009). Targeting anti-HIV drugs to the CNS. *Expert Opin Drug Deliv*.;6(8):771-784.
27. Cundy KC, Lynch G, Lee WA. Antiviral Research. 1997;35(2):113-122. doi:10.1016/j.antiviral.2009.11.004.
28. Dale Purves, George J Augustine, David Fitzpatrick, Lawrence C Katz, Anthony-Samuel LaMantia, James O McNamara and SMW, (2001). *Neuroscience*. 2nd ed. Sunderland (MA): Sinauer Associates.
29. Gizurarson S (2012). Anatomical and histological factors affecting intranasal drug and vaccine delivery. *Curr Drug Deliv*. 2012;9(6):566-582.
30. Pelvig DP, Pakkenberg H, Stark AK, Pakkenberg B. (2008). Neocortical glial cell numbers in human brains. *Neurobiol Aging*.;29(11):1754-1762.
31. Ginhoux F, Lim S, Hoeffel G, Low D, Huber T. (2013). Origin and differentiation of microglia. *Front Cell Neurosci*.;7(April):45.
32. Filiano AJ, Gadani SP, Kipnis J., (2014). Interactions of innate and adaptive immunity in brain development and function. *Brain Res*. 2015;1617:18-27.
33. GW K. The First Line of Defense in Brain Pathologies. (1995). *Drug Res (Stuttg)* ;45(1):357–360.
34. Krol S., (2012). Challenges in drug delivery to the brain: Nature is against us. *J Control Release*. 2012;164(2):145-155.
35. Gaillard PJ, Visser CC, Appeldoorn CCM, Rip J., (2012). Enhanced brain drug delivery: Safely crossing the blood-brain barrier. *Drug Discov Today Technol*.;9(2):e155-e160.

36. Wong HL, Wu XY, Bendayan R. (2012). Nanotechnological advances for the delivery of CNS therapeutics. *Adv Drug Deliv Rev*.;64(7):686-700.

37. Chen Y, Liu L., (2012). Modern methods for delivery of drugs across the blood-brain barrier. *Adv Drug Deliv Rev*.;64(7):640-665.

38. Rausch DM, Stover ES., (2011). Neuroscience research in AIDS. *Prog Neuro-Psychopharmacology Biol Psychiatry*. 2001;25(1):231-257.

39. Park K. (2008). Trojan monocytes for improved drug delivery to the brain. *J Control Release*. ;132(2):75.

40. Varatharajan L, A TS., (2009). The transport of anti-HIV drugs across blood–CNS interfaces: Summary of current knowledge and recommendations for further research. *Antiviral Res*.;82(2):A99-A109.

41. Sozio P, Cerasa LS, Laserra S, et al., (2013). Memantine-sulfur containing antioxidant conjugates as potential prodrugs to improve the treatment of Alzheimer's disease. *Eur J Pharm Sci*.;49(2):187-198.

42. Perioli L, Ambrogi V, Bernardini C, et al., (2004). Potential prodrugs of non-steroidal anti-inflammatory agents for targeted drug delivery to the CNS. *Eur J Med Chem*. ;39(8):715-727.

43. Ikeda M, Bhattacharjee AK, Kondoh T, Nagashima T, Tamaki N (2002),. Synergistic effect of cold mannitol and Na(+)/Ca(2+) exchange blocker on blood-brain barrier opening. *Biochem Biophys Res Commun*.;291(3):669-674.

44. Qin LJ, Gu YT, Zhang H, Xue YX. (2009). Bradykinin-induced blood-tumor barrier opening is mediated by tumor necrosis factor-α. *Neurosci Lett*. 2009;450(2):172-175.

45. Hynynen K (2007). Focused ultrasound for blood – brain disruption and delivery of therapeutic molecules into the brain.:27-35.

46. Vykhodtseva N, McDannold N, Hynynen K., (2008). Progress and problems in the application of focused ultrasound for blood-brain barrier disruption. *Ultrasonics*;48(4):279-296.

47. Liu L, Guo K, Lu J, et al., (2008). Biologically active core/shell nanoparticles self-assembled from cholesterol-terminated PEG-TAT for drug delivery across the blood-brain barrier. *Biomaterials*;29(10):1509-1517.

48. Pang Z, Lu W, Gao H, et al., (2008). Preparation and brain delivery property of biodegradable polymersomes conjugated with OX26. *J Control Release*. 2008;128(2):120-127.

49. Rohit B, Pal KI., (2013). A Method to Prepare Solid Lipid Nanoparticles with Improved Entrapment Efficiency of Hydrophilic Drugs. *Curr Nanosci*.;9(2):211-220.

50. Delivery AD., (2009). Nanotechnology for Antiretroviral Drug Delivery. *J Am Chem Soc*.:21-23.

51. Bhanushali RS, Gatne MM, Gaikwad R V, Bajaj AN, Morde MA., (2015). Nanoemulsion based Intranasal Delivery of Antimigraine Drugs for Nose to Brain Targeting;71(6):707-709.

52. Mishra V, Kesharwani P., (2016). Dendrimer technologies for brain tumor. *Drug Discov Today*.;21(5):766-778.

53. Ingallina C, Rinaldi F, Bogni A, et al., (2016). Niosomal approach to brain delivery: Development, characterization and in vitro toxicological studies. *Int J Pharm*. ;511(2):969-982.

54. Kozlovskaya L, Stepensky D., (2013). Quantitative analysis of the brain-targeted delivery of drugs and model compounds using nano-delivery systems. *J Control Release*;171(1):17-23.

55. Van der Meel R, Vehmeijer LJC, Kok RJ, Storm G, van Gaal EVB., (2013). Ligand-targeted particulate nanomedicines undergoing clinical evaluation: Current status. *Adv Drug Deliv Rev*.;65(10):1284-1298.

56. Serralheiro A, Alves G, Fortuna A, Falcao A. (2015). Direct nose-to-brain delivery of lamotrigine following intranasal administration to mice. *Int J Pharm*. ;490(1-2):39-46.

57. Woensel M Van, Wauthoz N, Rosière R, et al., (2013). Formulations for Intranasal Delivery of Pharmacological Agents to Combat Brain Disease: A New Opportunity to Tackle GBM:1020-1048.

58. Kumar M, Misra A, Babbar AK, Mishra AK, Mishra P, Pathak K., (2008) Intranasal nanoemulsion based brain targeting drug delivery system of risperidone. *Int J Pharm*.;358(1-2):285-291.

59. Patel S, Chavhan S, Soni H, , Babbar AK, Mathur R MA and SK., (2011). Brain targeting of risperidone-loaded solid lipid nanoparticles by intranasal route. *J Drug Target*.;19(6):468–474.

60. Seju U, Kumar A, Sawant KK., (2011). Development and evaluation of olanzapine-loaded PLGA nanoparticles for nose-to-brain delivery: In vitro and in vivo studies. *Acta Biomater*.;7(12):4169-4176.

61. Kaur IP, Bhandari R, Bhandari S, Kakkar V., (2008). Potential of solid lipid nanoparticles in brain targeting. *J Control Release*.;127(2):97-109.

62. Attama A , Momoh MA, Builders PF. Lipid Nanoparticulate Drug Delivery Systems: A Revolution in Dosage Form Design and Development (2012). *Recent Adv Nov Drug Carr Syst*. 2012:107-140.

63. Mehnert W, Mäder K., (2012). Solid lipid nanoparticles. *Adv Drug Deliv Rev*. 2012;64:83-101.

64. Blasi P, Giovagnoli S, Schoubben A, et al., (2011). Lipid nanoparticles for brain targeting I. Formulation optimization. *Int J Pharm*.;419(1-2):287-295.

65. Yasir M, Sara UVS., (2014). Solid lipid nanoparticles for nose to brain delivery of haloperidol: in vitro drug release and pharmacokinetics evaluation. Acta Pharmaceutica Sinica B;4(6):454-463.63.

66. Sharma N, Mishra N., (2014). Importance of Lipid Nanoparticles in the Treatment of Epilepsy: a Focus on Nasal Delivery. *J Pharm Sci Innov*.;3(3):199-207.

67. Mistry A, Stolnik S, Illum L., (2009). Nanoparticles for direct nose-to-brain delivery of drugs;379:146-157.

68. Edition S. Ophthalmic Drug Delivery Systems. *Clin Res*. 966:80-87.

69. Abbas Z., (2012). Mucoadhesive in situ gels as nasal drug delivery systems : an overview. ;7(3):168-180.

70. Ravi PR, Aditya N, Patil S, Cherian L., (2013). Nasal in-situ gels for delivery of rasagiline mesylate: improvement in bioavailability and brain localization. *Drug Deliv*. ;7544:1-8.

71. Qiu Y, Park K., (2001). Environment-sensitive hydrogels for drug delivery. ;53:321-339.

72. Dumortier G, Grossiord JL, Agnely F, Chaumeil , (2006). Expert Review A Review of Poloxamer 407 Pharmaceutical and Pharmacological Characteristics.;23(12):11095.

73. Arbelaez-Camargo D, Suñé-Negre JM, Roig-Carreras M, et al., (2016). Preformulation and characterization of a lidocaine hydrochloride and dexamethasone sodium phosphate thermo-reversible and bioadhesive long-acting gel for intraperitoneal administration. *Int J Pharm*.;498(1-2):142-152.

74. Morsi N, Ghorab D, Refai H, Teba H., (2016). Ketoroloac tromethamine loaded nanodispersion incorporated into thermosensitive in situ gel for prolonged ocular delivery. *Int J Pharm*.;506(1-2):57-67.

75. Burkoth AK, Anseth KS. A review of photocrosslinked polyanhydrides: in situ forming degradable networks. *Biomaterials*. 2000;21(23):2395-2404.

76. Lochhead JJ, Thorne RG., (2012). Intranasal delivery of biologics to the central nervous system. *Adv Drug Deliv Rev*.;64(7):614-628.

77. Eskandari S, Varshosaz J, Minaiyan M, Tabbakhian M., (2011). Brain delivery of valproic acid via intranasal administration of nanostructured lipid carriers: in vivo pharmacodynamic studies using rat electroshock model. *Int J Nanomedicine*. ;6:363-371.

78. Lochhead JJ, Thorne RG., (2012). Intranasal delivery of biologics to the central nervous system. *Adv Drug Deliv Rev*.;64(7):614-628.

79. Sood S, Jain K, Gowthamarajan K., (2014). Optimization of curcumin nanoemulsion for intranasal delivery using design of experiment and its toxicity assessment. *Colloids Surfaces B Biointerfaces*;113:330-337.

80. Patel T, Zhou J, Piepmeier JM, Saltzman WM (2012). Polymeric nanoparticles for drug delivery to the central nervous system. *Adv Drug Deliv Rev*. 2012;64(7):701-705.

81. Johnson NJ, Hanson LR, Iliff JJ, Ph D, Androulakis IP., (2011). Trigeminal pathways deliver a low molecular weight drug from the nose to the brain and orofacilal structures;7(3):228-237.

82. Jogani V V, Shah PJ, Mishra P, Mishra AK, Misra AR., (2007). Nose-to-brain delivery of tacrine:1199-1205.

83. G.J. T. (1998) *Principles of Human Anatomy*. 8th ed. Mento Park: Benjamin/cummings

Science Publishing.

84. Adams G.L. , Boies L.R. HPA.(1989). *Fundamentals of Otolaryngology, A Textbook of Ear, Nose and Throat Diseases*. Philadelphia.
85. Sharma S, Lohan S, Murthy RSR., (2012). Potential of Chitosan for nose to brain drug delivery, *Int. J. Pharm. Sci. Rev. Res.*;16(1):47-55.
86. Kumar TP, Sirisha B, Raju PN, Reddy GN., (2013). Nasal Drug Delivery : A Potential Route for Brain Targetting. *pharma Innov*. 2013;2(1):77-85.
87. Djupesland PG, Mahmoud RA, Messina JC. (2013). Accessing the brain: the nose may know the way. *J Cereb Blood Flow Metab*.;33(5):793-794.
88. Ding J, Na L, Mao S., (2012). Chitosan and its derivatives as the carrier for intranasal drug delivery;7(October):349-361.
89. Singh AK SA and MN (2012). Nasal cavity: A promising platform for drug delivery and research approaches from nasal to brain targeting. *J drug del ther*.;2(3):22-33.
90. Zaki NM, Awad GAS, Mortada ND, Abd ElHady SS.(2006) Rapid-onset intranasal delivery of metoclopramide hydrochloride. Part I. Influence of formulation variables on drug absorption in anesthetized rats. *Int J Pharm*. 2006;327(1-2):89-96.
91. DrugBank: Efavirenz. [Online]. Available: http://www.drugbank.ca/drugs/DB00625. [Accessed November 12, 2015].
92. HIV Drug Interactions., (2011). Efavirenz PK Factsheet. [Online]. Available: http://www.hiv-druginteractions.org/.[Accessed November 12, 2015].
93. Marzolini C, Telenti A, Decosterd L a, Greub G, Biollaz J, Buclin T., (2001). Efavirenz plasma levels can predict treatment failure and central nervous system side effects in HIV-1-infected patients. *Aids*.:71-75.
94. Blasi P, Giovagnoli S, Schoubben A, Ricci M, Rossi C., (2007). Solid Lipid Nanoparticles For Targeted Brain Drug Delivery. *Adv Drug Deliv Rev*.;59(6):454-477.
95. McGinity JW, Harris MR, Patel K et. al., (1986). *Handbook of Pharmaceutical Excipients*. American Pharmaceutical Association. Washington-DC, USA; 1986.

CHAPTER 3
Materials & Methods

3.1 Materials and Equipments

Different materials and equipments used for the experimental investigations of the present wok along with their sources have been listed in Table 3.1 and 3.2 respectively.

TABLE 3.1 List of Materials used

Category	Name of Materials	Source / Supplier
Drugs	Efavirenz (EFV)	Sun Pharma Ltd. Sikkim, India
	Tenofovir Disoproxil Fumarate	Paradise Healthcare, Vadodara, India
Lipids	Glycerymonostearate	Ozone intermediate, Mumbai, India
	Compritol 888 ATO (Glyceryl behenate)	Gattefosse India Pvt. Ltd, Mumbai
	Tripalmitin (Glyceryl tripalmitate)	Sigma Aldrich
	Glyceryl palmitostearate	Chemdyes Corp., Rajkot
	Glyceryl distearate	Atur Enterprise
	Cetyl palmitate	National chemical, Vadodara
Surfactants	Poloxamer 188 (Pluronic F68)	Sigma Aldrich
	Poloxamer 407 (Pluronic F127)	Sigma Aldrich
	Poloxamer 245 (Pluronic P 85)	Chemdyes Corporation, Rajkot
	Polysorbate 20 (Tween 20)	S.D.Fine Chemicals. Ltd, Mumbai
	Polysorbate 60 (Tween 60)	S.D.Fine Chemicals. Ltd, Mumbai
	Polysorbate 80 (Tween 80)	Chemdyes Corporation, Rajkot
Gelling agents	Chitosan	Chemdyes Corporation, Rajkot
	Carbopol 934P	S.D.Fine Chemicals. Ltd, Mumbai

Thermo-sensitive polymers	Poloxamer 188 (Pluronic F68)	Sigma Aldrich
	Poloxamer 407 (Pluronic F127)	Sigma Aldrich
Solvents	Methanol	S.D. Fine Chemicals Ltd., Mumbai
	Acetonitrile	S.D. Fine Chemicals Ltd., Mumbai
	Isopropyl Alcohol	S.D. Fine Chemicals Ltd., Mumbai
Other chemical Reagents	Potassium bromide	Merck Millipore
	Disodium hydrogen phosphate	Allied Chemical Corporation, Baroda
	Potassium dihydrogen phosphate	Allied Chemical Corporation, Baroda
	Sodium Chloride	Fischer scientific , Mumbai
	Sodium hydroxide	Fischer scientific , Mumbai
	Orthophosphoric acid	Fischer scientific , Mumbai
Dialysis Membrane	110 (LA 395)	Himedia
Nasal mucosa	Freshly excised goat	Slaughter house
Blood/ plasma	-	PASM Hospital, Vadodara, Gujarat

TABLE 3.2 List of Instruments used

Instruments	Model	Manufacturer
Digital weighing balance	CWS103C RB-1201	Scaletec Mechatronics Pvt. Ltd., Vadodara Raptec (Reputed Micro systems, Ahmedabad)
Melting Point Apparatus	VMP-D	Veego Inst. corp., Mumbai
FTIR Spectrophotometer	Alpha -1	Bruker Optics, Germany
UV-spectrophotometer	UV-1800	Shimadzu corporation, Japan
HPLC	2695	Waters (Allience)
Freeze Centrifuge	BL-35 R	BioLab, Israel
Vortex mixer	Spinix	Spinix Corporation, Danville CA, USA
Water bath	Digital Shaker	NOVA Inst. Pvt. Ltd., Ahmedabad
Particle size analyzer	Nanoseries Nano-ZS	Malvern instrument, UK
High Speed Homogenizer	Silent Crusher M	Heidolph, Germany
High Pressure Homogenizer	Panda Plus / GEA Niro Soavi	Inkarp Instruments Pvt. Ltd., Hyderabad, India
Magnetic Stirrer	DBK	Remi Equipments, Mumbai, India
Sonicator	CV334, Sonico Vibra Cell	Sonics Incorporation, USA
Bath Sonicator	Fast Clean ultrasonic cleaner,	Skymen Cleaning Equipment Shwnzhen Co.Ltd./ Lelesil Innovative system
Hot Plate	-	Sunbim, Mumbai, India
pH meter	LI 615	Elico India, Hyderabad
Brookfield Viscometer	DV-I Prime	Brookfield Pvt. Ltd, USA
Franz diffusion cell	-	D. K. Scientific Laboratories, Ahemedabad
TEM	Tecnai 20	Philips, Holland
Inverted Microscope	(NIKION TS -100)	Nikon corporation, Japan
Stability chamber	Humidity controlled chamber	Thermolab Pvt. Ltd., India

3.2. Identification of Drug

Identification of the procured drug is one of the important preliminary tests to be performed for verification and ensuring the purity of the drug sample prior to formulation development. Identification test is also included as a compendial test to provide an aid in verifying the identity of articles as they are purpoted [1]. Identification of drug sample in the present investigations was based on its appearance, solubility, melting point and was confirmed by fourier-transform infrared (FT-IR) spectroscopic determination of various functional groups present in the powder drug sample.

3.2.1 Appearance: The procured drug sample was visually observed for its color and was compared with the reported appearance of the drug.

3.2.2 Solubility: Quantitative solubility tests are performed as a test for purity [1]. Solubility of drug was determined in water and methanol. 10 mg sample was taken in a clean dry test tube and solvent was added gradually in aliquots of 0.1 ml with continuous shaking until it dissolved completely [2]. Amount of solvent required for solubilization of the drug powder was recorded and the solubility was compared with the reported values.

3.2.3 Melting point: Melting point is one of the identification test method for organic substances. Hence, it was determined for the sample by capillary method using melting point apparatus (VMP-D, Veego). Small amount of the sample was filled in a capillary tube (closed at one end) and placed in the melting point apparatus. The temperature at which the substance started to convert into liquid and the temperature at which the solid completely disappeared was recorded.

3.2.4 Infrared Absorption: Fourier Transform Infrared (FT-IR) is an important complementary tool for the solid-state characterization of pharmaceutical solids [3]. Identification of drug was done by infrared spectroscopy technique using Alpha Bruker FTIR spectrophotometer. The sample was prepared by disc method. The drug was triturated

with potassium bromide (about 5 mg sample with 100 mg dry potassium bromide) in a mortar-pestle to produce fine and uniform mixture. The pellets were prepared by compressing the powder at 20 psi for 10 min using potassium bromide press. Prepared sample disc was placed in the sample compartment. Sample was scanned at transmission mode in the region of 4000-400 cm^{-1}. The IR spectrum obtained was compared with standard spectrum of pure drug.

3.3 Analytical methods

Analytical methods for the estimation of drug content were needed at various stages of the investigations in the present work, such as at preformulation, optimization and evaluation stages. At preformulation and optimization stages, it was required to determine the entrapment efficiency of the formulation for selection of material and optimization of their concentrations. The analytical methods were needed for the *in-vitro* and *ex-vivo* drug release studies and evaluation of samples of stability testing. Analytical method was also required for estimation of drug in plasma and brain post-administration of the formulations. Hence, suitable analytical methods were required to be selected or developed for the accurate, precise and convenient analysis of the drug.

3.3.1 UV- Spectrophotometric estimation of Efavirenz

UV spectrophotometric methods have been reported for the estimation of efavirenz in formulations [4, 5]. Calibration curves were plotted in methanol:water (50% v/v) and in methanolic phosphate-buffered saline (PBS) (pH 6.4, 40%v/v) as solvents using UV-1800 spectrophotometer (Shimadzu) at 247 nm.

3.3.1.1 Calibration curve in methanol:water (50 %v/v) as solvent :

The calibration curve of the drug in methanol:water (50 %v/v) as solvent was useful to determine the entrapment efficiency and for analysing the stability samples.

Preparation of stock solutions: 100 mg accurately weighed quantity of EFV was transferred to 100 ml volumetric flask. It was dissolved and the volume was made up to the mark with methanol:water (50 %v/v) to get the final concentration of the stock-1 solution as 1000 µg/ml of drug. 1 ml of the stock-1 solution was further diluted to 10 ml with the same solvent to obtain stock-2 solution (100µg/ml).

Preparation of samples for the calibration plot: Appropriate aliquots of the stock-2 solution of EFV (0.3, 0.6, 0.9, 1.2, 1.5, 1.8 ml) were accurately pipetted out into 10ml volumetric flasks and were made up to the mark with the solvent to get the final concentration of the drug in the range 3 – 18 µg/ml. The drug-free solvent was used as blank. Scanning was performed in the range 200-400 nm to determine the λ_{max}. The absorbance of all the prepared solutions was obtained at λ_{max}. The procedure was repeated in triplicate and the observations were recorded. Mean value of the absorbance (n=3) were plotted graphically against concentration to obtain the calibration curve.

3.3.1.2 Calibration curve in methanolic phosphate-buffered saline (pH 6.4, 40%v/v):

The calibration curve was also plotted in methanolic phosphate-buffered saline (pH 6.4, 40%v/v) and regression equation was determined for the release studies of drug from the formulations. The pH was selected based on the nasal mucosal pH (5.5-6.5) and methanol being added to maintain the sink condition [6, 7].

Preparation of Phosphate-buffered saline pH 6.4 [8]: 1.79 g of disodium hydrogen phosphate, 1.36 g of potassium dihydrogen phosphate and 7.02 g of sodium chloride was dissolved in sufficient water to produce 1000 ml.

Preparation of stock solutions: 100 mg accurately weighed quantity of EFV was transferred to 100 ml volumetric flask. It was dissolved and the volume was made up to the mark with methanolic PBS (pH 6.4, 40%v/v) to get the final concentration of the stock-1 solution as 1000 µg/ml of EFV. 1 ml of the stock-1 solution was further diluted to 10 ml with the same solvent system to obtain stock-2 solution (100µg/ml).

Preparation of samples for the calibration plot: Appropriate aliquots of the stock-2 solution of EFV (0.3, 0.6, 0.9, 1.2, 1.5, 1.8 ml) were accurately pipetted out into 10ml volumetric flasks and were made up to the mark with the solvent to get the final concentration of the drug in the range 3 – 18 µg/ml. The drug-free methanolic PBS (pH 6.4, 40%v/v) was used as blank. Scanning was performed in the range 200-400 nm to determine the λ_{max}. The absorbance of all the prepared solutions was obtained at λ_{max}. The procedure was repeated in triplicate and the observations were recorded. Mean value of the absorbance (n=3) were plotted graphically against concentration to obtain the calibration curve.

3.3.2 High Performance Liquid Chromatographic Method (HPLC method) Development & Validation

High performance liquid chromatographic method was developed and validated using HPLC with UV Detector - Waters (Allience) for the estimation of EFV in plasma and brain samples for the pharmacokinetic / biodistribution studies. Tenofovir disoproxil fumarate (TDF) was used as the internal standard.

Preparation of standard solution : Stock solution of EFV (0.5 mg/ml) and TDF (1 mg/ml) were prepared by dissolving 50 mg EFV and 100 mg of TDF respectively in 100 ml diluent (Methanol:Water, 50 %v/v). Further dilution of 5 ml of stock solution to 100 ml with diluent was done to produce 25 ppm EFV solution and 50 ppm TDF solution for trial batches. The working standards of EFV in concentrations ranging from 1–300 µg/ml were prepared by spiking appropriate amount of the standard solution in drug-free plasma.

Sample Preparation in plasma: The normal pooled plasma sample from 20 people was obtained from Parul Arogya Seva Mandal (PASM) hospital. The plasma sample of 250µl was transferred to tubes in which 100µL of TDF (internal standard) and 50µL of Efavirenz were added, followed by 1 ml of ethyl acetate. The samples were vortexed for 1 min. The samples were then centrifuged using freeze centrifuge (BL – 135 R) at 10000 RPM (4^0C) and organic phase was evaporated via nitrogen purging. The solid residue was reconstituted with 100µL of mobile phase and was injected into the HPLC column [9-11].

3.3.2.1 Analytical Method development

Standard solution of EFV (25 ppm) and TDF (50 ppm) were scanned in the range of 200-400 nm for determination of detection wavelength in HPLC. Various trials were taken by varying the column, mobile phase, pH of mobile phase, flow rate, etc. at λ_{max} to optimize the analytical method to give good peaks with suitable retention time [12, 13].

3.3.2.2 Analytical method validation

The developed analytical method was validated for various parameters like linearity, precision, accuracy, specificity, robustness as per ICH guidelines and data obtained were statistically analyzed [14, 15].

A. Linearity and Range

The linearity was established in the range of 1 to 300 µg/ml concentrations (1, 5, 10, 20, 25, 50, 100, 200, 300 µg/ml) of EFV. The concentration of TDF (internal standard) was 50µg/ml. All the experiments were replicated thrice. The linear regression analysis of the area ratios (analyte/ internal standard) vs. concentration curve was determined. The linearity was verified using estimates of correlation coefficient.

B. Precision

The precision (repeatability) of the analytical method was determined by assaying six samples at 100% test concentration and estimating standard deviation (SD) and % relative standard deviation (RSD). The intra-day and inter-day precisions were also determined by analyzing three samples at three different times of the same day and on three consecutive days respectively and determining SD & % RSD and analyzing the data statistically using ANOVA.

C. Accuracy

Accuracy was assessed at three concentration levels. Six replicates were analyzed at 100%

concentration level and three replicates each at 50% and 150% concentrations. Assessment of accuracy was accomplished by evaluating the percent recovery of the analyte.

D. Limit of Detection (LOD) and Limit of Quantification (LOQ)

LOD : Signals for known low concentration (six replicates of 0.01 µg/ml) of analyte was compared with blank sample. Signal to noise ratio was found and compared with acceptable value (2:1) [14].

LOQ: Determination of the signal to noise ratio was performed by comparing measured signals from samples with known low concentrations (six replicates of 0.05 µg/ml) of analyte with those of blank samples and was compared with typically accepted signal-to –noise ratio of 10:1[14].

E. Specificity

Specificity is the ability to assess unequivocally the analyte in the presence of components which may be expected to be present. The specificity was assessed by analyzing the analyte in the presence of placebo. The results were based on three replicate analyses.

F. Robustness

The robustness of the analytical procedure was measured from its capacity to remain unaffected by small, but deliberate variations in method parameters - flow rate ($\pm$ 0.2), wavelength ($\pm$ 2), pH of mobile phase ($\pm$ 0.2) which provided an indication of its reliability during normal usage.

G. Stability of analytical solution:

Stability of the analytical solution was tested at 2, 4, 6, 12, 18, 24 hours and after 10 days in plasma and compared with chromatograms of freshly prepared sample. Experiments were replicated three times.

H. System suitability test

For system suitability six replicates of drug samples were run at 25 µg/ ml and 50µg/ml concentration of EFV and TDF respectively. Repeatability with respect to peak height and peak area in six replicates, peaks symmetry (tailing factor), resolution between the peaks of drugs, theoretical plates of the column (column efficiency) and retention time were determined.

I. Statistical analysis :

The data obtained were statistically evaluated with the help of Microsoft Excel. Linearity was assessed by determination of standard deviation, correlation coefficient and linear regression equation. While accuracy of the developed analytical method was assessed by % recovery method, standard deviation (SD) and relative standard deviation (% RSD) were determined for confirming the precision, robustness, etc. Intraday and interday precision was statistically analyzed using ANOVA from Analysis Toolpak of Microsoft Excel. Signal-to-noise ratios were determined for LOD and LOQ.

3.4 Design of experiment

Product should be designed to meet patients' needs and the intended product performance. Pharmaceutical development should include defining of quality target product profile (QTPP), identifying and determining potential critical quality attributes (CQAs), selecting an appropriate manufacturing process, defining a control strategy, identifying, through e.g., prior knowledge, experimentation, and risk assessment, the material attributes and process parameters that can have an effect on product CQAs. The systematic approach could facilitate product development and continual improvement and innovation throughout the product lifecycle [16-18]. In the present work, various preformulation investigations were performed like identification of drug, selection of different materials, compatibility studies, etc. followed by formulation and optimization of various parameters by factorial design to achieve minimize particle size and maximum encapsulation efficiency of the drug in SLN

[19, 20]. As per the literature review, the entrapment efficiency is mainly influenced by the formulation ingredients, their concentrations and the technique used for its formulation, hence was considered as one of the response parameter for optimization of formulation variables [21-23]. The SLN were further incorporated in the *in-situ* gel system and investigated for various performance parameters.

3.5 Preformulation studies

The major components for the solid lipid nanoparticulate system include the drug, lipid and surfactant. After the identification of the drug, various materials were screened as components for the proposed system. These selections were based on the solubility of the drug and their ability to produce small sized particles. The selections were also based on the safety profile and approval status of the components.

3.5.1 Selection of Lipid

Different lipids were screened on the basis of solubility studies. The solubility of the drug was determined in different lipids. Amount of drug dissolved in known amount of each lipid at a temperature 5^0C above the melting point of the respective lipid was determined using digital shaker water bath (NOVA Inst Pvt. Ltd., Ahmedabad, India) and the lipid showing maximum solubility for the drug was proposed to have maximum drug loading capacity and was selected for further investigations [24-26].

3.5.2 Selection of Surfactant

With the selected lipid, nanoparticles were prepared using different surfactants and were evaluated with respect to the particle size, PDI and entrapment efficiency. The particle size and PDI was determined using Malvern Zetasizer Nanoseries Nano-ZS, UK. Selection of the surfactant was made based on minimum particle size and PDI with maximum entrapment efficiency [27].

3.5.3 Drug-Excipient Compatibility Study

IR spectra of pure drug, and the physical mixtures of drug and selected excipients stored at 25 ± 2 ^{O}C, 60% ± 5% relative humidity for a period of 7 days were recorded using FT-IR spectrophotometer (Bruker Alpha-one, Bruker Optik, Germany) in the range of 4000–400 cm^{-1} and compared for any significant change [28, 29].

3.6 Selection of formulation Technique

Various techniques for SLN formulation are high shear homogenization and ultrasound, high pressure homogenization, solvent emulsification and evaporation technique, microemulsion based SLN preparation technique, etc [26, 30-34]. The selection of the technique was made based on the evaluation of particle size, PDI and entrapment efficiency of the nanoparticles obtained with the trial batches using the commonly used and reported to be reliable and powerful techniques.

3.6.1 High Pressure Homogenization

There are two general homogenization techniques (hot homogenization and cold homogenization) which can be used for the production of SLN [30]. In the present study, hot homogenization technique was investigated. The drug was incorporated into the melted lipid. The drug loaded lipidic phase was dispersed in a hot aqueous surfactant solution under continuous stirring to form a coarse o/w emulsion. It was then homogenized at the temperature above the melting point of the lipid using high pressure homogenizer (Panda Plus / GEA Niro Soavi, Parma, Italy) to form o/w nanoemulsion which was cooled to room temperature for solidification and formation of solid lipid nanoparticles [27, 34].

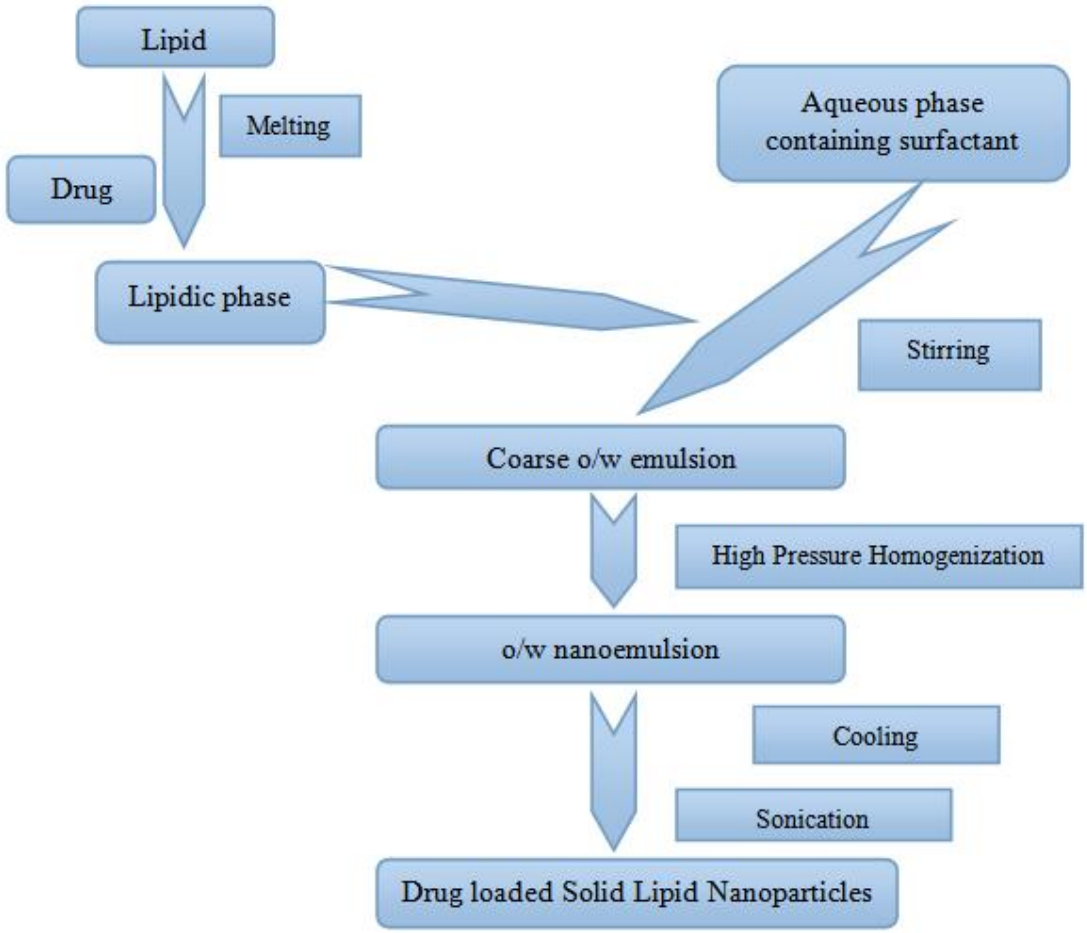

FIGURE 3.1: Formulation of solid lipid nanoparticles by high pressure homogenization

3.6.2 Solvent Evaporation method

The lipophilic drug was dissolved in a water-immiscible organic solvent and was emulsified in an aqueous phase containing the surfactant under continuous stirring on a magnetic stirrer. The organic solvent was evaporated and nanoparticulate dispersion was formed by precipitation of the lipid in the aqueous medium [19, 30, 31].

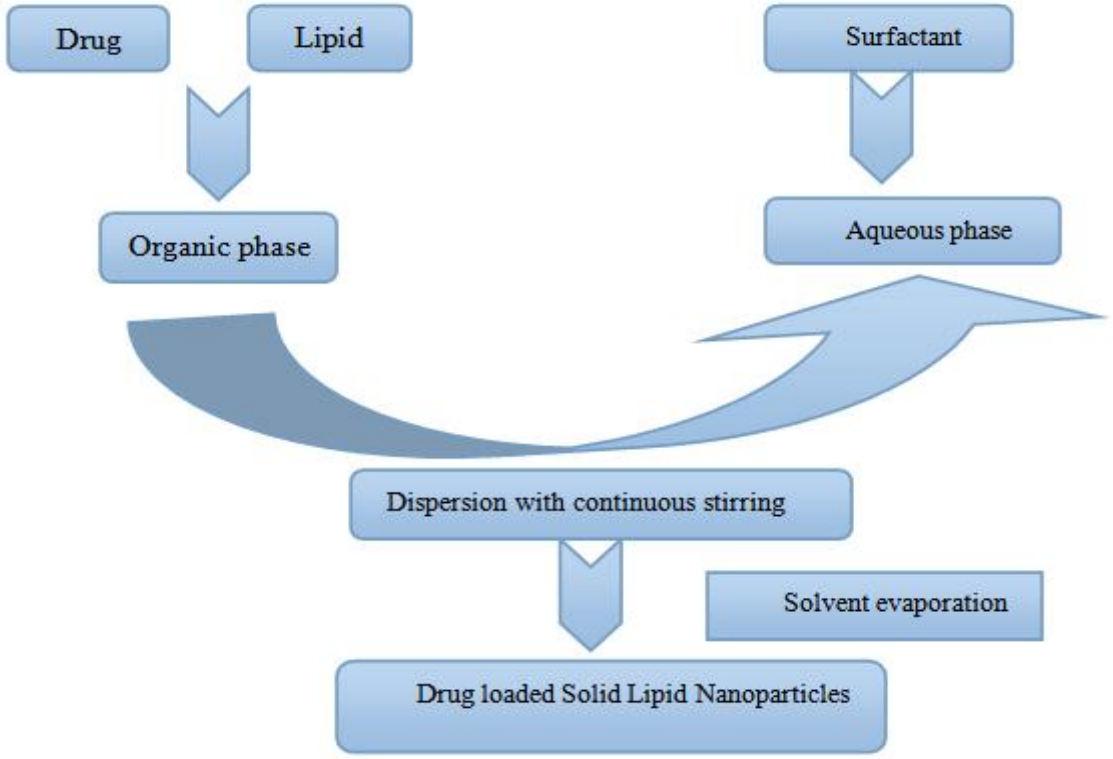

FIGURE 3.2: Formulation of solid lipid nanoparticles by solvent evaporation technique

3.7 Optimization of Process Variables

On the basis of literature survey and a few trial batches, various critical process variables which may have significant effect on the critical quality attributes were identified for each step involved in the formulation and were subjected to optimization. Preliminary optimization of stirring time, RPM and temperature were done by conducting the experiments at three levels of each process variables involved during stirring of the hot aqueous surfactant solution while addition of the drug incorporated lipidic phase for the formation of coarse emulsion. Critical process variables involved during the high pressure homogenization was optimized using 3^2 factorial design with Design Expert 9.0.3.1 software (Stat-Ease, Inc., USA). The pressure and number of cycles were selected as independent variables and the response on particle size and PDI were investigated. Sonication time and amplitude were optimized for the sonication of the nanoparticulate dispersion after homogenization [7, 20].

3.8 Optimization of Formulation Variables

3^2 factorial design was employed for optimization of formulation variables and Design Expert 9.0.3.1 software was used for statistical analysis by ANOVA, generating model equations and constructing contour plots and 3D surface plots for each response. Amount of drug with respect to lipid and concentration of surfactant were investigated as independent variables at three levels and the critical quality attributes selected were particle size, PDI and entrapment efficiency as responses [18, 35].

3.9 Formulation and Optimization of *In-situ* Gel

Chitosan and carbopol 934 P were screened as gelling and/or mucoadhesive agents based on literature review. Out of these two, one was selected based on their gelling properties with SLN dispersion [36]. Poloxamer 188 and poloxamer 407 were selected as thermosensitive polymers based on literature [37, 38]. The compatibility of the drug and all the excipients in the final formulation including the gelling, mucoadhesive and thermosensitive polymers were again evaluated using FTIR-spectroscopy. Ratio of poloxamer 188 and poloxamer 407 were optimized based on their gelling behaviour at different temperatures. The concentration of carbopol 934P was optimized based on gelling behaviour observed visually in the presence of selected thermo-sensitive polymers particularly at the nasal temperature (34^0C) [39, 40].

3.10 Evaluation of optimized formulation

3.10.1 Particle size, Polydispersity index (PDI) and Zeta potential

The average particle size, PDI and zeta potential of the solid lipid nanoparticles were determined using Zetasizer Nanoseries Nano-ZS, Malvern Instruments, Malvern, UK. In-built dynamic light scattering, DLS, and Laser Doppler Electrophoresis were used for the determinations of particle size and for zeta potential. The samples were put in 'folded capillary cells' and results obtained for size, PDI and zeta-potential were recorded.

3.10.2 Entrapment efficiency

Entrapment efficiency was determined by determining the amount of free drug spectrophotometrically at 247 nm in the supernatant after centrifugation of the known amount of nanoparticulate dispersion at 10000 RPM using freeze centrifuge (BL – 135 R) for 15 minutes. The entrapment efficiency was calculated using (4.1) [41, 42]

$$\text{Entrapment efficiency} = \frac{\text{Amount of entrapped drug}}{\text{Amount of total drug}} \times 100$$

$$= \frac{\text{Weight of drug added in the formulation} - \text{Weight of free drug}}{\text{Weight of drug added in the formulation}} \times 100$$

$$= [(W_T - W_F)/W_T] \times 100 \quad \textbf{Equation 3.1}$$

3.10.3 Evaluation of SLN based *in-situ* gel

The formulated SLN based gel was evaluated for gelation temperature, gelation time, pH, viscosity, transmittance, mucoadhesive strength and spreadability.

3.10.3.1 Gelation temperature / Sol–gel transition temperature ($T_{sol-gel}$): Sol-gel transitions play a critical role in establishing effectiveness of the formulations. 2 ml sample was taken in a glass vial and was placed on a magnetic stirrer (15 rpm) with heating arrangement. The temperature was gradually increased at the rate of 1^0C/min. The temperature at which the rotation of the magnetic bead was stopped was recorded as the gelation temperature [39].

3.10.3.2 Gelation time: The time required for gelation was also investigated for determining the lag time. 2 ml sample was taken in a glass vial and was placed on a magnetic stirrer (15 rpm) at the temperature of gelation and the time required for gelation was recorded [38, 43].

3.10.3.3 pH: pH of the nasal formulations are also important for avoiding the irritation to the nasal mucosa. Hence, the pH of the formulation was determined using pH meter (Li 615, Elico India, Hyderabad) and was compared with the reported pH in nasal cavity.

3.10.3.4 Viscosity: Viscosity is also one of the parameter to be evaluated for the *in-situ* gels. The viscosity of the formulations should be such that it remains convenient during their administration by the patient. Viscosity of the formulation was determined at 25^0C (ambient temperature) and 34^0C (nasal temperature) using brookfield viscometer (DV-I Prime).

3.10.3.5 Transmittance: The EFV nanoparticles loaded in-situ gel was diluted with distilled water (10 times dilution) and the resulting dispersion was observed visually for any turbidity. Thereafter, its % transmittance was measured at 650 nm using UV spectrophotometer (UV-1800, Shimadzu) against distilled water as the blank.

3.10.3.6 Mucoadhesive strength:

The mucoadhesive force was determined using modified two-pan balance method [37]. As per the literature review, in spite of numerous studies concerning the *in-vitro* and *in-vivo* performance of mucoadhesive drug delivery systems, surprisingly, there has not been any standard technique designed for mucoadhesive measurement or any analytical method that can be employed to qualify mucoadhesive strength. *In-vitro* tests including two-pan balance method are the most common and convenient methods to assess the mucoadhesive properties of formulations [43, 44]. In this method, one side of the balance was provided with blocks at the top for balancing and the other side had a receptacle for water as shown in Figure 3.3. 20 µl gel test sample was applied on the perfectly horizontal surface and was just touched with the cellophane membrane (1 cm^2) sticked at the horizontal end opposite to that of water receptacle. Gradually water was added drop by drop till the cellophane membrane got detatched from the gel. Weight in grams of water required to separate the two surfaces was measured and mucoadhesive force was calculated using (3.2)

$$F = w \times g \quad \text{……..……..Equation 3.2}$$

Where F is the mucoadhesion force (dynes / cm^2),

w is the minimum weight required to break the bond (grams),

g is the acceleration due to gravity (cm/s^2).

FIGURE 3.3: Apparatus used for determining the mucoadhesive strength of gel

3.10.3.7 Spreadability: Spreadability of the gel was determined by taking 0.5 g gel between two cellophane membranes and placing 100 g weight on it for 1 minute. The diameter of the area in which the gel got spread was measured.

3.10.4 Transmission Electron Microscopic Evaluation

The surface morphology of the optimized SLN was investigated using transmission electron microscope [7, 46]. Briefly, it was carried out by operating at an acceleration voltage of 200 kV. A drop of SLN dispersion was placed on grid. Approximately 2 min after sample deposition (1-2 µl), the grid was tapped with filter paper to remove surface water and air dried. The image was taken using transmission electron microscope with CCD camera (TEM Philips Tecnai 20, Holland).

3.10.5 Histopathological studies

Histological studies were carried out using isolated goat nasal mucosa. Freshly isolated goat nasal mucosa was sectioned in four pieces. One piece was treated with PBS pH 6.4 (as negative control), the other with a mucociliary toxicity agent - isopropyl alcohol (as positive control) and the other two with the SLN formulations (SLN dispersion and SLN gel) [6]. After 24 hours, all the samples were washed properly with distilled water, fixed, processed

for dehydration, embedded into paraffin wax and stained with hematoxylin and eosin. DPX was used as mounting medium and microtoming was performed using microtome (model 0126, yorco, India). The histopathological examinations for determination of damage/irritation due to the formulation were performed using inverted microscope (NIKION TS -100) [37, 47].

3.11 Drug Release Profile

3.11.1 *In-vitro* drug diffusion profile

In-vitro drug diffusion profile of the SLN dispersion and EFV loaded SLN gel were obtained by dialysis-bag/dialysis-sac method [7, 24, 48] as well as by using Franz-diffusion cell [18, 36, 48].

For dialysis bag method, SLN dispersion and plain drug suspension were filled in activated dialysis membrane bags (Dialysis membrane 110 (LA 395), Himedia, cut off 12000 Da) and suspended in glass beakers containing 50 ml methanolic phosphate buffer saline (pH 6.4, 40%v/v) [6, 7]. The beakers were placed on magnetic stirrers and stirred with magnetic beads and were covered with paraffin film to prevent any evaporative loss during the experimental run [46]. Aliquots were withdrawn from the receptor compartments at periodic time intervals for 24 hours, replaced with equivalent amounts of fresh diffusion medium. The aliquots were analyzed spectrophotometrically at 247 nm. All the experiments were performed in triplicate.

For *in-vitro* release studies using Franz diffusion cell, the activated dialysis membrane (Dialysis membrane 110 (LA 395), Himedia, cut off 12000 Da) were mounted on a Franz diffusion cells with methanolic phosphate buffer saline (pH 6.4, 40%v/v) filled in receptor compartments. The cells were placed on magnetic stirrers and EFV formulations (0.5 ml) were placed in the donor compartments. Aliquots were withdrawn from the receptor compartments at periodic time intervals for 24 hours, replaced with equivalent amounts of

fresh diffusion medium. The aliquots were analyzed spectrophotometrically at 247 nm. All the experiments were performed in triplicate.

3.11.2 *Ex-vivo* drug release profile

The *ex-vivo* release studies were performed with freshly isolated goat nasal mucosa procured from slaughter house using Franz diffusion cells [18, 39]. The nasal membrane was removed carefully and made free from adhered tissues. The excised nasal membrane was mounted on Franz diffusion cells with methanolic phosphate buffer saline (pH 6.4, 40%v/v) filled in receptor compartments. The cells were placed under mild agitation on magnetic stirrers and temperature was maintained at 34 ± 0.5 ^{0}C.EFV formulations (0.5 ml) were placed in the donor compartments. Aliquots were withdrawn from the receptor compartments at periodic time intervals for 24 hours, replaced with equivalent amounts of fresh diffusion medium. The aliquots were analyzed spectrophotometrically at 247 nm. All the experiments were performed in triplicate.

3.11.3 Kinetics of drug release

In order to examine the release mechanism of EFV from the prepared SLN dispersion and the EFV loaded SLN gel, the results of the *ex-vivo* release study were examined according to following equations [49-53].

3.11.3.1 Zero Order Release

$$\mathbf{Q = K_0 t}$$

Where, Q = Amount of drug release at time t,

K_0 =Zero order release constant,

t = Time.

Regression coefficient (R^2) value obtained from the plot of amount of drug released (Q) versus time (t), nearer to 1 indicates zero order release signifying the release to be concentration-independent.

3.11.3.2 First Order Release Equation

$\ln (100-Q) = \ln Q_0 - K_1 t$

Where, Q = Amount of drug release at time t,

K_1= First order release constant

The regression coefficient (R^2) value obtained from the log % ARR (Amount Remaining to Release) versus time, nearer to 1 indicates first order release signifying the release to be concentration-dependent.

3.11.3.3 Higuchi Square Root of Time Model

$Q = K_h t^{1/2}$

Where, Q= Amount of drug release at time t,

K_h= Higuchi square root of time release constant

The regression co-efficient of percentage drug release versus square root of time nearer to 1 indicates Higuchi's drug release model indicating Fickian diffusional release.

3.11.3.4 Hixon-Crowell Cube Root Model

$\sqrt[3]{Q_0} - \sqrt[3]{Q_t} = K_H C.t$

Where, Q_0 = initial concentration of drug present

Qt = amount of drug release at time t

R^2 values nearer to 1 for the plot of amount of drug released versus cube root time indicate Hixon – Crowell model.

3.11.3.5 Korsmeyer And Peppas Model

$Q_t / Q_\infty = K \times t^{\lambda}$

$\text{Log} (Q_t/Q_\infty) = \text{Log } K + \Lambda \text{ Log } t$

Where,

Q_∞ = Total drug released after infinite time.

Q_t/Q_∞ = Fractional drug released at time t

K = Kinetic constant incorporating structural and geometrical characteristic of the drug/polymer system (devices).

Λ = Diffusion exponents that characterizes the mechanism of drug release

t = Time

A plot of log (Q_t/ Q_∞) versus log t gives straight line of gradient λ and an intercept of log K. Values of exponent Λ and the corresponding release mechanism are given in Table 3.3.

TABLE 3.3 Values of exponent Λ and the corresponding release mechanism

Exponent λ			Release Mechanism
Thin film	**Cylinder**	**Sphere**	
0.5	0.45	0.43	Fickian diffusion
0.5 < Λ < 1.0	0.45 < Λ <0.89	0.43< Λ <0.85	Anamolous transport
1.0	0.89	0.85	Zero-order

3.12 *In-vivo* studies

In-vivo studies were performed on adult Wistar albino rats. A protocol for animal studies was approved by Institutional Animal Ethics Committee (IAEC) and Committee for the Purpose of Control and Supervision of Experiments on Animals (CPCSEA) [Protocol no. PIPH 04/15 CPCSEA921/PO/Ere/S/05/CPCSEA]. Animals were housed in polypropylene rat cages. Rice husk was used as the bedding material. Laboratory rat pellet feed and pure drinking water was supplied ad libitum. The rats were divided into two groups. Group I (test group) consisting of 6 animals were administered with the developed SLN formulation (equivalent to 0.06mg efavirenz) intranasally. The second group (standard) consisting of 6 animals were given the marketed formulation - EFAVIR - efavirenz capsules IP orally. (powder equivalent to 25 mg Efavirenz from capsule dispersed in 1 ml water). The dose was calculated based on human equivalent dose (HED) as per guideline by FDA [54].

The plasma samples from each animal were collected and the animals were sacrificed by an overdose of pentobarbital sodium at 24 hour. The brains were isolated, weighed, homogenized in PBS pH 6.4 at 5000 rpm using Silent crusher M homogenizer (Heidolph, Germany),

centrifuged and the supernatant were collected for determination of drug concentration [55]. The amount of drug in plasma and the brain homogenate were determined by the method developed and validated for estimation of efavirenz in plasma using HPLC. Tenofovir disoprxil fumarate was used as internal standard. Brain:Plasma ratio, bioavailable fraction and relative bioavailability were calculated using the formula

Brain: plasma = Conc. of drug in brain/Conc. of drug in plasma

Bioavailable fraction

= Bioavailable dose/ Administered dose

Relative bioavailability

=Systemic availability of drug/systemic availability of an oral standard of same drug

3.13 Stability Studies

The stability of the formulation were assessed under different storage conditions as per ICH guidelines, namely, 5 + 3 and 25 ± 2 ◦C/60 ± 5% RH [41, 56, 57]. The samples were evaluated at 0, 0.5, 1, 2, 3, 6 and 12 months for physical appearance, average particle size, PDI and zeta potential and drug content. All the studies were conducted in triplicate.

3.14 Data analysis

The data obtained were analysed statistically using t-test and ANOVA. The data obtained for the optimization of process and formulation variables were statistically analysed by analysis of variance (ANOVA) with in-built software design of Design Expert 9.0.3.1 software (Stat-Ease, Inc., USA). It was used to determine the significance and the magnitude of the effects of different variables and their interactions. Probability values less than 0.0500 were considered as statistically significant.

3.15 References:

1. The United States Pharamcopoeial convention, (2011), Standards A. General Notices and Requirements. USP 34; 6.
2. The National Toxicology Program (NTP) Interagency Center for the Evaluation of,

Alternative Toxicological Methods (NICEATM). Test Method Protocol for Solubility Determination Phase III. 2003:1-10.

3. Dole MN, Patel PA, Sawant SD, Shedpure PS., (2011) Advance applications of fourier transform infrared spectroscopy. *Int J Pharm Sci Rev Res*.;7(2):159-166.
4. Kumar YA, Rao NR., (2010). Development of Rapid UV Spectrophotometric Method for the Estimation of Efavirenz in Formulations. *E-Journal Chem*. ;7(3):856-860.
5. Kadam AA, Babu CJG, Permal RV, Channabasavaraj K, Mani TT., (2012) Development and Validation of Method for the Quantitative Estimation of Efavirenz in Bulk and Phrmaceutical Dosage Form. *Am J PharmTech Res*.;2(1):324-330.
6. Seju U, Kumar A, Sawant KK., (2011). Development and evaluation of olanzapine-loaded PLGA nanoparticles for nose-to-brain delivery: In vitro and in vivo studies. *Acta Biomater*.;7(12):4169-4176.
7. Sharma D, Maheshwari D, Philip G, et al., (2014) Formulation and optimization of polymeric nanoparticles for intranasal delivery of Lorazepam using box-behnken design: in vitro and in vivo evaluation. *Biomed Res Int*.;2014:156010.
8. Government of India, Ministry of Health and Family Welfare. *Indian Pharmacopoeia*. The Indian Pharmacopoeia commission; 1996:A-147.
9. Ramachandran G, Kumar. KH, Swaminathan S, Venkatesan P, Kumaraswami V, Greenblatt DJ., (2006). Simple and rapid liquid chromatography method for determination of efavirenz in plasma. *J Chromatogr B Anal Technol Biomed Life Sci*. 2006;835(2):131-135.
10. Kamble RN, Mehta P., (2015). Development of simple HPLC method to estimate the blood plasma concentration of Efavirenz in rat after oral administration, Innovare Academic Sciences, *Int. J Pharm & Pharm. Sci.*;7(7):7-10.
11. Lakshmi Sailaja, Kishore Kumar K, Ravi Kumar DVR, Mohan Kumar C, Yugandhar NM, Srinubabu G., (2007). Development and Validation of a Liquid Chromatographic Method for Determination of Efavirenz in Human Plasma. *Chromatographia*.;65(5-6):359-361.
12. Velpandian T, Mathur R, Agarwal NK, Arora B, Kumar L, Gupta SK., (2004). Development and validation of a simple liquid chromatographic method with ultraviolet

detection for the determination of imatinib in biological samples. *J Chromatogr B Anal Technol Biomed Life Sci*.;804(2):431-434.

13. Vikram Singh A, Nath LK, Pani NR., (2011). Development and validation of analytical method for the estimation of lamivudine in rabbit plasma. *J Pharm Anal*. ;1(4):251-257.
14. ICH. ICH Topic Q2 (R1) Validation of Analytical Procedures : Text and Methodology. *Int Conf Harmon*. 2005;1994(November 1996):17.
15. Ramaswamy A, Arul Gnana Dhas AS., (2014). Development and validation of analytical method for quantitation of Emtricitabine, Tenofovir, Efavirenz based on HPLC. *Arab J Chem*., 1-7.
16. Nagar M, Panwar KS, Chopra VS, Bala I, Trivedi P., (2010). Quality by design: A systematic approach to pharmaceutical development. *Der Pharm Lett*.;2(2):111-130.
17. Journals H, Article R, Parameters P, Kakodkar SSS, Gajare P., (2015). Pharmaceutical Quality-by-Design (QbD): Basic Principles;(1):1-19.
18. Sood S, Jain K, Gowthamarajan K., (2014). Optimization of curcumin nanoemulsion for intranasal delivery using design of experiment and its toxicity assessment. *Colloids Surfaces B Biointerfaces*;113:330-337.
19. Curic A, Keller B-L, Reul R, Moschwitzer J, Fricker G., (2015). Development and lyophilization of itraconazole loaded poly(butylcyanoacrylate) nanospheres as a drug delivery system. *Eur J Pharm Sci*.;78:121-131.
20. Pawar YB, Purohit H, Valicherla GR, et al., (2012). Novel lipid based oral formulation of curcumin: Development and optimization by design of experiments approach. *Int J Pharm*.;436(1-2):617-623.
21. Severino P, Santana MH a, Souto EB., (2012). Optimizing SLN and NLC by 2 2 full factorial design: Effect of homogenization technique. *Mater Sci Eng C*. ;32(6):1375-1379.
22. Rohit B, Pal KI., (2013). A Method to Prepare Solid Lipid Nanoparticles with Improved Entrapment Efficiency of Hydrophilic Drugs. *Curr Nanosci*. ;9(2):211-220.
23. Peter Christoper G V., Vijaya Raghavan C, Siddharth K, Siva Selva Kumar M, Hari Prasad R., (2014). Formulation and optimization of coated PLGA - Zidovudine nanoparticles using factorial design and in vitro in vivo evaluations to determine brain

targeting efficiency. *Saudi Pharm J*.;22(2):133-140.

24. Gupta S, Chavhan S, Sawant KK., (2011). Self-nanoemulsifying drug delivery system for adefovir dipivoxil: Design, characterization, in vitro and ex vivo evaluation. *Colloids Surfaces A Physicochem Eng Asp*.;392(1):145-155.
25. Blasi P, Giovagnoli S, Schoubben A, Ricci M, Rossi C., (2007). Solid lipid nanoparticles for targeted brain drug delivery. *Adv Drug Deliv Rev*.;59(6):454-477.
26. Silva C, Gonzalez-Mira E, Garcia ML, et al., (2011). Preparation, characterization and biocompatibility studies on risperidone-loaded solid lipid nanoparticles (SLN): High pressure homogenization versus ultrasound. *Colloids Surfaces B Biointerfaces*.;86(1):158-165.
27. Shegokar R, Singh KK, Müller RH., (2011). Production & stability of stavudine solid lipid nanoparticles - From lab to industrial scale. *Int J Pharm*. ;416(2):461-470.
28. Pani NR, Nath LK, Acharya S, Bhuniya B., (2011). Application of DSC, IST, and FTIR study in the compatibility testing of nateglinide with different pharmaceutical excipients. *J Therm Anal Calorim*.;108(1):219-226.
29. Bozdağ-Pehlivan S, Subaşi B, Vural I, Ünlü N, Çapan Y., (2011). Evaluation of drug-excipient interaction in the formulation of celecoxib tablets. *Acta Pol Pharm - Drug Res*. ;68(3):423-433.
30. Mehnert W, Mäder K., (2012). Solid lipid nanoparticles. *Adv Drug Deliv Rev*. ;64:83-101.
31. Park JH, Ban SJ, Ahmed T, et al., (2015). Development of DH-I-180-3 loaded lipid nanoparticle for photodynamic therapy. *Int J Pharm*. 2015;491(1-2):393-401.
32. Omwoyo WN, Melariri P, Gathirwa JW, et al., (2016). Development, characterization and antimalarial efficacy of dihydroartemisinin loaded solid lipid nanoparticles. *Nanomedicine Nanotechnology, Biol Med*.;12(3):801-809.
33. Jeannot V, Mazzaferro S, Lavaud J, et al., (2016). Targeting CD44 receptor-positive lung tumors using polysaccharide-based nanocarriers: Influence of nanoparticle size and administration route. *Nanomedicine Nanotechnology, Biol Med*. ;12(4):921-932.
34. Blasi P, Schoubben A, Traina G, et al., (2013). Lipid nanoparticles for brain targeting III. Long-term stability and in vivo toxicity. *Int J Pharm*.;454(1):316-323.

35. Blasi P, Giovagnoli S, Schoubben A, et al., (2011). Lipid nanoparticles for brain targeting I. Formulation optimization. *Int J Pharm*. ;419(1-2):287-295.
36. Das Neves J, Sarmento B., (2014). Mucosal delivery of biopharmaceuticals: Biology, challenges and strategies. *Mucosal Deliv Biopharm Biol Challenges Strateg*. 9781461495:1-601.
37. Naik A, Nair H., (2014). Formulation and Evaluation of Thermosensitive Biogels for Nose to Brain Delivery of Doxepin. *Biomed Res. Int.*;2014.1-10.
38. Lun H, Chattopadhyay N, Yu X, Bendayan R., (2010). Nanotechnology applications for improved delivery of antiretroviral drugs to the brain. *Adv Drug Deliv Rev*. ;62(4-5):503-517.
39. Ravi PR, Aditya N, Patil S, Cherian L., (2013). Nasal in-situ gels for delivery of rasagiline mesylate: improvement in bioavailability and brain localization. *Drug Deliv*. 2013;7544:1-8.
40. Kumar A, Garg T, Sarma GS, Rath G, Goyal AK., (2015). Optimization of combinational intranasal drug delivery system for the management of migraine by using statistical design. *Eur J Pharm Sci*.;70:140-151.
41. Yasir M, Sara UVS., (2014). Solid lipid nanoparticles for nose to brain delivery of haloperidol: in vitro drug release and pharmacokinetics evaluation. Acta Pharmaceutica Sinica B;4(6):454-463.
42. Morsi NM, Ghorab DM, Badie HA., (2012). Bioadhesive Brain Targeted Nasal Delivery of an Ant ischemic Drug.;3(5):1067-1076.
43. Das Neves J, Amiji MM, Bahia MF, Sarmento B.,(2010). Nanotechnology-based systems for the treatment and prevention of HIV/AIDS. *Adv Drug Deliv Rev*.;62(4-5):458-477.
44. Morsi N, Ghorab D, Refai H, Teba H., (2016). Ketoroloac tromethamine loaded nanodispersion incorporated into thermosensitive in situ gel for prolonged ocular delivery. *Int J Pharm*.;506(1-2):57-67.
45. Arbelaez-Camargo D, Suñé-Negre JM, Roig-Carreras M, et al., (2016). Preformulation and characterization of a lidocaine hydrochloride and dexamethasone sodium phosphate thermo-reversible and bioadhesive long-acting gel for intraperitoneal administration. *Int*

J Pharm.;498(1-2):142-152.

46. Avachat AM, Parpani SS., (2015). Formulation and development of bicontinuous nanostructured liquid crystalline particles of efavirenz. *Colloids Surfaces B Biointerfaces*.;126:87-97.
47. Pathak R, Prasad R, Misra M., (2014). Role of mucoadhesive polymers in enhancing delivery of nimodipine microemulsion to brain via intranasal route. *Acta Pharm Sin B*.;4(2):151-160.
48. Gupta S, Chavhan S, Sawant KK., (2011). Self-nanoemulsifying drug delivery system for adefovir dipivoxil: Design, characterization, in vitro and ex vivo evaluation. *Colloids Surfaces A Physicochem Eng Asp*.;392(1):145-155.
49. Venkateswarlu V, Manjunath K., (2004). Preparation, characterization and in vitro release kinetics of clozapine solid lipid nanoparticles. *J Control Release*.;95(3):627-638.
50. Singhvi G, Singh M., (2011). In-vitro drug release characterization models. Int. J Pharm. Studies and Res.;2 (1):77-84.
51. Hilip, LR, Peppas A., (1987). Fickian and anomalous release from swellable devices. *J Control Release*.;5:37-42.
52. Macheras, P., Liadis A., (2006). *Modelling in Biopharmaceutics, Pharmacokinetics and Pharmacodynamics: Homogeneous and Heterogeneous Approaches. Series: Interdisciplinary Applied Mathematics*. Springer, New York.
53. Ren S, Park MJ, Sah H, Lee BJ., (2008). Effect of pharmaceutical excipients on aqueous stability of rabeprazole sodium. *Int J Pharm*.;350(1-2):197-204.
54. FDA. Guidance for Industry Starting Dose in Initial Clinical Trials Guidance for Industry Estimating the Maximum Safe. *FDA*. 2005;(July):27.
55. Kumar S, Randhawa JK., (2013). High melting lipid based approach for drug delivery: Solid lipid nanoparticles. *Mater Sci Eng C*. ;33(4):1842-1852.
56. Guidance for Industry Q1A(R2) Stability Testing of New Drug Substances and Products. U.S. Department of Health and Human Services, Food and Drug Administration, Center for Drug Evaluation and Research (CDER) Center for Biologics Evaluation and Research (CBER); (2003); (November):1–22.
57. SADC. Registration of Medicines Stability. *SADC Guidel Stab Test*. 2004;(March):1-44.

CHAPTER 4
Results & Discussions

4.1 Identification of Drug

Identification of the procured drug sample and ensuring its purity is a prerequisite before proceeding with the formulation development. The identification tests and the inferences for the drug sample based on its appearance, solubility and melting point determination are summarized in Table 4.1.

TABLE 4.1: Identification tests for EFV with the inferences

Parameters	Observations	Reported [1]	Inferences
Appearance	White powder	White to almost white powder	Complies
Solubility	Practically insoluble in water (10 mg insoluble in >100 ml) Freely soluble in methanol (10 mg in < 1 ml)	Practically insoluble in water Freely soluble in methanol	Complies Complies
Melting point	139-142^{0}C	138 – 142 ^{0}C	Complies

Compliance of the observations with respect to the reported specifications verifies the sample to be of the drug efavirenz. Various functional groups present in the powder drug sample was determined by fourier-transform infrared (FT-IR) spectroscopic and compared with the standard spectra of EFV for confirmation [2]. The observed and reported IR spectra of EFV are shown in Figure 4.1.

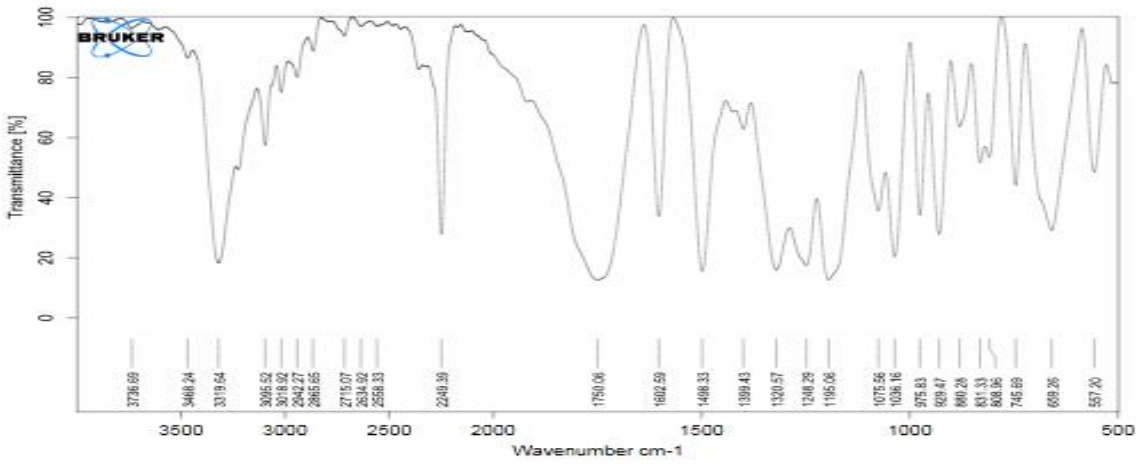

(a)

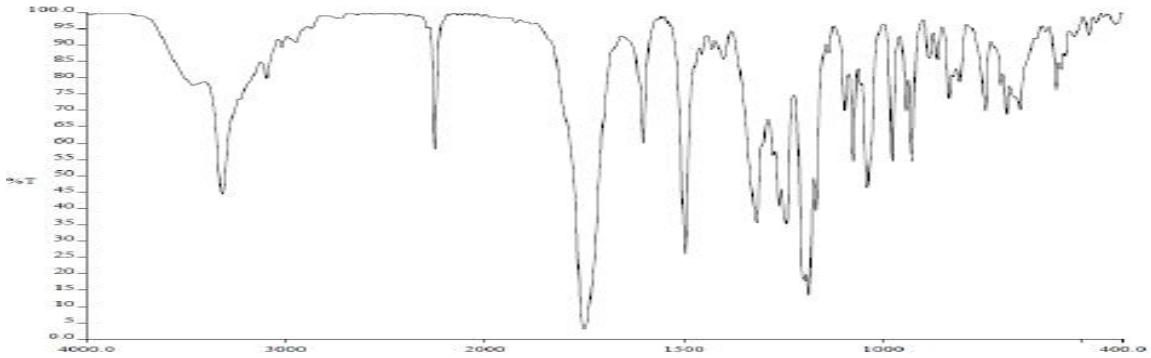

(b)

FIGURE 4.1: IR spectra (a) Observed spectra of EFV (b) Reported spectra of EFV

The major IR peaks observed and reported for EFV molecule (shown in Figure 4.2) is summarized in Table 4.2 [3].

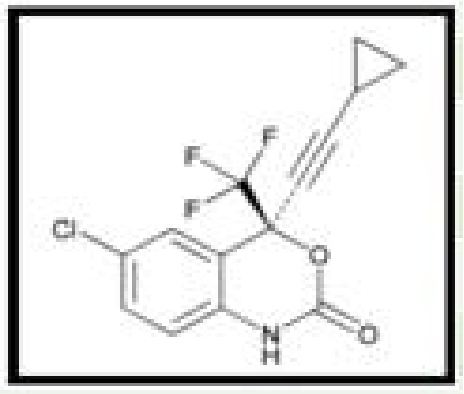

FIGURE 4.2: Structure of efavirenz (EFV)

TABLE 4.2: Major peaks observed and reported for EFV in IR spectra:

Observed (cm^{-1})	Reported (cm^{-1})	Inferences [3]
3319.64	3500-3100	N-H stretching
2249.39	2250-2100	C= C (Alkyne)
1750.06	1750-1730	C=O of ester
1602.59	1680-1630	C=O of amide
1498.33	1350-1000	C-N
1036.16	1300-1000	C-O

From the observations of Table 4.1, Table 4.2 and Figure 4.1, it was verified and concluded that the procured sample was of efavirenz and the sample was used for all further investigations.

4.2 Analytical Methods

Simple, rapid and reliable analytical methods for the estimation of drug content were required to determine the entrapment efficiency of the formulation, which in turn was needed for selection of right material, optimization of their concentrations, characterization of the optimized formulation and for stability testing. The analytical methods were also needed for the *in-vitro* and *ex-vivo* drug release studies and for estimation of drug in plasma and brain post-administration of the formulations.

4.2.1 UV- Spectrophotometric estimation of efavirenz

Simple, sensitive, accurate, precise and rapid ultraviolet (UV) spectrophotometric methods have been reported to be developed and validated for the estimation of efavirenz in pure form, its formulations and stability samples [4, 5]. Hence, calibration curves were obtained using methanol:water (50% v/v) and methanolic phosphate buffer saline (PBS) (pH 6.4, 40%v/v) as solvents respectively for determining the entrapment efficiency and *in-vitro* drug release studies.

4.2.1.1 Calibration curve in methanol:water:: 50:50 %v/v as solvent :

Calibration curves were plotted in methanol:water (50% v/v) at 247 nm in the concentration range of 3-18 µg/ml of efavirenz using UV- spectrophotometer (UV-1800, Shimadzu) for determining the entrapment efficiency and for analysing the stability samples. The data obtained for calibration curve is shown in Table 4.3 and the overlay spectra of EFV at different concentrations and the calibration curve is shown in Figure 4.3 respectively.

TABLE 4.3: Calibration data for EFV in methanol:water (50% v/v)

S.No.	Concentration (µg/ml)	Mean Absorbance* ± S.D.
1	3	0.152 ± 0.009
2	6	0.309 ± 0.008
3	9	0.461 ± 0.009
4	12	0.634 ± 0.007
5	15	0.785 ± 0.005
6	18	0.951 ± 0.013

(*Mean of n=3 determinations)

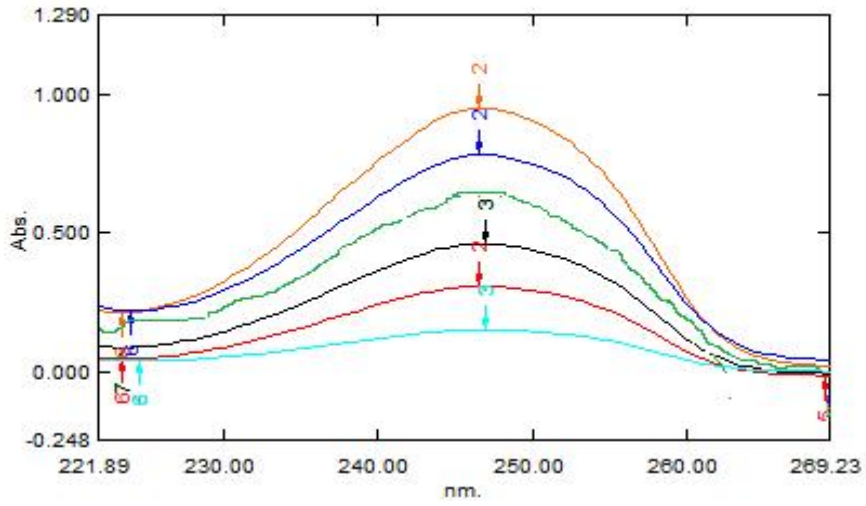

FIGURE 4.3(a): Overlay spectra of EFV at different concentrations

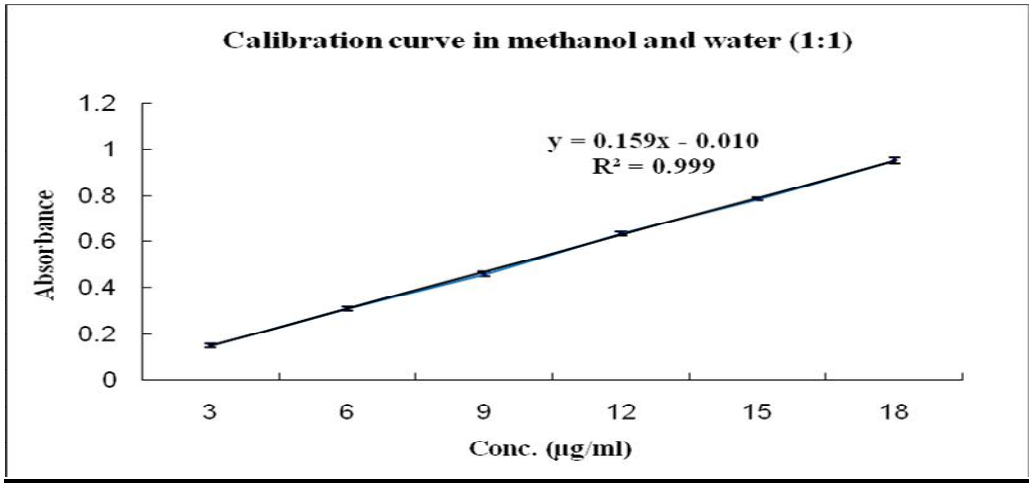

FIGURE 4.3 (b): Calibration curve for efavirenz in methanol and water (1:1)

The calibration curve was found to be linear in the concentration range of 3 – 18 µg/ml with correlation coefficient (R^2) value of 0.999.

4.2.1.2 Calibration curve in methanolic phosphate buffer saline (pH 6.4, 40%v/v):

The calibration curve for efavirenz in methanolic phosphate buffer saline (pH 6.4, 40% v/v) is shown in Figure 4.4 and the data is given in Table 4.4. The pH was selected based on the nasal mucosal pH (5.5-6.5) and methanol being added to maintain the sink condition. Efavirenz has limited solubility in buffer but is soluble in methanol, hence methanol was added in PBS pH 6.4 to maintain the perfect sink conditions [6, 7].

TABLE 4.4 Calibration data for EFV in methanolic PBS (pH 6.4, 40% v/v).

S.No.	Concentration (µg/ml)	Mean Absorbance* ± S.D.
1	3	0.179 ± 0.002
2	6	0.382 ± 0.004
3	9	0.576 ± 0.003
4	12	0.758 ± 0.006
5	15	0.967 ± 0.005
6	18	1.136 ± 0.008

(*=Mean of 3 determinations)

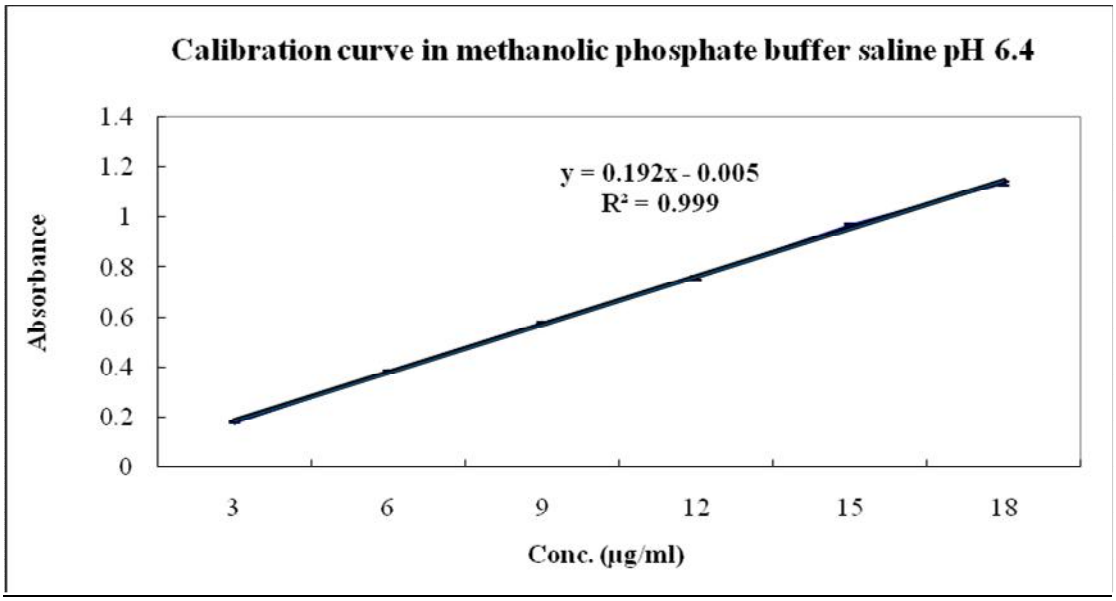

FIGURE 4.4 Calibration curve for efavirenz in 40% methanolic phosphate buffer saline pH 6.4

The calibration curve was found to be linear with R^2 value of 0.999. The regression equation was determined in the methanolic phosphate buffer saline (pH 6.4. 40%v/v) for the release studies of drug from the formulations.

4.2.2 HPLC Method Development & Validation

Standard solution of EFV (25 ppm) and TDF (50 ppm) were scanned in the range of 200-400 nm as shown in Figure 4.5 and from that the detection wavelength (λ_{max}) was selected at 260 nm.

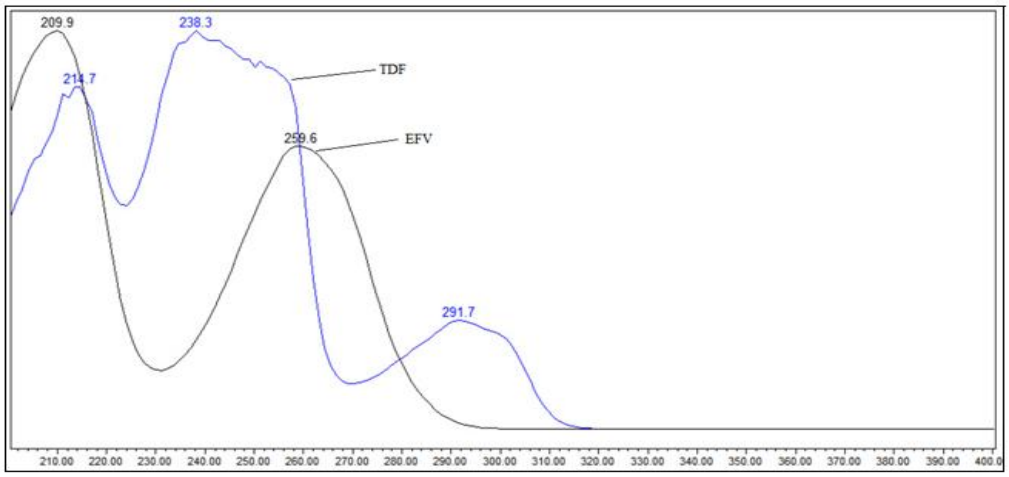

FIGURE 4.5: Spectra obtained for EFV and TDF for selection of wavelength

Several trials were taken with various columns, mobile phase, pH of the mobile phase to select the chromatographic conditions giving good peak characteristics. The initial chromatographic conditions were as given in Table 4.5.

TABLE 4.5 Initial chromatographic conditions for trial batches

Column	Inertsil ODS, 150X4.6mm, 5.0µm
Mobile Phase	Mobile phase-A : 0.1% Orthophosphoric acid in water, Mobile phase B : Acetonitrile (30:70)
Flow rate	1.0 ml/min
Detection wavelength	260 nm
Column Temperature	30^0C
Sample cooler temperature	5 ^{0}C
Injection volume	5µl
Run Time	9 minutes

4.2.2.1 Selection and optimization of chromatographic conditions

Several trials were taken for EFV sample first, followed by addition of TDF sample as internal standard and plasma.

Trial 1: Starting with the chromatographic conditions mentioned in Table 4.5, the chromatogram obtained with 25 ppm EFV sample is as shown in Figure 4.6.

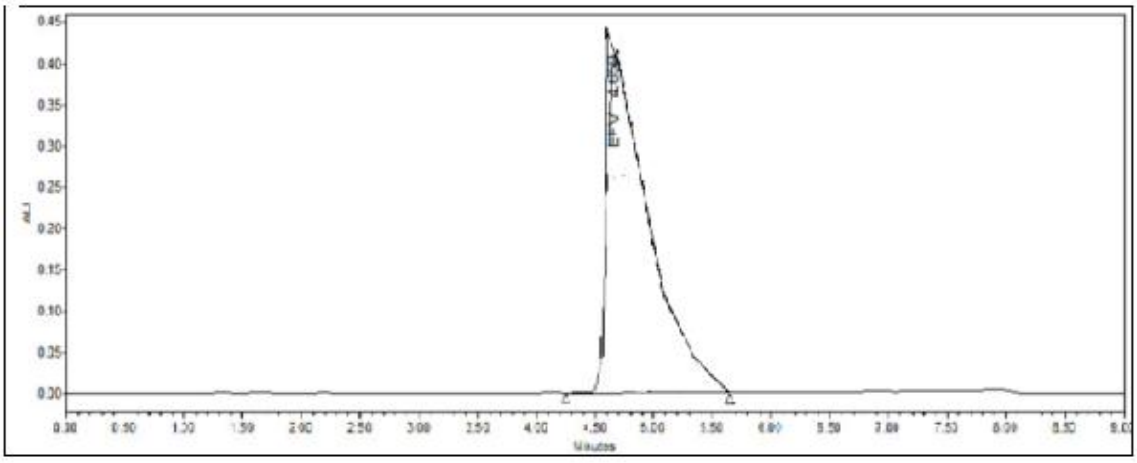

FIGURE 4.6: Trial 1 for HPLC method development

It can be observed from Figure 4.6 that the peak characteristics of EFV were not acceptable showing tailing in the peak.

Trial 2: With same sample of 25 ppm solution of EFV, trials were taken with change of column. Waters symmetry shield C18, 150 x 4.6mm, 5.0µm column was used with other other chromatographic conditions as mentioned in Table 4.5. The chromatogram obtained is shown in Figure 4.7.

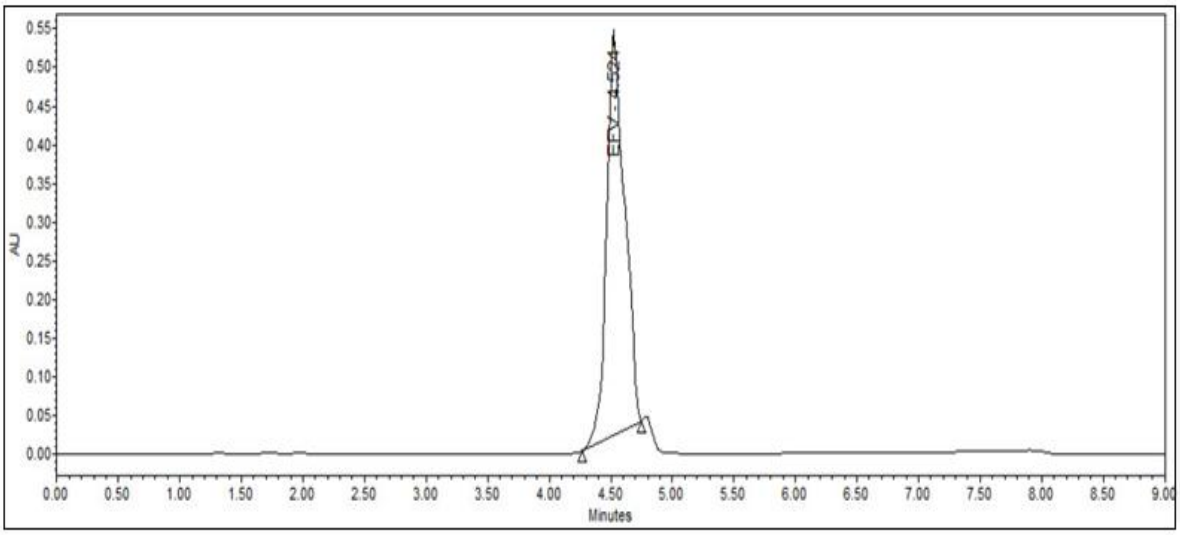

FIGURE 4.7: Trial 2 for HPLC method development

It was observed that the base of the peak was not found good, hence there was need to take more trials to improve peak shape.

Trial 3: To improve the peak shape, mobile phase was changed from acidic to little basic to check improvement in peak shape. Hence, 10 mM ammonium acetate was used instead of 0.1% orthophosphoric acid as mobile phase. The chromatogram obtained with 10mM ammonium acetate buffer and acetonitrile (30:70) as mobile phase and Waters symmetry shield C18, 150 x 4.6mm, 5.0µm column is shown in Figure 4.8.

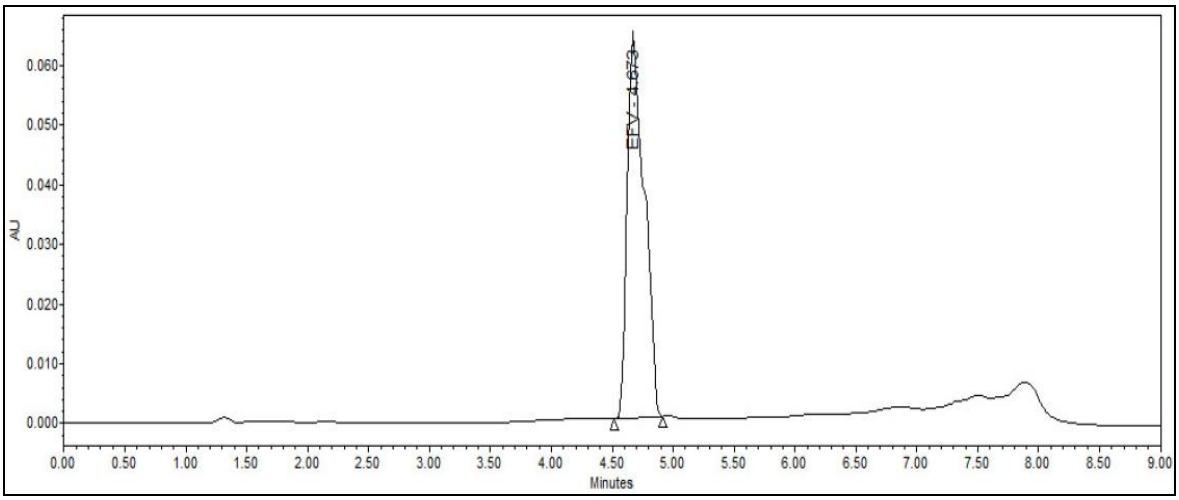

FIGURE 4.8: Trial 3 for HPLC method development

It was observed that peak shape was not improved and more trials were required with change of pH of the mobile phase.

Trial 4: The trial was taken by adjusting the pH of the mobile phase to 5.5 with rest of the chromatographic parameters similar to that of the trial 3. The chromatograms obtained for trial 4 is shown in Figure 4.9.

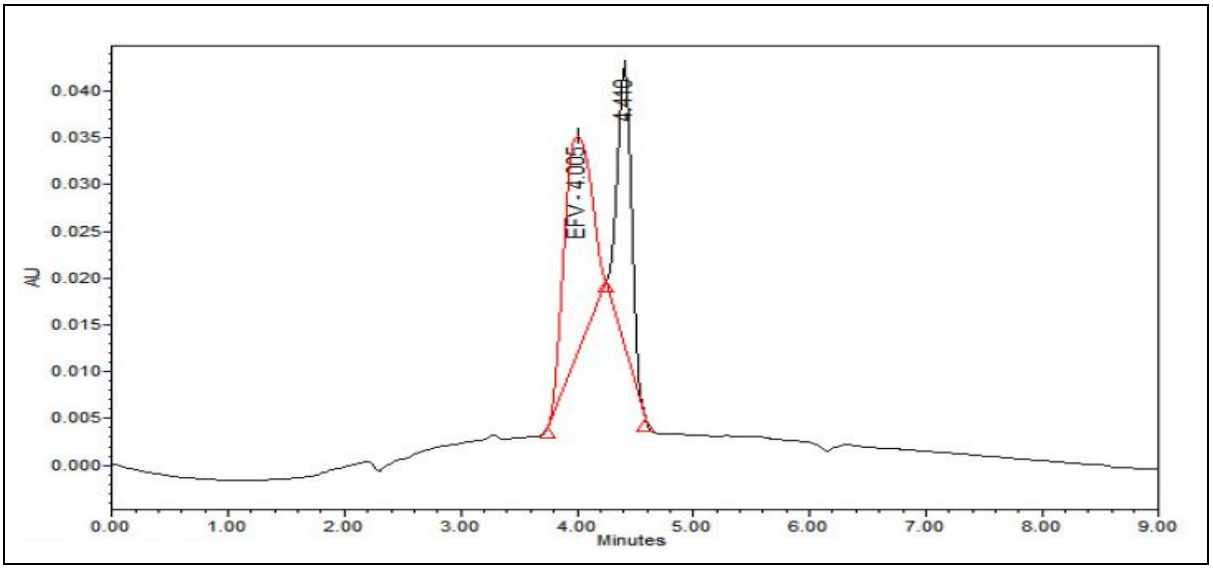

FIGURE 4.9: Trial 4 for HPLC method development

As can be observed from Figure 4.9, splitting of the peak was obtained with mobile phase consisting of ammonium acetate buffer pH 5.5. Hence, it was concluded that more trials are required to be taken.

Trial 5: In this trial, the effect was checked by changing the buffer in mobile phase from acetate to phosphate buffer with acidic pH. Thus, the chromatogram obtained with 10 mM phosphate buffer pH 2.5 and Acetonitrile (30:70) is as shown in Figure 4.10.

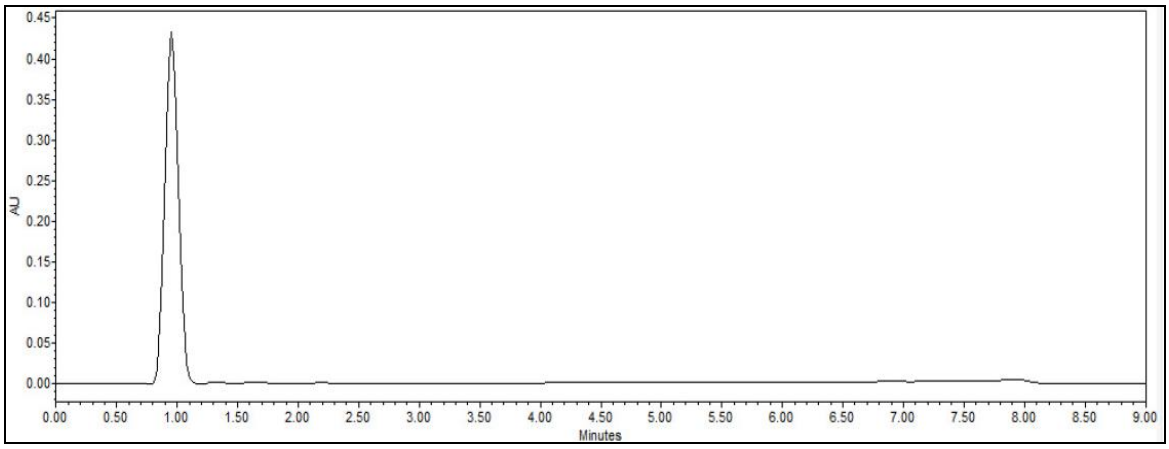

FIGURE 4.10: Trial 5 for HPLC method development

It was observed from Figure 4.10 that the shape of efavirenz peak was good and symmetrical, but it eluted near void volume, next trial to be taken with mobile phase pH changed from highly acidic to less acidic.

Trial 6: In order to increase the retention time, this trial was taken with increased pH of the mobile phase. Thus, mobile phase for this trial was phosphate buffer pH 3.5 and acetonitrile and remaining all parameter were same as that for trial 5. The chromatogram obtained was as shown in Figure 4.11.

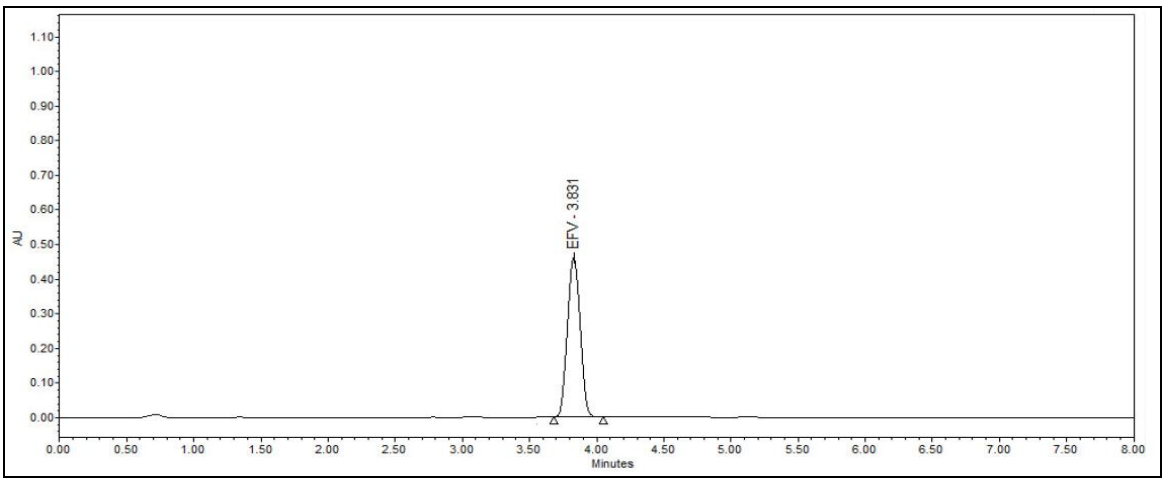

FIGURE 4.11: Trial 6 for HPLC method development

The shape and symmetry of the chromatographic peak for EFV obtained in this trial was observed to be good, hence the similar chromatographic conditions were used for further analytical method developmental investigations.

Trial 7: To check peak shape of internal standard in above chromatographic condition, 50 ppm of TDF was prepared and injected. The chromatogram obtained with the sample consisting of 25 ppm EFV and 50 ppm TDF prepared using methanol:water (50%v/v) as diluents is shown in Figure 4.12.

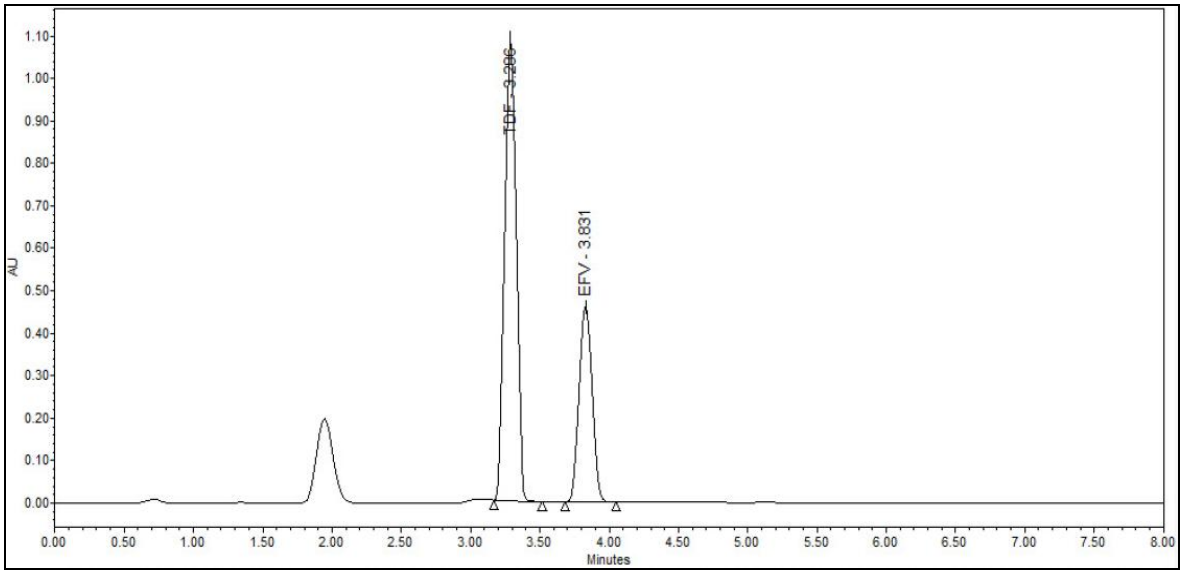

FIGURE 4.12: Trial 7 for HPLC method development

In the chromatogram obtained with trial 7, it can be observed that the peak shape for both the drug (EFV) and internal standard (TDF) were found good, but resolution between both the peaks was not appropriate, hence more trials for good separation between both the peaks were needed.

Trial 8: In order to improve resolution between the peaks of EFV and TDF, HPLC column was changed with smaller sorbent particle size (3.5 µm). The chromatogram obtained with the mixed sample of EFV and TDF using Waters X-Terra Shield, RP18 50 x 4.6 mm, 3.5 µm column is shown in Figure 4.13.

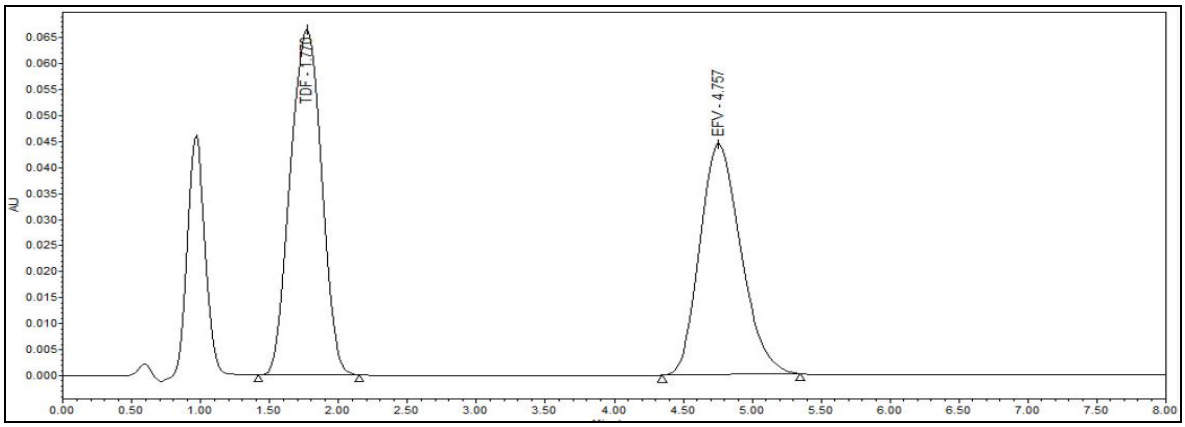

FIGURE 4.13: Trial 8 for HPLC method development

The peak shapes were found to be good, but peak of TDF eluted near to void volume, hence next trials were taken with gradient chromatographic program.

Trial 9:

In this trial, the gradient chromatographic program was used as shown in Table 4.6. Flow rate was also changed from 1.0 to 1.5 ml/min and mixture of the standard EFV and TDF was injected. The chromatogram obtained is shown if Figure 4.14.

TABLE 4.6: Gradient Program used for HPLC method development

Time (Minutes)	Mobile phase-A (%v/v) (Phosphate buffer pH 3.5)	Mobile phase-B (%v/v) (Acetonitrile)
0	95	5
1	95	5
5	20	80
6	20	80
6.1	95	5
8	95	5

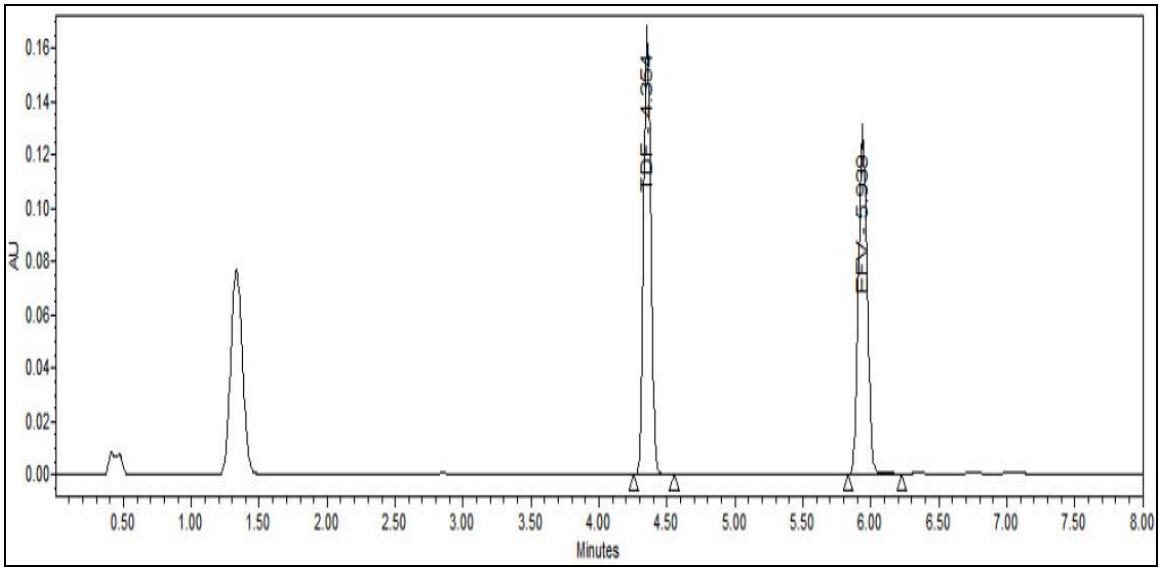

FIGURE 4.14: Trial 9 for HPLC method development

It can be observed from Figure 4.14 that peak characteristics including its shape, symmetry, resolution, etc. were found to be good. An extra peak eluted at about 1.5 minutes was also observed. It was assumed to be the peak of fumarate. In order to confirm this, 20 ppm fumaric acid was injected with the same chromatographic conditions. The peak observed with fumaric acid is shown in Figure 4.15.

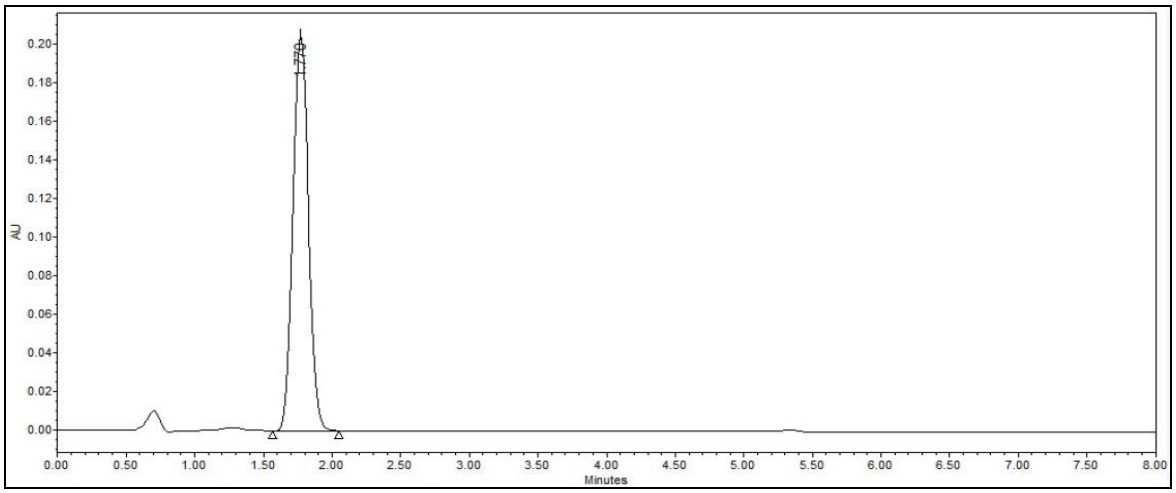

FIGURE 4.15: Chromatogram of 20 ppm fumaric acid

The peak observed at about 1.5 minutes in Figure 4.15, confirms that the extra peak observed in trial 9 was due to fumarate. Hence, the chromatographic conditions were further tested for plasma samples. The chromatogram obtained with the sample in plasma is shown in Figure 4.16.

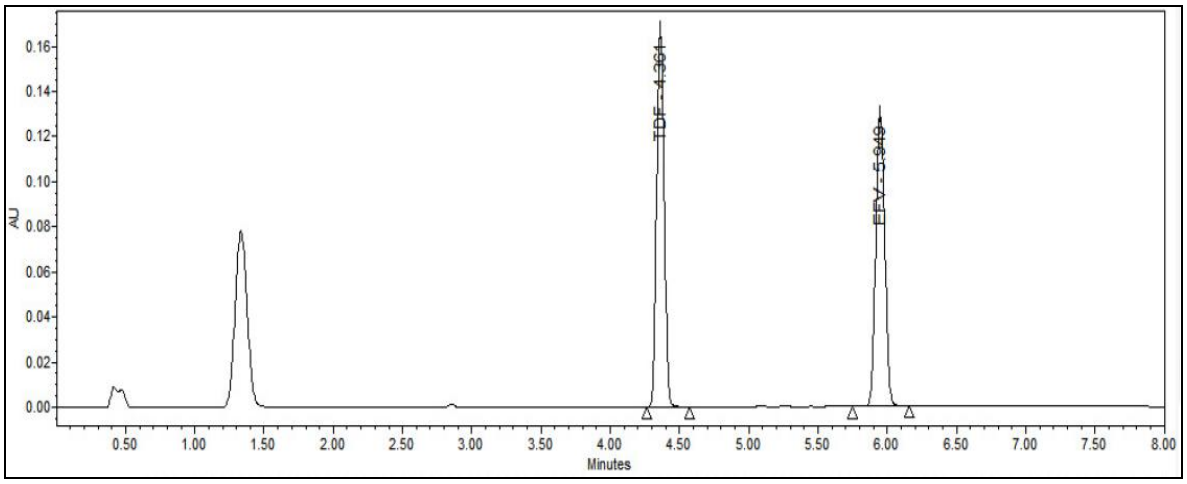

FIGURE 4.16: Chromatogram of EFV and TDF in plasma samples

From the Figure 4.16, it was concluded that no significant interference was observed with the presence of plasma. Thus, the chromatographic conditions summarized in Table 4.7 can be used for estimation of EFV from plasma after the validation of the developed method.

TABLE 4.7: Optimized Chromatographic conditions for HPLC method

Equipment	HPLC with UV Detector - Waters (Alliance)
Mobile phase	Mobile phase-A : Phosphate buffer pH 3.5 , Mobile phase B : Acetonitrile
Column	Waters X-Terra Shield, RP18 50 x 4.6 mm, 3.5 µm
Column temperature	Ambient
Sample cooler	5°C
Injection volume	5 µL
Flow rate	1.5 mL/min
Wavelength	260 nm
Diluent	Water:Methanol (50 %v/v)

It was observed that with the optimized chromatographic parameters shown in Table 4.7, the retention time was significantly reduced to 5.949 min in comparison to reported retention times in literature [8-10]. This can reduce the run time and the cost of analysis of samples. All the reagents used are also commonly available. While the composition of mobile phase was similar consisting of phosphate buffer and acetonitrile as in various other reported methods [8,

11], the retention time of EFV was observed to be drastically reduced in comparison to the reported values (from 13.2 min to 5.951 min) [8]. This may be due to the use of column of different dimension 50 x 4.6 mm, 3.5 µm instead of 250 × 4.6 mm, 5 µm. With the use of the analytical column 150 x 4.6 mm, 3 µm, the retention time of 6.9 min [11] and with 75 x 4.6 mm, 3.5 µm, retention time of 6.45 min have been reported [10]. While the pH of the mobile phase reported are higher than 3.5 [8, 11], peak was observed to be split at higher pH in the present investigation. Better results were obtained at a pH of 3.5. Most of the investigations reported in literature have used flow rate of 1 ml/min [8, 11] or less [10, 12], in the present investigation TDF peak was observed to be very close to the void volume at flow rate of 1 ml/min. Proper retention time for EFV and TDF were observed with flow rate of 1.5 ml/min. Higher flow rate would have also contributed for lowering the retention time of EFV. The lower retention time can help to reduce the time required for analysis. With the use of the gradient elution method, improved resolution, increased detection, shorter analysis time and increased efficiency was observed.

4.2.2.2 Analytical Method Validation

Various parameters such as linearity and range, precision, accuracy, sensitivity (limit of detection, limit of quantification), specificity, robustness/ruggedness, stability, were evaluated for validating the developed analytical method as per ICH guidelines [13].

A. Linearity and Range

The linearity of an analytical procedure is its ability (within a given range) to obtain test results which are directly proportional to the concentration (amount) of analyte in the sample. Calibration curve was constructed by plotting the peak area ratios (analyte/internal standard) v/s concentration. The overlay chromatogram obtained for linearity study is shown in Figure 4.17(a) and the calibration plot with regression equation and correlation coefficient was determined as shown in Figure 4.17(b). The calibration plot revealed linearity in the concentration range of 1-300 µg/ml with the correlation coefficient of 0.999. Tables 4.8(a) and 4.8(b) indicate the sample preparation and area ratios obtained for linearity study respectively.

TABLE 4.8(a): Sample Preparation for linearity studies:

Sample	Stock solution		Dilution		Conc. (µg/ml)
	Wt taken (mg)	Total Volume (ml)	Volume of stock solution taken (ml)	Final Volume (ml)	
TDF	100.51	100	5.0	100	50.255
EFV	50.17	100	0.2	100	1.003
EFV	50.17	100	1.0	100	5.017
EFV	50.17	100	2.0	100	10.034
EFV	50.17	100	4.0	100	20.068
EFV	50.17	100	5.0	100	25.085
EFV	50.17	100	10.0	100	50.170
EFV	50.17	100	20.0	100	100.340
EFV	50.17	100	40.0	100	200.680
EFV	50.17	100	60.0	100	301.020

TABLE 4.8(b): Concentration, Area and Area ratio for linearity study:

S.No.	Concentration (µg/ml)		Area		Area Ratio (Analyte/IS)
	Efavirenz (Analyte)	Tenofovir (IS)	Efavirenz (Analyte)	Tenofovir (IS)	
1	1.003	50.255	1030189	7804463	0.132
2	5.017	50.255	1225301	7804463	0.157
3	10.034	50.255	1462147	7804463	0.187
4	20.068	50.255	2901725	7804463	0.372
5	25.085	50.255	3602156	7804463	0.462
6	50.170	50.255	7404312	7804463	0.949
7	100.340	50.255	14708624	7804463	1.885
8	200.680	50.255	29417248	7804463	3.769
9	301.020	50.255	43225872	7804463	5.539

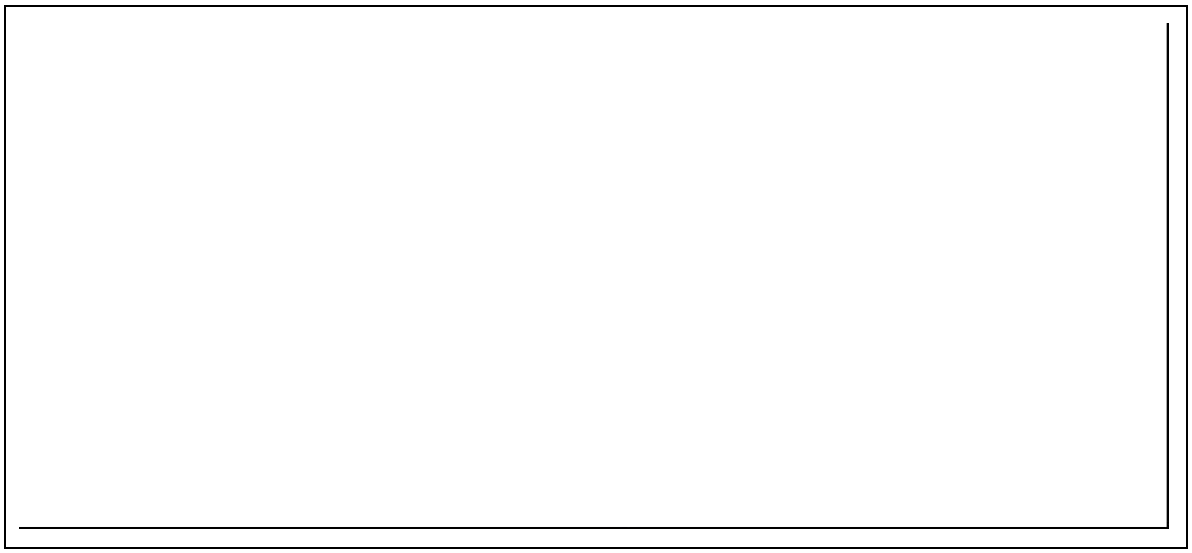

(a)

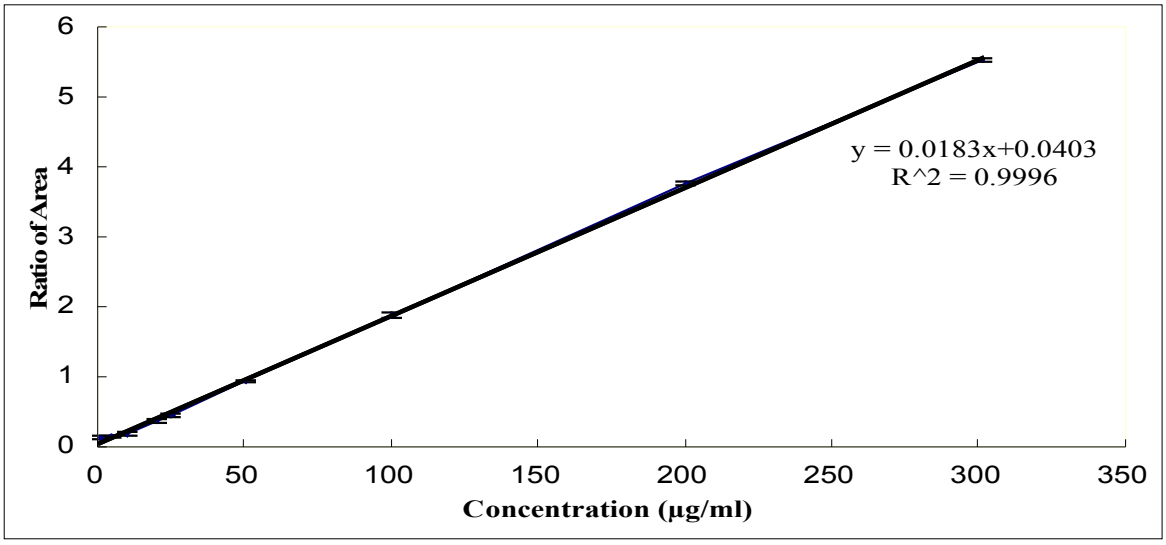

(b)

FIGURE 4.17: (a) Chromatogram for linearity study (b) Calibration plot for linearity

As per the extensive literature review, most of the methods were reported to give linear relation in the concentration range upto 10 µg/ml [10, 11, 14, 15]. Only a few had reported linearity at higher concentration of 0.1- 100 µg/ml [9]. In one of the reported methods for simultaneous estimation of Emtricitabine, Tenofovir and Efavirenz, the linearity was investigated in the concentration range of 200-280 µg/ml [16]. The present investigation assures the linearity in a wider range of 1-300 µg/ml required for the intended application of the procedure.

B. Precision

The precision of an analytical procedure expresses the closeness of agreement (degree of scatter) between a series of measurements obtained from multiple sampling of the same homogeneous sample under the prescribed conditions. The precision (repeatability) of the analytical method was determined by assaying six samples at 100% test concentration. The chromatograms obtained for the precision study is shown in Figure 4.18. RSD was determined to be 0.497 (NMT 2.0%) as shown in Table 4.9.

The intra-day and inter-day precisions were also assessed by analyzing three samples at three different times of the same day and on three consecutive days respectively and RSD were found to be less than 1.0 % as shown in Table 4.10 and 4.11 respectively which is within the normal acceptable range (NMT 2.0%). RSD of upto 8.6% have been reported in the literature for precision of the analytical methods for estimation of EFV [11, 15]. Although many authors have not analyzed the data statistically with ANOVA [5, 9-11, 14], a few have [12, 15]. In the present investigations, no significant differences were observed for results obtained for intra-day and inter-day data when statistically analyzed with ANOVA ($p>0.05$) as shown in Table 4.12 and Table 4.13.

FIGURE 4.18: Chromatogram for precision study

TABLE: 4.9 Area ratios and RSD calculation for Precision study (Repeatability):

Sample	Stock solution		Dilution		Conc. (µg/ml)
	Wt taken (mg)	Total Volume (ml)	Volume of stock solution taken (ml)	Final Volume (ml)	
Efavirenz	50.17	100	5.0	100	25.085
Tenofovir	100.51	100	5.0	100	50.255
S.No.	**Concentration (µg/ml)**		**Area**		**Area Ratio (Analyte/IS)**
	Efavirenz	**Tenofovir (IS)**	**Efavirenz**	**Tenofovir (IS)**	
1	25.085	50.255	3594121	7816671	0.460
2	25.085	50.255	3614721	7804413	0.463
3	25.085	50.255	3600781	7863229	0.458
4	25.085	50.255	3612480	7821009	0.462
5	25.085	50.255	3607115	7831118	0.461
6	25.085	50.255	3586470	7844471	0.457
Mean			3602615	7830152	0.460
S.D.			10957	21109	0.002
% RSD			0.304	0.270	0.497

TABLE: 4.10 Intraday Precision studies:

Drug	Conc. (µg/ml)	Area			Average	SD	%RSD
		at 10 am	at 1 pm	at 4 pm			
EFV	25.085	3594121	3612480	3624812	3610471	15444	0.428
	25.085	3614721	3607115	3628599	3616812	10894	0.301
	25.085	3600781	3586470	3617955	3601735	15764	0.438
TDF	50.255	7816671	7821009	7810063	7815914	5512	0.071
	50.255	7804413	7831118	7866541	7834024	31166	0.398
	50.255	7863229	7844471	7852116	7853272	9432	0.120

TABLE: 4.11 Inter-day Precision studies:

Drug	Conc. (µg/ml)	Area			Average	SD	%RSD
		on Day 1	on Day 2	on Day 3			
EFV	25.085	3598121	3612151	3620012	3610095	11089	0.307
	25.085	3612721	3614561	3610124	3612469	2229	0.062
	25.085	3600781	3616589	3616479	3611283	9095	0.252
TDF	50.255	7816671	7820041	7832017	7822910	8065	0.103
	50.255	7804413	7862535	7814250	7827066	31108	0.397
	50.255	7863229	7821451	7825599	7836760	23017	0.294

TABLE: 4.12 Summary of ANOVA analysis for precision study (intra-day)

Groups	Count	Sum (Analyte/IS)	Average	Variance
I (at 10:00 am)	3	1.385817084	0.461939028	4.6643E-06
II (at 01:00 pm)	3	1.38504671	0.461682237	1.75399E-06
III (at 04:00 pm)	3	1.375885473	0.458628491	3.54619E-06

Source of Variation	Sum of Squares	Degree of Freedom	Mean of Squares	F	P-value	F critical
Between Groups	2.0351E-05	2	1.01755E-05	3.063522248	0.121112463	5.143253
Within Groups	1.9929E-05	6	3.3215E-06			
Total	4.028E-05	8				

TABLE: 4.13 Summary of ANOVA analysis for precision study (inter-day)

Groups	Count	Sum (Analyte/IS)	Average	Variance
I (Day 1)	3	1.381147701	0.460382567	6.20602E-06
II (Day 2)	3	1.384022629	0.461340876	2.03014E-06
III (Day 3)	3	1.386333712	0.462111237	1.19046E-08

Source of Variation	Sum of Squares	Degree of Freedom	Mean of Squares	F	P-value	F critical
Between Groups	4.5001E-06	2	2.25006E-06	0.81839427	0.484977346	5.143253
Within Groups	1.6496E-05	6	2.74936E-06			
Total	2.0996E-05	8				

C. Accuracy

The accuracy of an analytical procedure expresses the closeness of agreement between the value which is accepted either as a conventional true value or an accepted reference value and the value found. The accuracy of the developed HPLC method was determined by recovery study. Six replicates were analyzed at 100% concentration level and three replicates each at 50% and 150% concentrations. Assessment of accuracy was accomplished by evaluating the percent recovery of the analyte as shown in Table 4.14.

TABLE 4.14: Data of recovery study for Accuracy Parameter

Sample details		Area of EFV	Area of TDF	Ratio	Amount found (µg/ml)	Amount added (µg/ml)	% Recovery
Recovery at 50% level	Set-1	1852461	7812521	0.237	12.617	0.987	100.6
	Set-2	1843251	7832151	0.235	12.519	0.979	99.8
	Set-3	1838369	7842611	0.234	12.467	0.982	99.4
Recovery at 100% level	Set-1	3624812	7810063	0.464	25.229	2.014	100.6
	Set-2	3648599	7896541	0.462	25.114	2.005	100.1
	Set-3	3617955	7852116	0.461	25.042	1.999	99.8
	Set-4	3602488	7821562	0.461	25.032	1.998	99.8
	Set-5	3624851	7862140	0.461	25.058	2.000	99.9
	Set-6	3638412	7831411	0.465	25.255	2.016	100.7
Recovery at 150% level	Set-1	5391453	7821663	0.689	37.739	3.010	100.3
	Set-2	5422757	7812320	0.694	38.007	3.032	101.0
	Set-3	5451369	7892113	0.691	37.819	3.017	100.5

It can be observed that the percent recovery determined falls in the range of 99 to 101%. As per the literature review, % recovery achieved with several of the reported methods are between 97-103% [8, 11] or even wider range [14, 15].

D. Limit of Detection (LOD) and Limit of Quantification (LOQ)

The detection limit of an individual analytical procedure is the lowest amount of analyte in a sample which can be detected but not necessarily quantitated as an exact value. The quantitation limit of an individual analytical procedure is the lowest amount of analyte in a sample which can be quantitatively determined with suitable precision and accuracy. Out of the various methods described, LOD and LOQ were determined based on signal-to-noise ratio. A signal-to-noise ratio between 3 or 2:1 is generally considered acceptable for estimating the detection limit and a typical signal-to-noise ratio for LOQ is 10:1 [13].

Signal for known low concentration (six replicates of 0.01 µg/ml each) of analyte was compared with blank sample for the LOD. Average signal to noise ratio was found to be 4:1 which was in accordance with the acceptance criteria indicating the detection at concentration of even as low as 0.01 µg/ml concentration also with reliability.

Average signal-to-noise ratio of more than 10:1 were obtained with known low concentrations (six replicates of 0.05 µg/ml solution) of analyte which indicated that even 0.05 µg/ml of efavirenz may also be reliably quantified.

The reported therapeutic range of efavirenz is 1 – 4 µg/ml [17]. Hence the developed method has the potential to estimate even the minimum concentration of drug in effective therapeutic range.

The results obtained are similar with the reported LOD and LOQ determined by dispersive liquid-liquid micro-extraction coupled to high performance liquid chromatography (DLLME) with 0.01 and 0.1 µg/ml [9, 11], 0.02 and 0.05 µg/ml [14], as LOD and LOQ respectively.

E. Specificity

The peak areas of compounds co-eluting with one of the analytes should be less than 20% of the peak areas of the analyte at LOQ. For compounds co-eluting with the internal standard the peak area should be less than 5% of the internal standard area [18].

Specificity of the developed method was checked by recording chromatogram of placebo and comparing with chromatogram of EFV and TDF. No interference was observed at the retention time of EFV and TDF in placebo and diluent as shown in Figure 4.19 indicating the specificity of the analytical method.

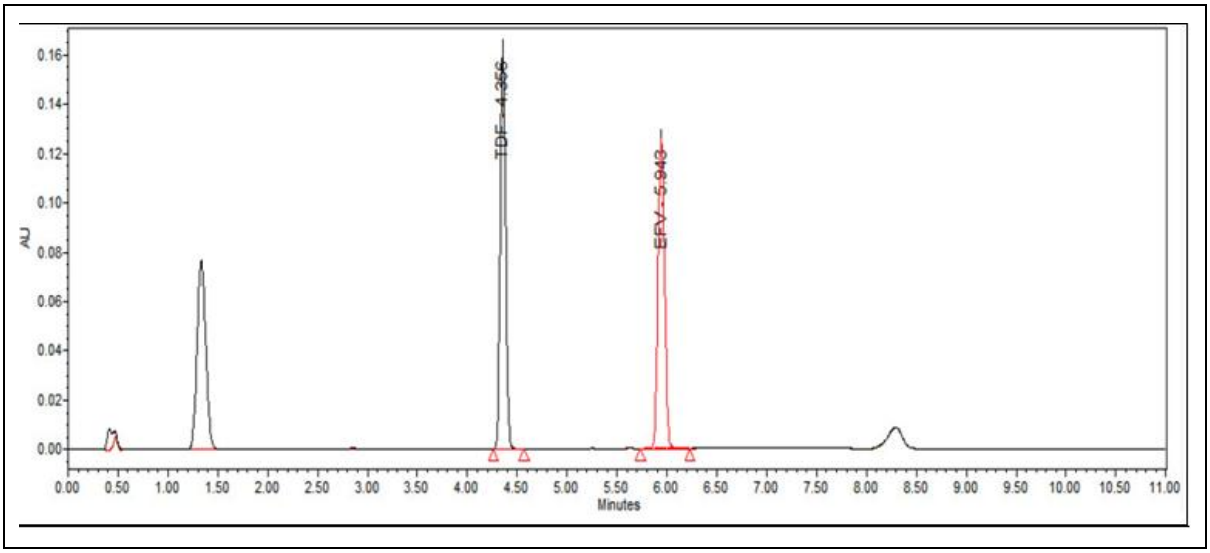

FIGURE 4.19: Chromatogram for specificity (Diluent, Placebo, Standard)

F. Robustness

The robustness of an analytical procedure is a measure of its capacity to remain unaffected by small, but deliberate variations in method parameters and provides an indication of its reliability during normal usage. The robustness of the method was studied by changing the flow rate (±0.2 ml/min), wavelength (±2 nm) and pH of mobile phase (±0.2). Robustness of the developed method was determined in terms of % RSD as shown in Table 4.15.

TABLE 4.15 (a) : Robustness data for change in flow rate

Drug	Param-eters	Flow rate (ml/min)	Injection 1	Injection 2	Injection 3	Injection 4	Injection 5	Injection 6	Mean	% RSD
EFV	RT	1.3	6.103	6.105	6.1	6.102	6.101	6.101	6.102	0.029
		1.5	5.94	5.941	5.941	5.94	5.941	5.942	5.941	0.013
		1.7	5.831	5.832	5.831	5.831	5.832	5.831	5.831	0.009
	Area	1.3	3644512	3642412	3669819	3672156	3652207	3695711	3662802	0.557
		1.5	3594121	3614721	3600781	3612480	3607115	3586470	3602614	0.304
		1.7	3542146	3551482	3540087	3556214	3549860	3556810	3549433	0.197

	Tailing factor	1.3	1	1	1	1	1	1	1.000	0.000
		1.5	1	1	1	1	1	1	1.000	0.000
		1.7	1	1	1	1	1	1	1.000	0.000
	Thear otical plates	1.3	11304	11921	11015	11465	11756	11685	11524	2.874
		1.5	12381	12014	13009	12571	12712	12880	12594	2.863
		1.7	14207	14220	14358	14097	15117	14586	14430	2.604
TDF	RT	1.3	4.521	4.52	4.521	4.523	4.521	4.52	4.521	0.022
		1.5	4.355	4.356	4.356	4.355	4.357	4.355	4.356	0.017
		1.7	4.123	4.128	4.122	4.121	4.125	4.125	4.124	0.056
	Area	1.3	7862141	7865211	7841208	7871190	7883971	7893601	7869553	0.212
		1.5	7816671	7804413	7863229	7821009	7831118	7844471	7830151	0.246
		1.7	7779148	7782547	7782197	7780128	7780224	7793221	7782910	0.061
	Tailing factor	1.3	1	1	1	1	1	1	1.000	0.000
		1.5	1	1	1	1	1	1	1.000	0.000
		1.7	1	1	1	1	1	1	1.000	0.000
	Theo plates	1.3	24364	24008	24971	24851	24739	24013	24491	1.581
		1.5	26752	26001	27021	27339	26987	26017	26686	1.905
		1.7	27658	27966	27845	27921	27332	28014	27789	0.842
Resolution		1.3	5.1	5.7	5.9	5.4	5.5	5.1	5.5	5.376
		1.5	5.3	5.1	5	5.1	5.1	5.6	5.2	3.846
		1.7	5.6	5.7	5.5	5.9	5.8	5.8	5.7	2.351

TABLE 4.15 (b) : Robustness data for change in wavelength

Drug	Param-eters	Wavelength (nm)	Injection 1	Injection 2	Injection 3	Injection 4	Injection 5	Injection 6	Mean	% RSD
EFV	RT	258	5.940	5.941	5.941	5.94	5.941	5.942	5.941	0.012
		260	5.940	5.941	5.941	5.94	5.941	5.942	5.941	0.012
		262	5.940	5.941	5.941	5.94	5.941	5.942	5.941	0.012
	Area	258	3593951	3614251	3601245	3612701	3608012	3586801	3602826	0.276
		260	3594121	3614721	3600781	3612480	3607115	3586470	3602614	0.278
		262	3594981	3614411	3600497	3613001	3607820	3586101	3602801	0.280
	Tailing factor	258	1	1	1	1	1	1	1.000	0.000
		260	1	1	1	1	1	1	1.000	0.000
		262	1	1	1	1	1	1	1.000	0.000
	Theor etical plates	258	12220	12178	12800	12621	12797	12725	12556	2.072
		260	12381	12014	13009	12571	12712	12880	12594	2.614
		262	12370	12103	12891	12709	12624	12768	12577	2.109

TDF	RT	258	4.355	4.356	4.356	4.355	4.357	4.355	4.356	0.017
		260	4.355	4.356	4.356	4.355	4.357	4.355	4.356	0.017
		262	4.355	4.356	4.356	4.355	4.357	4.355	4.356	0.017
	Area	258	7816210	7805214	7863524	7821280	7831331	7844921	7830413	0.246
		260	7816671	7804413	7863229	7821009	7831118	7844471	7830151	0.246
		262	7816241	7804124	7864517	7821987	7831127	7844678	7830445	0.252
	Tailing factor	258	1	1	1	1	1	1	1.000	0.000
		260	1	1	1	1	1	1	1.000	0.000
		262	1	1	1	1	1	1	1.000	0.000
	Theo plates	258	26801	26120	26987	27211	27108	26330	26759	1.504
		260	26752	26001	27021	27339	26987	26017	26686	1.905
		262	26802	26281	27178	27271	26721	26208	26743	1.505
Resolution		258	5.3	5.1	5	5.1	5.1	5.6	5.200	3.846
		260	5.3	5.1	5	5.1	5.1	5.6	5.200	3.846
		262	5.3	5.1	5	5.1	5.1	5.6	5.200	3.846

TABLE 4.15 (c) : Robustness data for change in pH of mobile phase

Drug	Parameters	pH	Injection 1	Injection 2	Injection 3	Injection 4	Injection 5	Injection 6	Mean	% RSD
EFV	RT	3.3	5.830	5.830	5.830	5.828	5.829	5.828	5.829	0.015
		3.5	5.940	5.941	5.941	5.940	5.941	5.942	5.941	0.012
		3.7	6.112	6.110	6.112	6.114	6.112	6.112	6.112	0.019
	Area	3.3	3544874	3562199	3584152	3555841	3561422	3499658	3551357	0.730
		3.5	3594121	3614721	3600781	3612480	3607115	3586470	3602614	0.278
		3.7	3599641	3597821	3600485	3610308	3661421	3658741	3621402	0.763
	Tailing factor	3.3	1.0	1.0	1.0	1.0	1.0	1.0	1.000	0.000
		3.5	1.0	1.0	1.0	1.0	1.0	1.0	1.000	0.000
		3.7	1.0	1.0	1.0	1.0	1.0	1.0	1.000	0.000
	Theoretical plates	3.3	14311	14368	14285	14268	14336	14451	14336	0.423
		3.5	12381	12014	13009	12571	12712	12880	12594	2.614
		3.7	11278	11721	11458	11774	11498	11338	11511	1.588
TDF	RT	3.3	4.112	4.112	4.115	4.113	4.11	4.112	4.112	0.036
		3.5	4.355	4.356	4.356	4.355	4.357	4.355	4.356	0.017
		3.7	4.449	4.448	4.451	4.452	4.446	4.448	4.449	0.045
	Area	3.3	7789211	7821146	7792351	7701236	7782971	7782399	7778219	0.473
		3.5	7816671	7804413	7863229	7821009	7831118	7844471	7830151	0.246
		3.7	7854742	7860045	7851468	7841136	7859941	7884263	7858599	0.167

	Tailing factor	3.3	1	1	1	1	1	1	1.000	0.000
		3.5	1	1	1	1	1	1	1.000	0.000
		3.7	1	1	1	1	1	1	1.000	0.000
	Theo plates	3.3	27568	27450	27005	26894	26993	26473	27063	1.341
		3.5	26752	26001	27021	27339	26987	26017	26686	1.905
		3.7	24200	24682	24791	24931	24013	24228	24474	1.396
Resolution		3.3	5.5	5.5	5.5	5.8	5.4	5.6	5.550	2.267
		3.5	5.3	5.1	5.0	5.1	5.1	5.6	5.200	3.846
		3.7	5.3	5.3	5.4	5.7	5.1	5.6	5.400	3.704

No significant changes in the chromatographic parameters were observed when changing the optimized experimental conditions (flow rate, wavelength, pH of mobile phase). Robustness of the developed method was determined in terms of % RSD as shown in Table 4.15(a), 4.15(b) and 4.15(c) which are summarized in Table 4.15(d). The RSD in all the investigations were found to be less than 5. Robustness with respect to change in flow rate, wavelength and pH has not been investigated in various reported results [10, 15, 18]. RSD values of up to 7.5 has been reported [9].

TABLE 4.15 (d): Summary of robustness data for change in different parameters

Parameters		**RSD**	
		EFV	**TDF**
Change in flow rate (±0.2 ml/min)	Retention time	2.288	4.602
	Area	1.573	0.554
	Tailing factor	0	0
	Resolution	4.604	4.604
Change in wavelength (±2 nm)	Retention time	2.391	4.042
	Area	1.009	0.521
	Tailing factor	0	0
	Resolution	3.262	3.262
Change in pH of mobile phase (±0.2)	Retention time	2.391	4.042
	Area	1.009	0.521
	Tailing factor	0	0
	Resolution	3.262	3.262

G. Stability of analytical solution:

Stability of the analytical solution was tested at 2, 4, 6, 12, 18, 24 hours and after 10 days, and compared with chromatograms of freshly prepared sample. No significant change ($p > 0.05$) was observed indicating the stability of the analytical solution for 10 days, the time being based on the expected duration of analysis. Stability of the samples up to 6 hours at room temperature has been reported in other similar investigations [10]. The stability of efavirenz in human plasma when stored at −20 ^{0}C has been reported for upto 30 days [14].

TABLE 4.16: Summary of validation Parameters

S.No.	Parameters	Results
1	Linearity range	1-300 µg/ml
2	Correlation coefficient	0.999
3	LOD	0.01 µg/ml
4	LOQ	0.05 µg/ml
5	Retention time	5.941 $\pm$ 0.013 min

Thus it can be concluded that a simple and sensitive reversed-phase HPLC gradient method has been developed and validated for the estimation of EFV in plasma using UV detector. The summary of the validation parameters has been presented in Table 4.16. A good resolution was obtained between EFV and TDF as internal standard with retention time 5.941 minutes and 4.356 min respectively. There were no interference peaks observed around the retention time of EFV and TDF. The method was found to be linear (R^2= 0.999) within the analytical range of 1-300 µg/ml. The results obtained proved that the method was accurate and reproducible and the drug was stable in plasma. Therefore, the developed chromatographic method can be used for estimation of EFV in plasma with good resolution to evaluate the pharmacokinetic parameters of EFV.

4.3 Design of Experiment

Literature survey was done to identify and determine the QTPP, CQAs, manufacturing procedures for SLN, various process and formulation attributes having effect on product CQAs. For the intended solid lipid nanoparticulate drug delivery system, almost all routes of administration – oral, parenteral, dermal, ocular, nasal, etc. have been reported for topical, systemic or central nervous system actions. For better absorption of the drug, minimum average size of the nanoparticles is desired. Hence, minimum particle size is one of the most important CQA along with minimum PDI (monodispersity), maximum entrapment efficiency, minimum zeta potential of ± 20 mV for stability [19] and no residual solvent for avoiding toxicity and ensuring safety. A CQA is a physical, chemical, biological, or microbiological property or characteristic that should be within an appropriate limit, range, or distribution to ensure the desired product quality [20, 21]. In the present investigation, different preliminary experiments were carried out for selection of suitable excipients/materials which may directly and/or indirectly influence critical quality attributes. The compatibility of the drug-excipient was checked before the optimization of various process and formulation variables. With the selected excipients, various critical process variables identified through literature were optimized sequentially as per the steps involved in the formulation. Finally, the formulation variables were optimized using 3^2 factorial design and design expert software for analyzing the data statistically and graphically using response surface plots [22-26].

4.4 Preformulation studies

The major components for the solid lipid nanoparticulate system include the drug, lipid and surfactant. After the identification of the drug, various materials were screened as components for the proposed system. These selections were based on the solubility of the drug and their ability to produce small sized particles. The selections were also based on the safety profile and approval status of the components.

4.4.1 Selection of lipid

Improved permeability of the drug is reported due to lipid content in SLN [27]. SLN contain

lipids which remain solid at room temperature and body temperature. The lipids are pure triglycerides (tristearin, tripalmitin, trimyristin, etc.), long chain alcohols (cetyl alcohol), waxes (bees wax, cetyl palmitate) and sterols (cholesterol) [28]. The selection of the lipid was primarily based on the solubility of the drug in lipid since higher the solvent capacity, higher will be the drug loading potential [29, 30]. The solubility of the drug was determined in six different lipids - Glycerymonostearate, Glyceryl behenate (Compritol 888 ATO), Glyceryl tripalmitate (Tripalmitin), Glyceryl palmitostearate, Glyceryl distearate and Cetyl palmitate. The results obtained are as shown in Table 4.17 and Figure 4.20.

TABLE 4.17: Selection of lipid based on solubility of drug in lipid

Lipids	Melting Point (^{0}C)	Solubility of drug in lipid (mg / g)
Glycerymonostearate	58-59	40-60
Compritol 888 ATO (Glyceryl behenate)	70-71	40-60
Tripalmitin (Glyceryl tripalmitate)	**66-68**	**110-130**
Glyceryl palmitostearate	53-57	60-80
Glyceryl distearate	65-77	20 -40
Cetyl palmitate	43-57	60-80

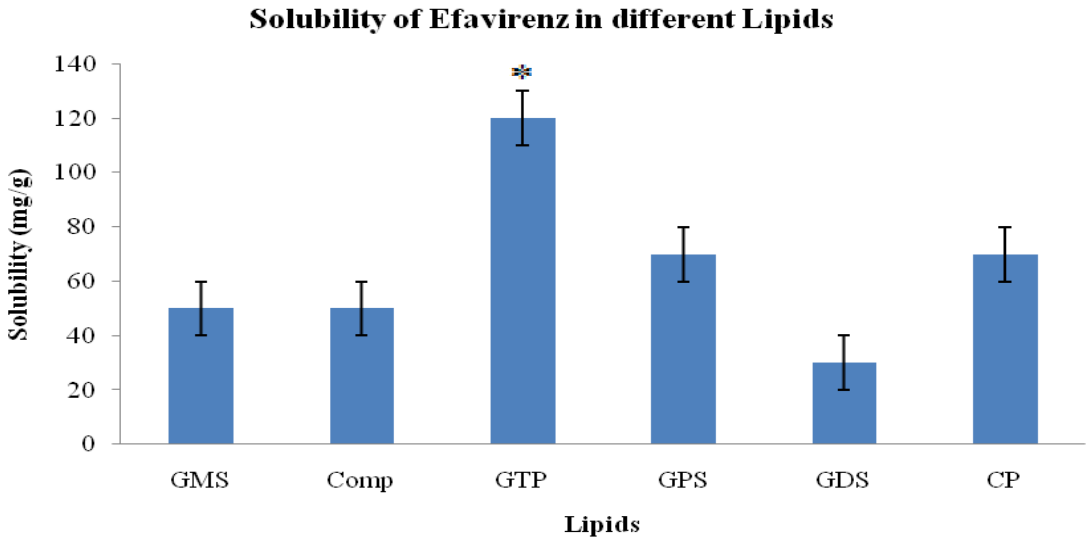

FIGURE 4.20: Solubility of Efavirenz in different lipids [GMS: Glycerymonostearate, Comp: Compritol 888 ATO (Glyceryl behenate), GTP: Glyceryl tripalmitate(Tripalmitin), GPS : Glyceryl palmitostearate, GDS: Glyceryl distearate, CP: Cetyl Palmitate]

Glyceryl tripalmitate (tripalmitin) showed maximum drug solubilizing capacity of 120 ± 10 mg drug / gram of lipid while glyceryl palmitostearate and cetyl palmitate showed next highest solubilizing capacity of 70 ± 10 mg drug / gram of lipid. Thus, the solubility of drug in glyceryl tripalmitate was found to be significantly higher than other lipids ($p < 0.05$). Medium and long chain fatty acids are also reported to have good solvent capacity in comparison to short chain fatty acids. Moreover, triglycerides have many advantages as the foundation of lipid-based delivery systems. They are commonly ingested in food, fully digested and absorbed, and therefore do not present any safety issues [30]. Tripalmitin also has GRAS status as per 21 CFR § 186.1555 and hence was selected for further investigations. Glyceryl tripalmitate is also reported to be used for SLN preparation during various investigations [31-34].

4.4.2 Selection of Surfactant

SLN are the colloidal system of nanoparticles made up of solid lipid as matrix medium which is stabilized in aqueous media by surfactants [28]. Solubilization of endothelial cell membrane lipids and membrane fluidization due to surfactant effect leads to improved permeability [27]. For the selection of surfactant, nanoparticles were prepared with six different surfactants using tripalmitin as lipid and were evaluated for particle size, PDI and entrapment efficiency. The results obtained are as shown in Table 4.18.

TABLE 4.18: Selection of Surfactant on the basis of Particle size, PDI and Entrapment Efficiency

S. No.	Lipid	Surfactant (1% w/w)	Particle size* (nm)	PDI*	Entrapment Efficiency* (%)
1	**Tripalmitin**	**Poloxamer 188 (Pluronic F68)**	**566.4±7.4#**	**0.494±0.2**	**23.93±0.31**
2	Tripalmitin	Poloxamer 407 (Pluronic F127)	891.1±8.1	0.363±0.3	16.50±0.51

3	Tripalmitin	Poloxamer 245 (Pluronic P 85)	628.3±9.3	0.488±0.3	18.31±0.57
4	Tripalmitin	Polysorbate 20	697.4±9.7	0.511±0.4	17.33±0.49
5	Tripalmitin	Polysorbate 60	620.5+8.9	0.500+0.3	20.14±0.63
6	Tripalmitin	Polysorbate 80	601.3±8.5	0.499±0.3	21.23±0.90

{PDI: Polydispersity Index, *Data expressed as mean ± SD (n = 3), # indicates statistical significance ($p < 0.05$)}

Poloxamer 188 (Pluronic F68) was found to give minimum particle size and PDI with maximum entrapment efficiency. The difference in particle size was found to be statistically significant in comparison to others ($p < 0.05$) while the differences observed in PDI and entrapment efficiency were statistically non-significant. Poloxamers are nonionic triblock copolymers composed of a central hydrophobic chain of polyoxypropylene (poly (propylene oxide)) flanked by two hydrophillic chains of polyoxyethylene (poly(ethylene oxide)). Poloxamers are also reported to sterically stabilize the nanoparticles and reduce the adsorption plasma proteins or opsonins on the surface of nanoparticles by providing hydrophilic property to the surface of nanoparticles, thus can prevent the clearance of drug containing SLN from circulation [28]. In general, bulky and non-ionic surfactants are reported to be less toxic than single-chain and ionic surfactants [30]. Hence, Poloxamer 188, also having GRAS status [35] was selected for further investigations for the formulation.

4.4.3 Drug-Excipient Compatibility Study

IR spectra of pure drug efavirenz, and the physical mixtures of efavirenz, tripalmitin and poloxamer 188 are shown in Figure 4.21.

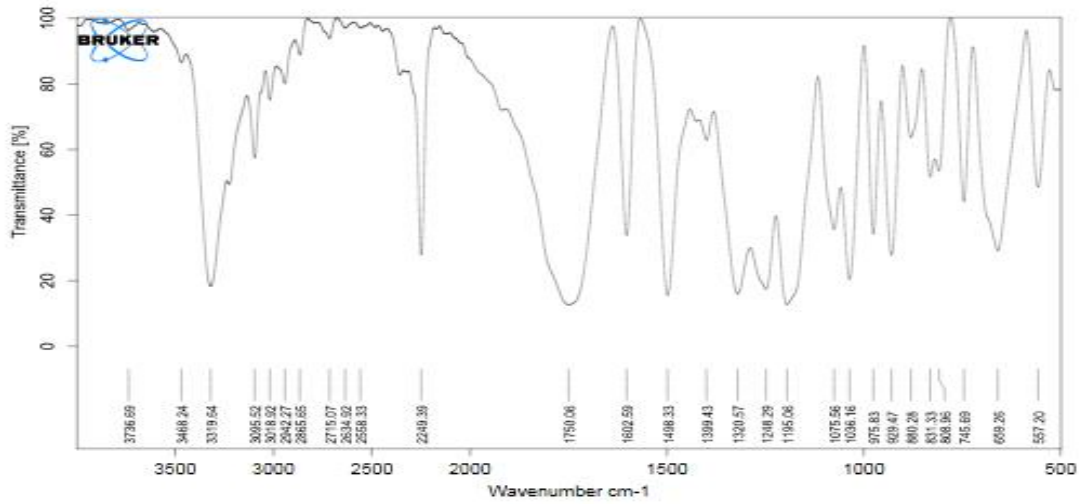

(a)

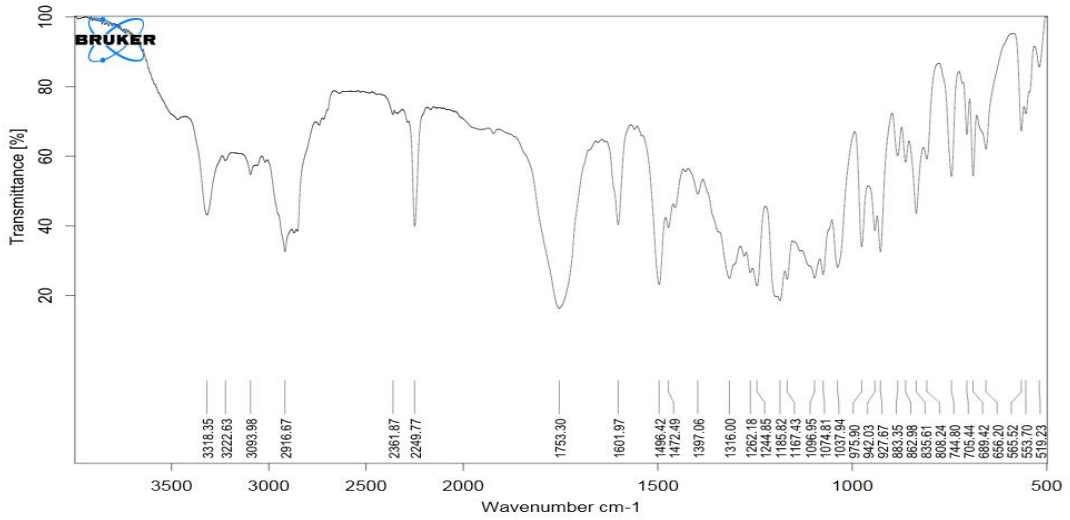

(b)

FIGURE 4.21: IR spectra of drug and physical mixture of drug and excipients. (a) IR spectrum of drug (Efavirenz) (b) IR spectrum of drug (Efavirenz) + Lipid (Tripalmitin) + Surfactant (Poloxamer 188)

It was observed from Figure 4.21, that all major peaks of the drug were obtained in the IR spectra as shown in Table 4.2 and no significant change was observed in the IR spectra of drug-excipients mixture (Figure 4.21(b)) indicating the compatibility of the drug with the selected excipients [36].

4.4.4 Selection of formulation Technique

SLN formulations were prepared by different techniques (as trials) and were compared with respect to particle size, PDI and entrapment efficiency. The results obtained are as shown in Table 4.19.

TABLE 4.19: Comparison of formulation techniques on the basis of Particle size, PDI and Entrapment Efficiency

S. No.	Batch No.	Technique	Particle size* (nm)	PDI*	Entrapment efficiency* (%)
1	SFT01	Solvent evaporation	479.7 ± 13.4	0.373 ± 0.113	42.24 ± 2.3
2	SFT02	**High Pressure Homogenization**	**376.3$^{\#}$ ± 9.5**	**0.380 ± 0.101**	**64.76$^{\#}$ ± 1.9**

{PDI: Polydispersity Index, *Data expressed as mean ± SD (n = 3), $^{\#}$indicates statistical significance ($p<0.01$)}

It was observed that lower particle size with higher entrapment efficiency was obtained by high pressure homogenization. The difference in particle size and entrapment efficiency obtained with two techniques were found statistically significant ($p<0.01$) while the difference in PDI was statistically insignificant. The results were found to be in accordance with the findings reported in the literature [37, 38]. There are no chances of residual organic solvent since the high pressure homogenization technique avoids the use of organic solvent. The use of organic solvents presents a major toxicological disadvantage with solvent evaporation technique [39, 40]. Another advantage of the high pressure homogenization technique is its scale up feasibility as it easily allows a laboratory, pilot or large scale production [41]. Hence, further investigations were carried out with high pressure homogenization technique.

4.5 Optimization of Process Variables

Various critical process variables which may have significant effect on the critical quality attributes were identified for each steps involved in the formulation i.e. stirring, high pressure homogenization and sonication. Preliminary optimization of stirring time and RPM of high speed homogenizer (Heidolph silent crusher) were carried out by conducting the experiments at three different RPM (5,000 to 10,000) for three time durations (10 to 20 minutes) at room temperature. From the results obtained in terms of particle size and PDI (as shown in Table 4.20), it was observed that as the homogenization time and/or homogenization speed increased, the particle size decreased which may be attributed to increased force of deforming droplets at higher speed leading to smaller particles [42]. The observation was in accordance to reported results [6]. It was also observed that with the increase in homogenization time PDI also increased which may be due to formation of foam and more aggregation in the formulation. Best results were obtained by stirring at 10,000 RPM for 15 minutes. Hence further investigations were done with homogenization/ stirring speed of 10000 RPM for 15 min.

TABLE 4.20: Optimization of stirring speed (rpm) and stirring on the basis of Particle size and PDI

S. No.	Batch No.	Stirring time (min)	Stirring speed (rpm)	Particle size (nm)	PDI
1	OST01	10	5000	904.3 ± 10.0	0.556 ± 0.221
2	OST02		7500	752.3 ± 8.3	0.433 ± 0.201
3	OST03		10000	354.3 ± 7.2	0.384 ± 0. 187
4	OST04	**15**	5000	886.6 ± 9.4	0.506 ± 0.203
5	OST05		7500	677.0 ± 7.8	0.454 ± 0.189
6	**OST06**		**10000**	**345.6 ± 5.4**[#]	**0.380 ± 0.175**
7	OST07	20	5000	847.6 ± 6.9	0.431 ± 0.116
8	OST08		7500	501.3 ± 5.8	0.549 ± 0.108
9	OST09		10000	308.0 ± 5.2	0.624 ± 0.019

{PDI: Polydispersity Index *Data expressed as mean ± SD (n = 3), [#] indicates statistical significance ($p<0.01$)}

To study the effect of temperature on the performance attributes, particle size and PDI were determined for the investigations carried out at three different temperatures (60-80^{0}C). Best results were obtained at 70^{0}C as observed from Table 4.21. It may be because the lipid would have remained at melted condition at this temperature as well as the temperature is much below the melting point of the drug, hence drug degradation due to temperature remains negligible. In general, higher temperatures result in lower particle sizes due to the decreased viscosity of the inner phase [43].

TABLE 4.21: Optimization of temperature during stirring on the basis of Particle size and PDI

S. No.	Batch No.	Stirring time min)	Stirring speed (rpm)	Temp (^{0}C)	Particle size (nm)	PDI
1	OT01	**15**	**10000**	60	466.7 + 5.1	0.503 + 0.123
2	**OT02**			**70**	**290.2 + 5.0$^{\#}$**	**0.242 +0.111**
3	OT03			80	371.9 + 4.9	0.565 + 0.112

{PDI: Polydispersity Index, *Data expressed as mean ± SD (n = 3), $^{\#}$indicates statistical significance ($p<0.01$)}

Critical process variables involved during the high pressure homogenization were pressure and number of cycles. These were optimized using 3^2 factorial design with Design Expert 9.0.3.1 software (Stat-Ease, Inc., USA). Thirteen runs were carried out with pressure (500 to 900 bars) and number of cycles (3 to 7) as independent variables at three levels and particle size and PDI as dependent variables. Full factorial design used for optimization of process variables is shown in Table 4.22.

TABLE 4.22: Full factorial design with coded and actual values used for optimization of process variables. (Independent variable : Pressure and Number of cycles; Dependent Variable: Particle size and Polydispersity index- PDI)

S. No.	Batch No.	Coded Values		Actual Values		Particle size (nm)	PDI
		Pressure (bar)	No. of Cycles	Pressure (bar)	No. of Cycles		
1	OPC01	-1	-1	500	3	501.0	0.469
2	OPC02	0	-1	700	3	403.1	0.440
3	OPC03	1	-1	900	3	309.8	0.412
4	OPC04	-1	0	500	5	457.7	0.386
5	OPC05	0	0	700	5	376.3	0.380
6	OPC06	1	0	900	5	246.1	0.259
7	OPC07	-1	1	500	7	379.9	0.326
8	OPC08	0	1	700	7	352.7	0.359
9	OPC09	1	1	900	7	235.6	0.261
10	OPC10	0	0	700	5	390.2	0.253
11	OPC11	0	0	700	5	405.5	0.301
12	OPC12	0	0	700	5	389.9	0.286
13	OPC13	0	0	700	5	399.3	0.298

ANOVA was applied to determine the significance and the magnitude of the effects of the variables and their interactions. ANOVA for Response Surface Quadratic model for Response 1 (Particle size) and Response 2 (PDI) are shown in Table 4.23(a) and 4.23(b) respectively.

TABLE 4.23(a): Response Surface Quadratic Model for Particle size (p < 0.0001)

Response 1 - PS (Particle Size)						
ANOVA for Response Surface Quadratic Model						
Analysis of Variance table (Partial sum of squares - Type III)						
Source	**Sum of Squares**	**Df**	**Mean Square**	**F value**	**P-value Prob > F**	
Model	64116.53	5	12823.31	42.26	<0.0001	Significant
A- Pressure	49886.40	1	49886.40	164.42	<0.0001	Significant
B-No. of cycle	10061.42	1	10061.42	33.16	0.0007	Significant
AB	549.90	1	549.90	1.81	0.2202	Not significant
A^2	2681.72	1	2681.72	8.84	0.0207	Significant
B^2	73.55	1	73.55	0.24	0.6375	Not significant
Residual	2123.88	7	303.41	-	-	-
Lack of Fit	1634.49	3	544.83	4.45	0.0915	Not significant
Pure Error	489.39	4	122.35	-	-	-
Cor Total	66240.41	12	-	-	-	-

TABLE 4.23(b): Response Surface Quadratic Model for PDI (p = 0.0272)

Response 2 - PDI (Polydispersity Index)						
ANOVA for Response Surface Quadratic Model						
Analysis of Variance table (Partial sum of squares - Type III)						
Source	**Sum of Squares**	**Df**	**Mean Square**	**F value**	**P-value Prob > F**	
Model	0.049	5	9.838E-003	5.11	0.0272	Significant
A- Pressure	0.010	1	0.010	5.37	0.0536	Not significant
B-No. of cycle	0.023	1	0.023	12.18	0.0101	Significant
AB	1.600E-005	1	1.600E-005	8.314E-003	0.9299	Not significant
A^2	9.659E-005	1	9.659E-005	0.050	0.8291	Not significant
B^2	0.014	1	0.014	7.25	0.0310	Significant
Residual	0.013	7	1.924E-003	-	-	-
Lack of Fit	4.726E-003	3	1.575E-003	0.72	0.5899	Not significant
Pure Error	8.745E-003	4	2.186E-003	-	-	-
Cor Total	0.063	12	-	-	-	-

As observed from Table 4.23 (a), for Response 1 (PS), the Model F-value of 42.26 implies the model is significant. There is only a 0.01% chance that a "Model F-Value" could occur due to noise. Values of "Prob > F" less than 0.0500 indicated model terms are significant. In this case, A (Pressure), B (Number of cycles) and A^2 are significant model terms. Values greater than 0.1000 indicate the model terms AB and B^2 are not significant.

Full model equation for Particle Size in terms of coded factors was obtained as

$PS = +389.62 - 91.18*A - 40.95*B +11.73*AB \quad -31.16 *A^2-5.16*B^2$

Final reduced polynomial equation for Particle Size in terms of coded factors was obtained as

$PS = +388.14 - 91.18*A - 40.95* B - 33.13*A^2$

As shown in Table 4.22(b), ANOVA results confirmed the adequacy of the quadratic model (Model Prob > F is less than 0.05) for PDI. The individual effect of number of cycles (B) was found to be significant (P value <0.05) and of pressure (A) was marginally significant (P value = 0.0536).

Full model equation for PDI in terms of coded factors was found to be

$PDI = +0.31 \quad - 0.042*A - 0.063*B - 2.000E-003*AB - 5.914E-003* A^2 + 0.071*B^2$

Final reduced polynomial equation for PDI in terms of coded factors

$PDI = +0.31 -0.042*A -0.063* B + 0.069*B2$

The regression model obtained was used to generate the contour plots, 3D Surface plots and the overlay plot for particle size and as shown in Figure 4.22 for analyzing interactions of the independent factors. It was observed from Figure 4.22(b) and 4.22(d) that as the pressure and/or number of cycles were increased, the particle size and PDI were found to reduce. The results were found to be in accordance to the findings of Furedi.et. al. [44], whereas it was in contrast to the investigations for production of SLN with cetyl palmitate as the solid lipid where particle size and PDI was observed to be increased with increase in pressure [45].

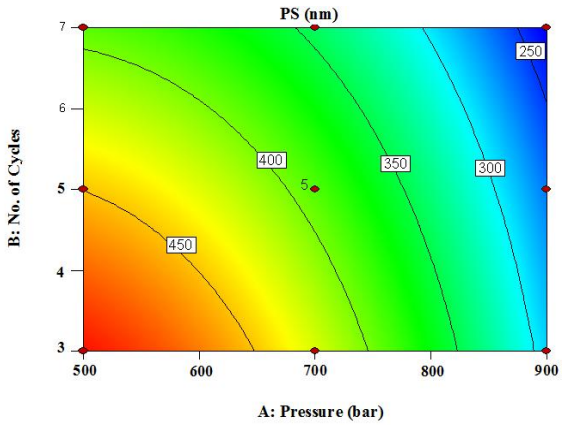

(a)

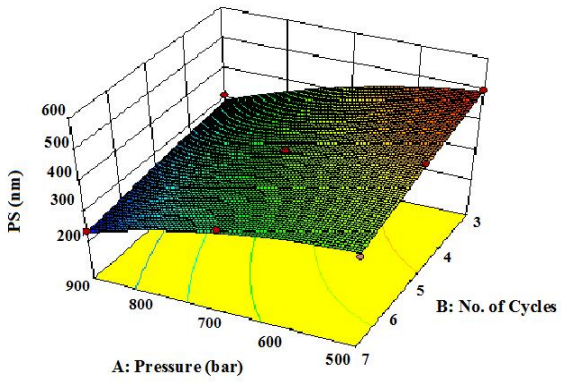

(b)

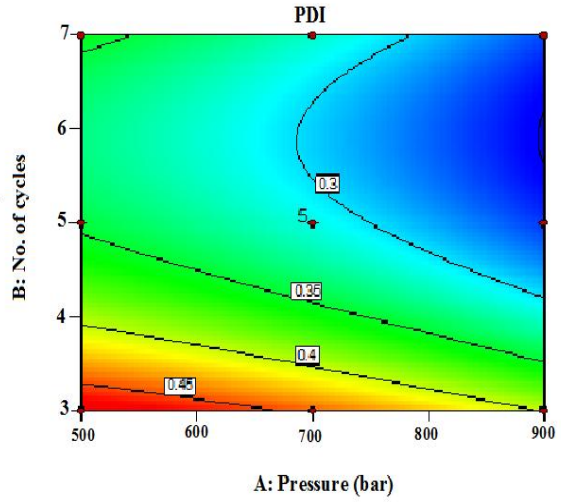

(c)

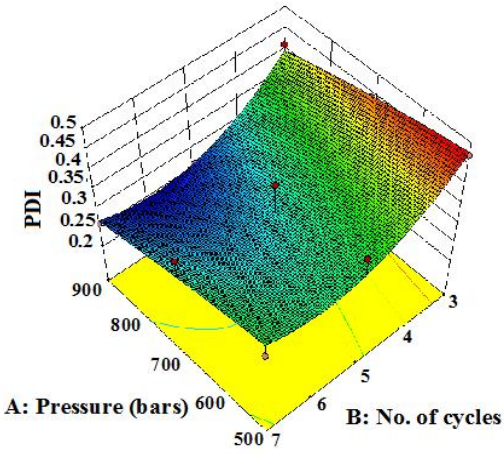

(d)

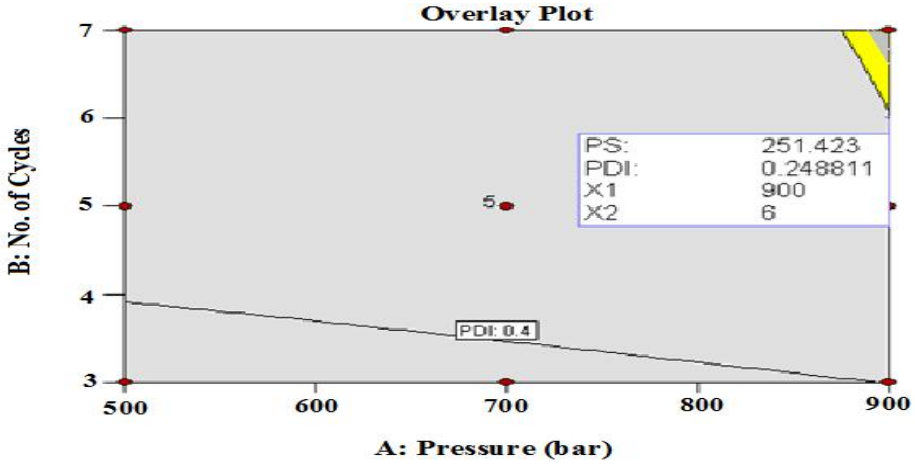

(e)

FIGURE 4.22: Contour plots, 3D surface plots and overlay plot for process variables (a) Contour plot for particle size (b) 3D Surface plot of Particle Size (c) Contour plot for PDI (d) 3D Surface plot of PDI (e) Overlay plot for optimization

4.5.1 Experimental validation of design space

(For process variables during high pressure homogenization)

The multidimensional combination and interaction of input variables and process parameters that have been demonstrated to provide assurance of quality is termed as the design space [24]. Design space could be determined from the common region of successful operating ranges for the two responses and is depicted with the yellow region in the overlay plot [Figure 4.22(e)]. Experimental validation of DoE trials was undertaken by preparation and characterization of nanoparticles at the check point batch suggested by software. The observed values (Particle size 259.7 nm and PDI 0.220) were in close agreement with the predicted values (Particle size 267.274 nm and PDI 0.263276) and established the reliability of the optimization procedure. For further reduction in particle size, the effect of sonication was also investigated and sonication time and amplitude were optimized. The experiments were carried out at three amplitudes for three time durations (data not shown). No significant effect was observed with change in amplitude. Particle size was found to reduce with increase in sonication time but PDI was increased with increased time. Homogenization followed by ultrasonication is reported to be suitable method to produce SLN of 60–380 nm size ranges [46].

4.6 Optimization of Formulation Variables

For the optimization of the formulation variables, %Drug w.r.t. lipid (Drug : Lipid) and concentration of emulsifier were selected as independent variables, each at three levels. Particle size, PDI and drug entrapment were selected as dependent variables (responses). The coded and actual values of the three levels independent variables are shown in Table 4.24. The effect of these independent variables on dependable variables was studied using 3^2 factorial design and Design Expert 9.0.3.1 software (Stat-Ease, Inc., USA). A total of 11 experiments were designed by the software with 2 centre points. Experiments were run in random order to increase the predictability of the model. . Full factorial design used for optimization of formulation variables is shown in Table 4.25.

TABLE 4.24: Coded and Actual values of independent variables of formulation optimization

Independent variables	Levels (Three)		
	Low (-1)	Medium (0)	High (+1)
% Drug w.r.t Lipid (Drug: Lipid)	4% (1:25)	7% (1:14)	10% (1:10)
Concentration of emulsifier	0.5%	1.0%	1.5%

TABLE 4.25: Full factorial design with coded and actual values used for optimization of formulation variables (Independent variable: Amount of drug with respect to lipid and concentration of surfactant; Dependent Variable: Particle size, Polydispersity index-PDI and entrapment efficiency - EE)

S. No.	Batch No.	Coded Values		Actual Values		Particle size (nm)	PDI	EE (%)
		Amt of drug w.r.t lipid (%)	Conc. of surfactant (%)	Amt of drug wrt lipid (%)	Conc. of surfactant (%)			
1	ODS01	-1	-1	4	0.5	259.3	0.250	54.4
2	ODS02	0	-1	7	0.5	246.1	0.247	62.0
3	ODS03	1	-1	10	0.5	194.9	0.306	68.5
4	ODS04	-1	0	4	1.0	175.8	0.172	51.2
5	ODS05	0	0	7	1.0	126.3	0.187	60.5
6	ODS06	1	0	10	1.0	106.3	0.18	66.3
7	ODS07	-1	1	4	1.5	197.4	0.187	34.5
8	ODS08	0	1	7	1.5	191.8	0.214	50.8
9	ODS09	1	1	10	1.5	159.6	0.218	67.2
10	ODS10	0	0	7	1.0	124.5	0.204	62.0
11	ODS11	0	0	7	1.0	137.9	0.197	61.5

ANOVA was also applied to determine the significance and the magnitude of the effects of the formulation variables and their interactions. ANOVA for Response 1 (Particle size), Response 2 (PDI) and Response 3 (% Entrapment) are shown in Table 4.26.

TABLE 4.26(a): Response Surface Linear Model for Particle size (p < 0.0001)

Response 1 - PS (Particle Size)						
ANOVA for Response Surface Linear Model						
Analysis of Variance table (Partial sum of squares - Type III)						
Source	**Sum of Squares**	**df**	**Mean Square**	**F value**	**P-value Prob > F**	
Model	19114.42	2	9557.21	73.31	<0.0001	significant
A-A	4913.48	1	4913.48	37.69	0.0003	significant
B-B	14200.94	1	14200.94	108.93	<0.0001	significant
Residual	1042.95	8	130.37	-	-	-
Lack of Fit	1024.26	6	170.71	18.27	0.0528	Not significant
Pure Error	18.69	2	9.34	-	-	-
Cor Total	20157.37	10	-	-	-	-

TABLE 4.26(b): Response Surface Linear Model for PDI (p = 0.0007)

Response 2- PDI (Poly Dispersity Index)						
ANOVA for Response Surface Linear Model						
Analysis of Variance table (Partial sum of squares - Type III)						
Source	**Sum of Squares**	**df**	**Mean Square**	**F value**	**P-value Prob > F**	
Model	0.013	2	6.560E-003	20.94	0.0007	Significant
A-Amt. of drug	1.504E-003	1	1.504E-003	4.80	0.0598	Non significant
B-Conc. of surf.	0.012	1	0.012	37.08	0.0003	Significant
Residual	2.506E-003	8	3.133E-004	-	-	-
Lack of Fit	2.360E-003	6	3.933E-004	5.39	0.1648	Not significant
Pure Error	1.460E-004	2	7.300E-005	-	-	-
Cor Total	0.016	10	-	-	-	-

TABLE 4.26(c): Response Surface Quadratic Model for % Entrapment (p = 0.0007)

Response 3 - EE (Entrapment Efficiency)						
ANOVA for Response Surface Quadratic Model						
Analysis of Variance table (Partial sum of squares - Type III)						
Source	**Sum of Squares**	**df**	**Mean Square**	**F value**	**P-value Prob > F**	
Model	949.81	5	189.96	34.80	0.0007	Significant
A- Amt. of drug	638.60	1	638.60	115.32	0.0001	Significant
B-Conc. of surf.	174.96	1	174.96	31.59	0.0025	Significant
AB	86.49	1	86.49	15.62	0.0108	Significant
A^2	4.65	1	4.65	0.84	0.4014	Significant
B^2	34.78	1	34.78	6.28	0.0541	Not significant
Residual	27.69	5	5.54	-	-	-
Lack of Fit	26.52	3	8.84	15.16	0.0625	Not significant
Pure Error	1.17	2	0.58	-	-	-
Cor Total	977.50	10	-	-	-	-

As observed from Table 4.19, the Model F-value of 73.31 for Response 1 (PS), 20.94 for Response 2 (PDI) and 34.80 for Response 3 (EE) implies the models are significant. Linear models were obtained for Particle size and PDI, while quadratic model showed the best fit for entrapment efficiency. There is only a 0.01% chance that a "Model F-Value" for Response 1 and 0.07% for Response 2 and 3 could occur due to noise. P-values less than 0.0500 indicate model terms are significant.

Polynomial equation for Particle size in terms of coded Factors

PS = +186.35 - 28.62*A - 48.65*B

Final equation for PDI in terms of coded Factors

PDI = +0.21 + 0.016* A -0.044* B

Polynomial equation for EE in terms of coded factors

$EE = +60.84 + 10.32* A - 5.40* B + 4.65* AB - 1.36* A^2 - 3.71* B^2$

The contour plots and 3D Surface plots for particle size, PDI and % entrapment are shown in Figure 4.23. It can be observed that particle size was found to reduce with increase in drug: lipid ratio and increase of concentration of surfactant. The results were found in agreement with the reported observations [42]. The reason may be that with increased drug: lipid ratio (decreased lipid content), less surface area of the lipid with high surface tension would have been exposed which could be easily reduced with less surfactant amount. The excess surfactant may be utilized for further reducing the surface tension due to creation of increased surface area due to reduction of particle size. PDI was also observed to reduce with increase in surfactant concentration. This may be because high concentrations of the surfactant would have reduced the surface tension and facilitated the particle partition during homogenization. The increase of the surface area during HPH occurs very rapidly due to reduction in size. The process of a primary coverage of the new surfaces competes with the agglomeration of uncovered lipid surfaces [27, 42].

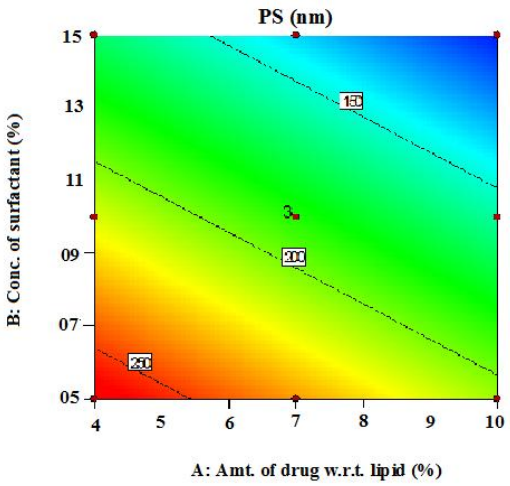

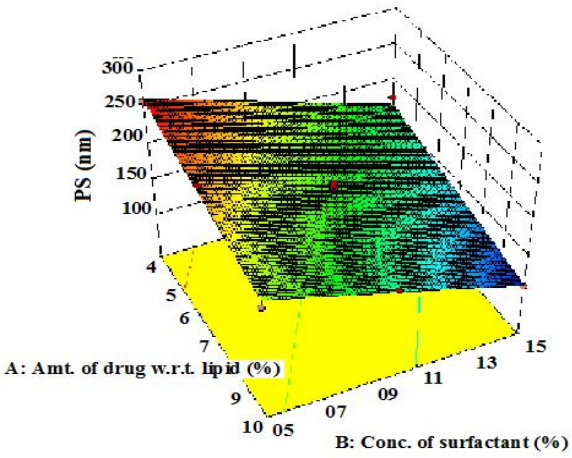

(a) **(b)**

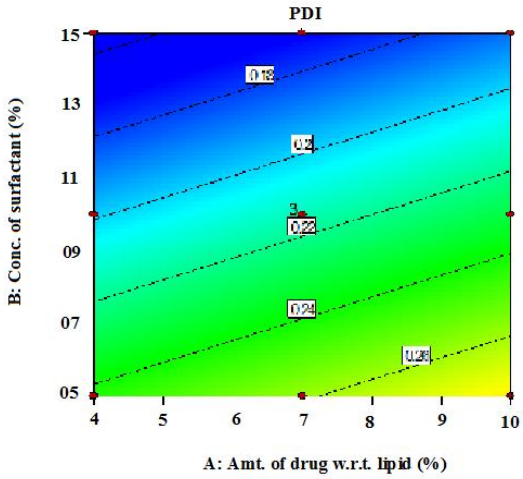

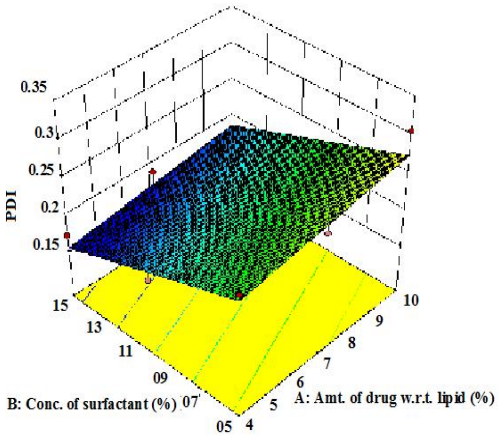

(c) **(d)**

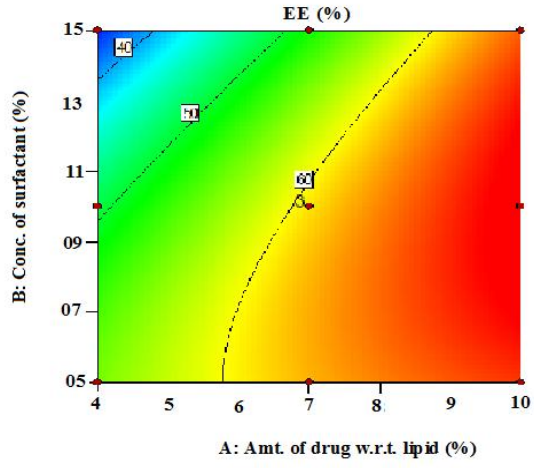

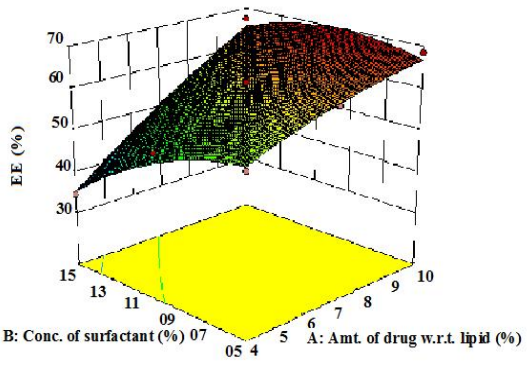

(e) **(f)**

FIGURE 4.23: Contour plots and 3D surface plots for formulation variables (a) Contour plot for particle size (b) 3D Surface plot of Particle Size (c) Contour plot for PDI (d) 3D Surface plot of PDI (e) Contour plot entrapment efficiency (f) 3D Surface plot of entrapment efficiency.

4.6.1 Experimental validation of design space

(For formulation variables)

Experimental validation of DoE trials for formulation variables was undertaken by formulation and characterization of nanoparticles at the check point batch suggested by the software. Figure 4.24 shows the overlay plot displaying the design space and optimized parameters as check point suggested by DoE software to obtain the desired responses. The observed values (Particle size 108.3 nm, PDI 0.172 and EE 64.9%) were comparable with the predicted values (Particle size 109.088 nm, PDI 0.186561 and EE 65.3482) establishing the reliability of the optimization procedure.

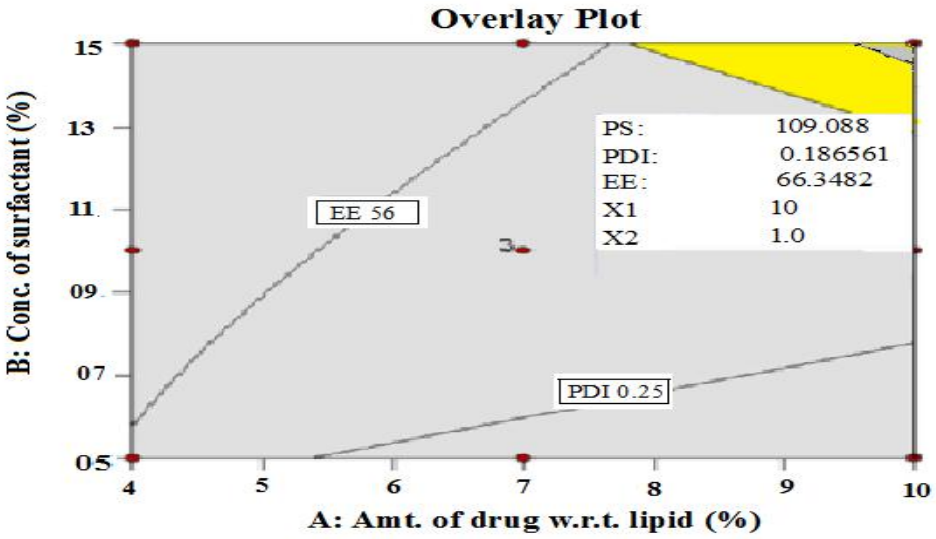

FIGURE 4.24: Overlay plot for optimization of formulation variables.

4.7 Formulation and Optimization of *In-situ* Gel

In order to increase the nasal residence time of the formulation, to achieve increased olfactory delivery to CNS and at the same time maintaining the ease of application of the formulation, *in-situ* gelling system incorporating the developed formulation was developed [47-49]. Olfactory delivery could be improved if nanoparticles are mucoadhesive [50]. Poloxamer 188 (Pluronic F68) and poloxamer 407 (Pluronic F127) were selected as thermo-sensitive polymers based on literature [48, 51-53]. Poloxamers are reported to have poor mucoadhesive properties. Hence, some mucoadhesive polymer is required to be added along with poloxamers to make effective *in-situ* intranasal gel formulation [48]. There are

various agents used for gelling and for mucoadhesive properties like chitosan, lectin, carbopol, etc. Chitosan is one of the naturally occurring biodegradable, biocompatible polysaccharide which is widely investigated and reported to significantly improve the CNS delivery of drug through intranasal route [50, 54, 55]. In the present investigations, different gelling and mucoadhesive agents were screened based on their gelling properties with SLN dispersion. Various trials conducted are shown in Table 4.27. Since proper gel formulation was not achieved with chitosan at nasal pH of 6.4 even on heating, carbopol 934P was selected as gelling/ mucoadhesive agent. No significant incompatibility was observed between drug and the selected excipients as observed with IR spectra of pure drug efavirenz, and the physical mixtures of efavirenz, tripalmitin, poloxamer 188, poloxamer 407 and carbopol 934P (shown in Figure 4.25).

TABLE 4.27 Different trials for selection of gelling/ mucoadhesive agent

S. No.	Trials	Observations
1	100 mg chitosan + 10 ml water →Magnetic stirring	Insoluble
2	100 mg chitosan + 10 ml water –heat--→Mag. stirring	No proper gel
3	100 mg chitosan+10ml warm water(40^0C) → Mag. stirring	Hydrated, lump formation
4	100 mg chitosan + Buffer pH 6.4→ Magnetic stirring	Insoluble
5	100mg chitosan+BufferpH6.4–heat--→Magnetic stirring	Insoluble
6	(100 mg chitosan+ 5 ml water) + (150 mg Pluronic F68 + 5 ml water) → Magnetic stirring	Insoluble
7	(100 mg chitosan + 5 ml water) + (150 mg Pluronic F68 + 5 ml water) –heat--→Magnetic stirring	No proper gel
8	50 mg chitosan + 5 ml SLN dispersion → Mag. stirring	No proper gel
9	100 mg chitosan + 10 ml 0.1 M HCl → Mag. stirring	Soluble/gelling
10	Acidic aqueous solution of chitosan + Buffer pH 6.4	Soluble / slight gelling
11	Carbopol 934P + water → Mag. Stirring	Gel formation
12	**Carbopol 934P + SLN dispersion → Mag. stirring**	**Gel formation**

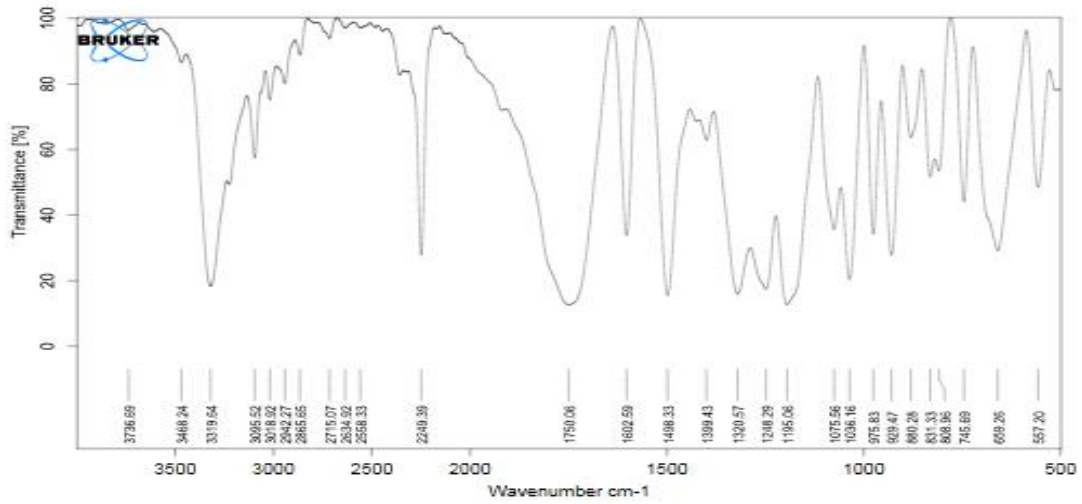

(a)

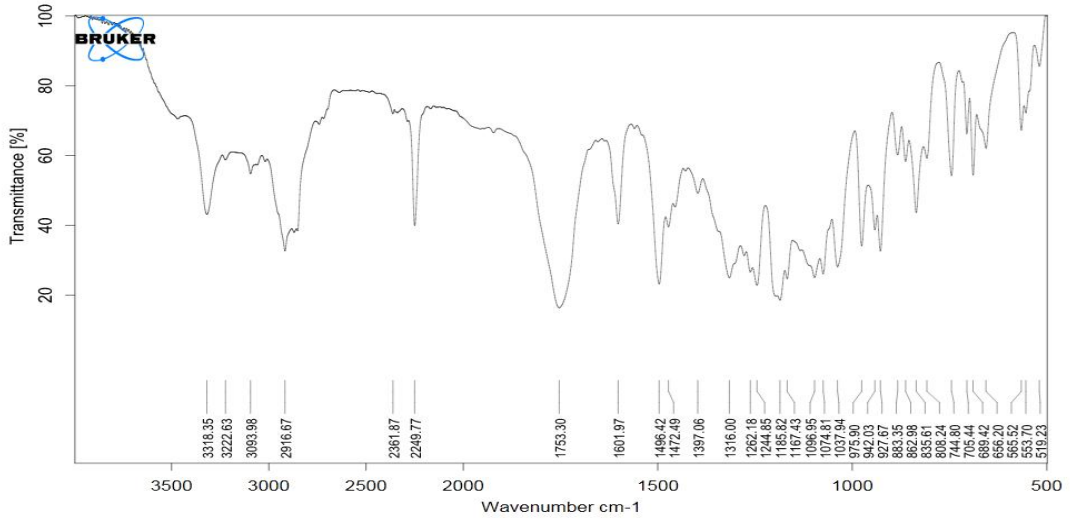

(b)

FIGURE 4.25: IR spectra of drug and physical mixture of drug and excipients. (a) IR spectrum of drug (Efavirenz) (b) IR spectrum of physical mixture of drug and excipients (Efavirenz + Tripalmitin + Poloxamer 188 + Poloxamer 407 + Carbopol 934P)

Ratio of poloxamer 188 and poloxamer 407 were optimized (1:2) based on their gelling behaviour at different temperatures as shown in Table 4.28. The concentration of carbopol 934P selected as gelling/ mucoadhesive was optimized to be 0.4% w/v in the presence of selected thermosensitive polymers as observed from Table 4.29.

TABLE 4.28: Optimization of ratio of poloxamer 188 and poloxamer 407 for gelling behaviour (- : Absence of gelling behaviour, + : slight gelling, ++ : Moderate gelling, +++: Considerable gelling)

S.No.	Pluronic F68: Pluronic F407	Gelling behavior at					
		30^0C	**32^0C**	**34^0C**	**36^0C**	**38^0C**	**40^0C**
1	1:1	-	-	+	+	+	++
2	**1:2**	**-**	**+**	**+**	**+**	**++**	**+++**
3	2:1	-	-	+	+	+	++

TABLE 4.29: Gelling behaviour of SLN dispersion containing thermoresponsive polymers at different concentrations of Carbopol 934P

S. No.	Conc. of Carpool 934 P (%w/v)	Temp (^{0}C)	Gelling behavior	
1	0.1	RT(29^0C) to 40^0C	+	Slight
2	0.2	RT(29^0C) to 40^0C	++	Moderate
3	0.3	RT(29^0C) to 40^0C	+++	Considerable
4	**0.4**	**RT(29^0C) to 40^0C**	**++++**	**Acceptable**
5	0.5	RT(29^0C) to 40^0C	+++++	High

Hence, the optimized formulation variables are as follows

Amount of drug w.r.t lipid : 10% w/w (Drug: lipid =1:10)

Conc. of surfactant: 1.0% w/v

Gelling agent:

Pluronic F68 : 1% w/v (Thermo-sensitive polymer)

Pluronic F127: 2%w/v (Thermo-sensitive polymer)

Carbopol 934P: 0.4% w/v (Mucoadhesive)

4.8 Evaluation of optimized formulation

4.8.1 Particle size, Polydispersity index (PDI), Zeta potential and Entrapment efficiency:

The average particle size, PDI, zeta potential and entrapment efficiency of the solid lipid nanoparticles, determined using Malvern Zetasizer Nanoseries Nano-ZS was found to be 108.3 nm, 0.172, -21.2 mV and 64.9% respectively as shown in Figure 4.26. Most SLN dispersions produced by high pressure homogenization (HPH) are characterized by an average particle size below 500 nm and low microparticle content. The attainable particle size is especially dependent on the composition and concentration of lipid and emulsifier [42]. As per reported observations, optimum size (224.8–266.3 nm) was achieved for Clozapine loaded SLN with different lipids including tripalmitin and 1% poloxamer concentration [31], 241 nm for dihydroartemisinin loaded solid lipid nanoparticles when formulated by single-emulsion solvent evaporation technique [56]. Particles of 200 nm were obtained with polyhydroxy surfactants [42], nanoparticles in the range of 180 – 190 nm were achieved with cetyl palmitate as lipid and are reported to be suitable for targeting to brain [57, 58], size of upto 140 nm was achieved for cetyl palmitate SLN when the formulation of lipid nanoparticles were optimized with the aid of a computer generated experimental design [57]. In general, Z-average size of 20-500 nm are reported depending on the drug, lipid, surfactants and the formulation technique used [31, 48].

Average particle size of less than 110 nm indicated the suitability of the formulation for administration through various routes with the potential of increased permeability and thus enhanced bioavailability of the poorly soluble drug efavirenz. Low PDI value (< 0.2) indicated the narrow distribution of size (monodispersity) and stability of the formulation was indicated by the zeta potential value (-21.2 mV).

Results

		Size (d.nm):	% Intensity:	St Dev (d.n...
Z-Average (d.nm): 108.5	Peak 1:	260.2	100.0	104.9
PdI: 0.172	Peak 2:	0.000	0.0	0.000
Intercept: 0.938	Peak 3:	0.000	0.0	0.000

Result quality : Good

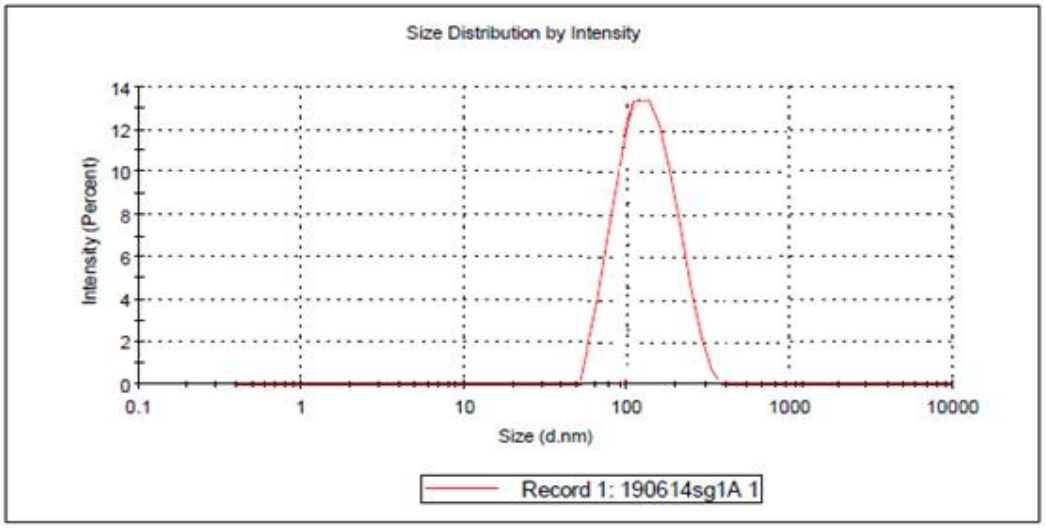

Results

		Mean (mV)	Area (%)	St Dev (mV)
Zeta Potential (mV): -21.2	Peak 1:	-21.2	100.0	6.23
Zeta Deviation (mV): 6.23	Peak 2:	0.00	0.0	0.00
Conductivity (mS/cm): 0.0980	Peak 3:	0.00	0.0	0.00

Result quality : Good

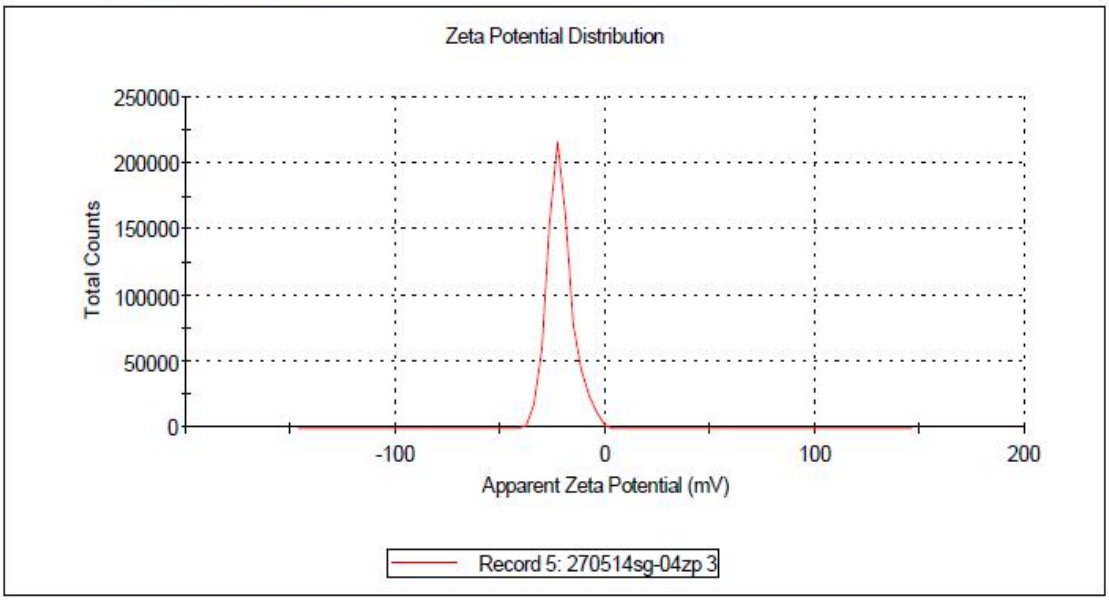

FIGURE 4.26: Size distribution and zeta potential distribution of optimized Efavirenz nanoparticles

Zeta potential is an important physicochemical parameter that influences the stability of nanosuspensions. Extremely positive or negative zeta potential values cause larger repulsive forces, whereas repulsion between particles with similar electric charge prevents aggregation of the particles and thus ensures easy redispersion. In the case of a combined electrostatic and steric stabilization achieved by large molecule weight stabilizers, a minimum zeta potential of ± 20 mV is desirable [59].

4.8.2 Evaluation of SLN based in-situ gel

4.8.2.1 Gelation temperature / Sol–gel transition temperature ($T_{sol-gel}$):

The gelation temperature determined with 2 ml of the sample taken in a glass vial and placed on a magnetic stirrer with heating arrangement was found to be 34^0C. The mean nasal mucosal temperature ranges from 30.2±1.7^{0}C to 34.4± 1.1 ^{0}C. Most of the thermo-reversible gels prepared and reported so far have gelation temperature ranging from 32 to 34 ^{0}C [60].

4.8.2.2 Gelation time:

The time required for complete gelation at 34^0C was found to be less than 1 minute. The gelation within a minute at nasal mucosal temperature ensures the prevention of flow of the formulation when administered and increase the residence time [51].

4.8.2.3 pH:

The pH of the formulation was determined to be 6.0 which indicated non-irritancy of the formulation owing to the pH similar to that of nasal mucosal secretions. The pH of the nasal mucosal secretions ranges from 5.5 to 6.5 in adults and 5.0 to 6.7 in children [61].

4.8.2.4 Viscosity:

Viscosity of the formulation is important since higher the viscosity of the formulation (after *in-situ* gelling on administration at nasal temperature), greater will be the contact time which increases the time for absorption. At the same time, highly viscous formulations may interfere with the normal functions like mucociliary clearance, etc [62]. Viscosity of the formulation was determined to be 19,000 cps at 25^0C (ambient temperature) and 24,500 cps

at 34^0C (nasal temperature).

4.8.2.5 Transmittance:

The EFV nanoparticles loaded *in-situ* gel diluted with distilled water (10 times dilution) was found to be visually clear without any turbidity. The % transmittance was measured to be 92% at 650 nm with reference to distilled water as blank.

4.8.2.6 Mucoadhesive strength:

The mucoadhesive force was determined using modified two-pan balance method [51]. 18.5 ml of water was required to be added to detach the cellophane membrane from the gel. Hence, the mucoadhesive force was calculated as 18150 dynes/cm^2 using Equation (3.2).

$$F = w \times g \quad \text{……..……..Equation 3.2}$$

$$= 18.5 \times 981 \text{ dynes/cm}^2$$

$$= 18148.5 \text{ dynes/cm}^2$$

Where F is the mucoadhesion force (dynes / cm^2),

w is the minimum weight required to break the bond (grams),

g is the acceleration due to gravity (cm/s^2).

4.8.2.7 Spreadability:

Spreadability of the gel was determined by taking 0.5 g gel between two cellophane membranes and placing 100 g weight on it for 1 minute. The diameter of the area in which the gel got spread was measured to be 10 cm/gm gel. Proper spread of the hydrogels on the nasal surface will ensure increased absorption of the drug after intra-nasal administration.

4.8.3 Transmission Electron Microscopy

The surface morphology of the optimized SLN was investigated using transmission electron microscope. The image taken using transmission electron microscope with CCD camera (TEM Philips Tecnai 20, Holland) is shown in Figure 4.27. Spherical particles were observed with drug incorporated in the lipid matrix.

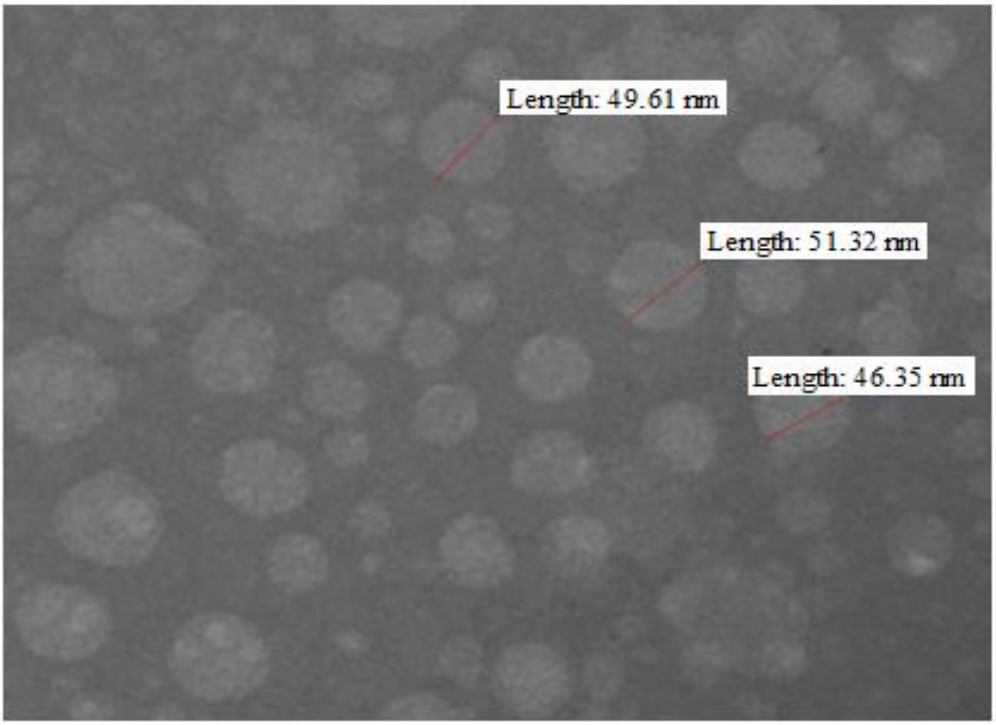

FIGURE 4.27: Transmission Electron Microscopic image of Efavirenz nanoparticles obtained using transmission electron microscope with CCD camera (TEM Philips Tecnai 20, Holland).

4.8.4 Histopathological studies

Histopathological condition of nasal mucosa after treatment with PBS pH 6.4 (negative control), isopropyl alcohol (positive control) and developed formulations are shown in Figure 4.28.

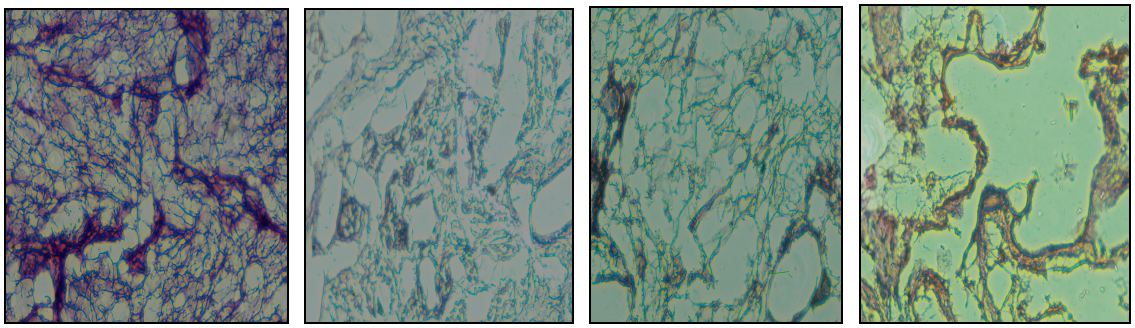

(a) (b) (c) (d)

FIGURE 4.28: Histopathological conditions of nasal mucosa after treatment with (a) Phosphate buffer saline - PBS pH 6.4 (b) SLN dispersion (c) SLN gel (d) Isopropyl alcohol

No significant damage /harmful effects on the microscopic structure of the nasal mucosa treated with SLN formulation was observed in comparison to that of sample treated with isopropyl alcohol indicating the safety of the SLN formulations for nasal adminstration. This was in accordance with the results obtained by Seju et al. [6]. Mucosa treated with isopropyl alcohol showed heavy loss of epithelial cells

4.8.5 Drug Release Profile

4.8.5.1 *In-vitro* drug diffusion profile

In-vitro drug diffusion profiles of the SLN dispersion and EFV loaded SLN gel along with the release profile of plain drug suspension (PDS) for comparison obtained by dialysis-bag/dialysis-sac method and by using Franz diffusion cell method are shown in Figure 4.29(a) and Figure 4.29(b) respectively.

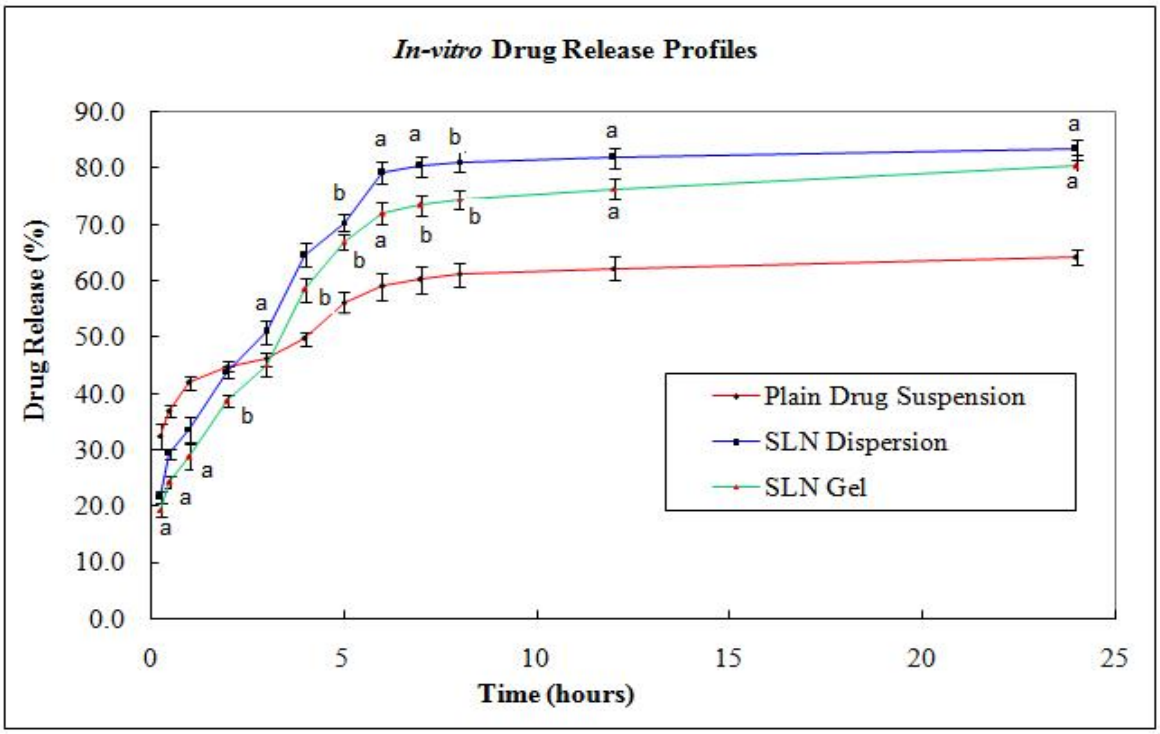

FIGURE 4.29(a): *In-vitro* Drug Release Profile by dialysis-bag method (Different letters indicate statistically significant difference relative to plain drug suspension; a indicate $p < 0.01$ and b indicate $p < 0.05$)

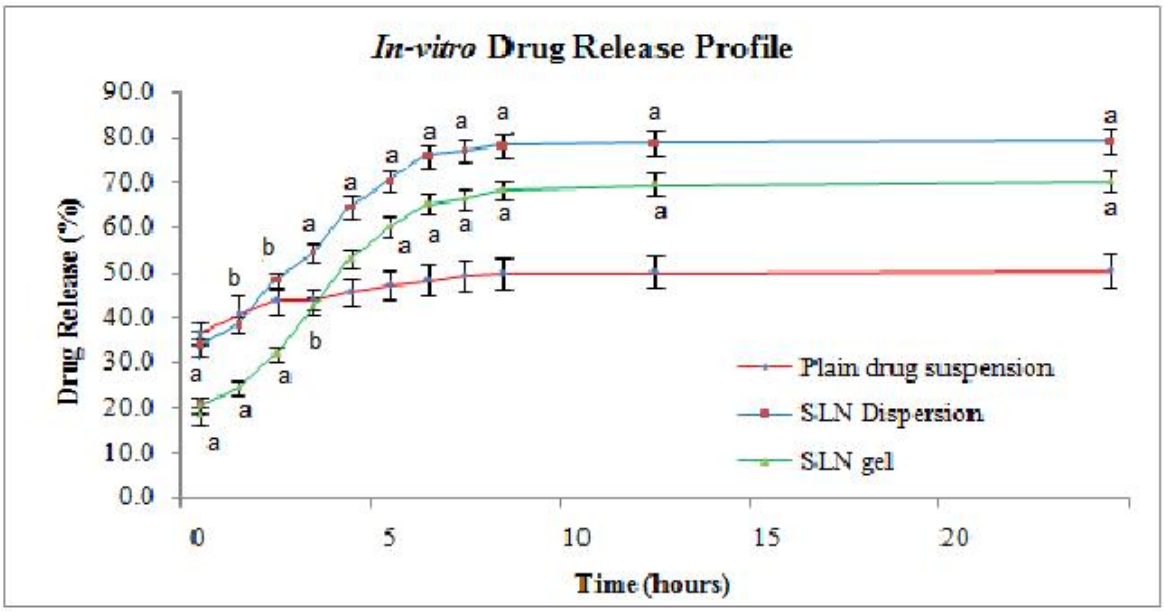

FIGURE 4.29(b): *In-vitro* drug release profile by using Franz-diffusion cell

(PDS: Plain drug suspension, Different letters indicate statistically significant difference relative to PDS; a indicate p < 0.01 and b indicate p < 0.05)

4.8.5.2 *Ex-vivo* drug release profile

The *ex-vivo* drug release profile of SLN dispersion, EFV loaded SLN gel and plain drug suspension (PDS) are shown in Figure 4.30.

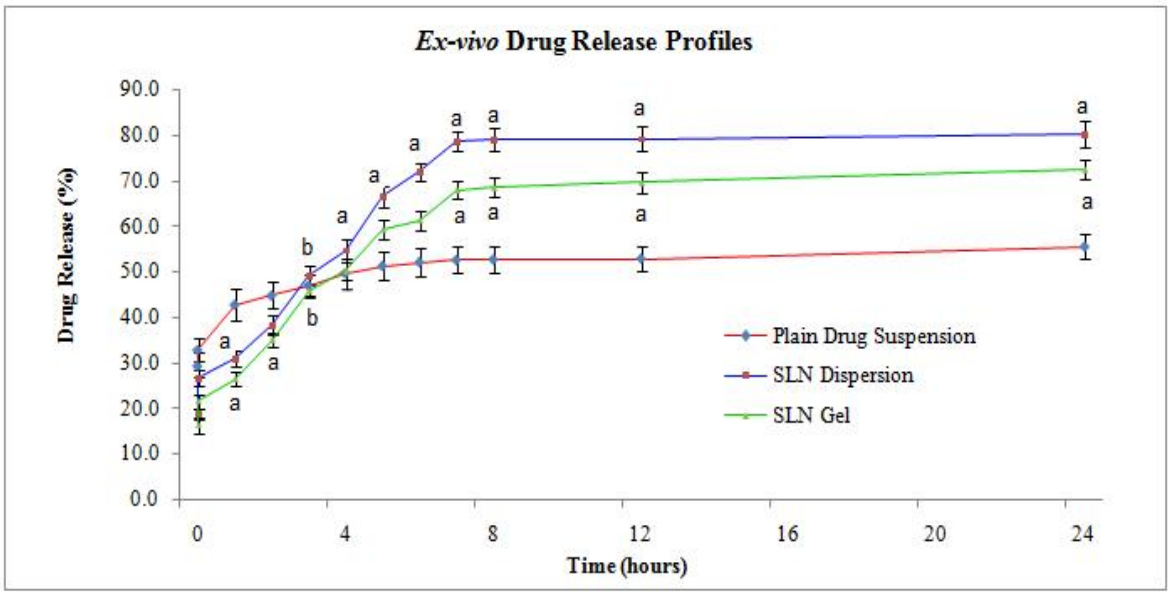

FIGURE 4.30: *Ex-vivo* drug release profile by using Franz-diffusion cell

(PDS: Plain drug suspension, Different letters indicate statistically significant difference relative to PDS; a indicate p < 0.01 and b indicate p < 0.05)

The release of drug from the SLN dispersion was found to be more consistent in comparison to the release from plain drug suspension. It showed initial burst release followed by a prolonged release in accordance with investigations by other researchers [63]. More than 80% drug release was observed in 24 hours with SLN formulations with considerable amount of release achieved within 8 hours in comparison to the drug release of less than 65% in 24 hours with plain drug suspension. The small size of nanoparticles and the presence of surfactant in the developed formulation may have improved the permeability, wetting, solubilization and the dissolution of the soluble surfactants to form pores in the matrix may have played the role for consistent and enhanced release of the drug from nanoparticulate formulations. Similar results are also observed and reported that nano-sized drug delivery systems can enhance nose-to-brain delivery of drugs compared to equivalent drug solutions formulations [7, 48, 64]. Protection of the drug from degradation and/or efflux back into the nasal cavity may partly be the reason for this effect of nanoparticles [65].

4.8.5.3 Kinetics of drug release/ Pharmacokinetic modeling

In order to examine the release mechanism of EFV from the prepared SLN dispersion and the EFV loaded SLN gel, the results of the *ex-vivo* release studies were examined according to various equations for pharmacokinetic modeling. Figures 4.31(a), 4.31(b), 4.31(c), 4.31(d) and 4.31(e) depicts graphs for various mathematical model fitting.

Zero order release:

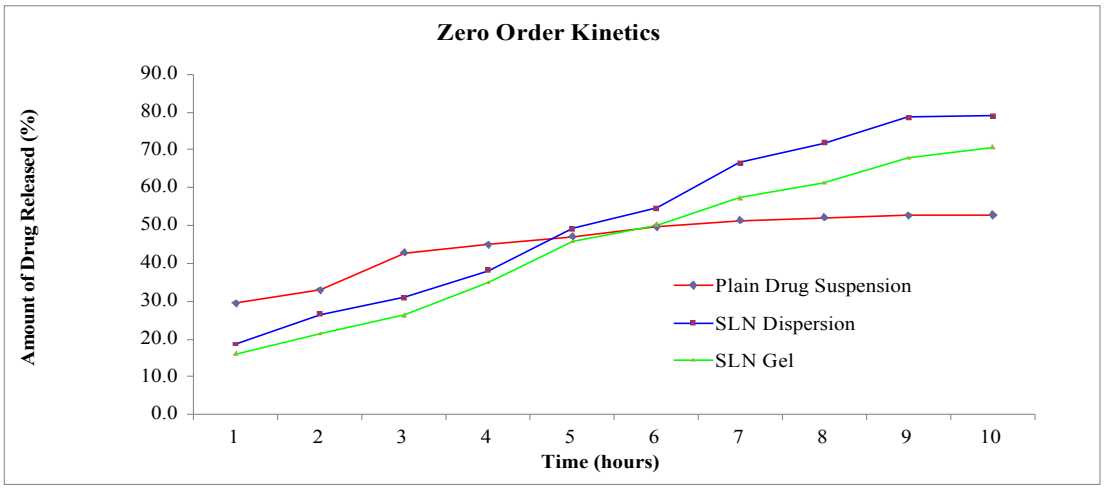

FIGURE 4.31(a): Zero order release kinetics.

First order release:

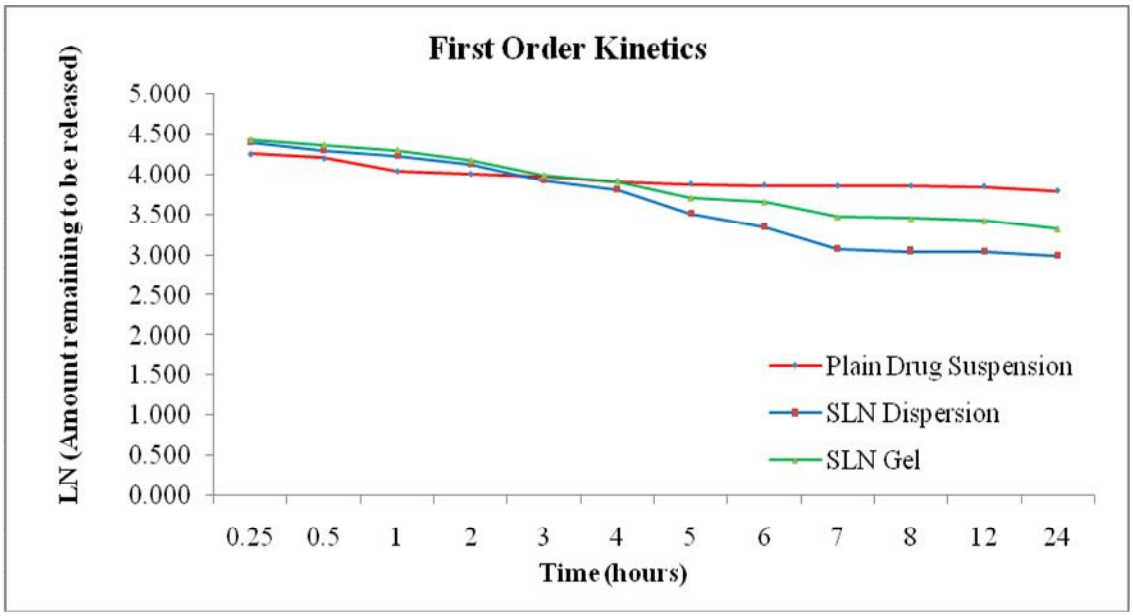

FIGURE 4.31(b): First order release kinetics.

Higuchi Model:

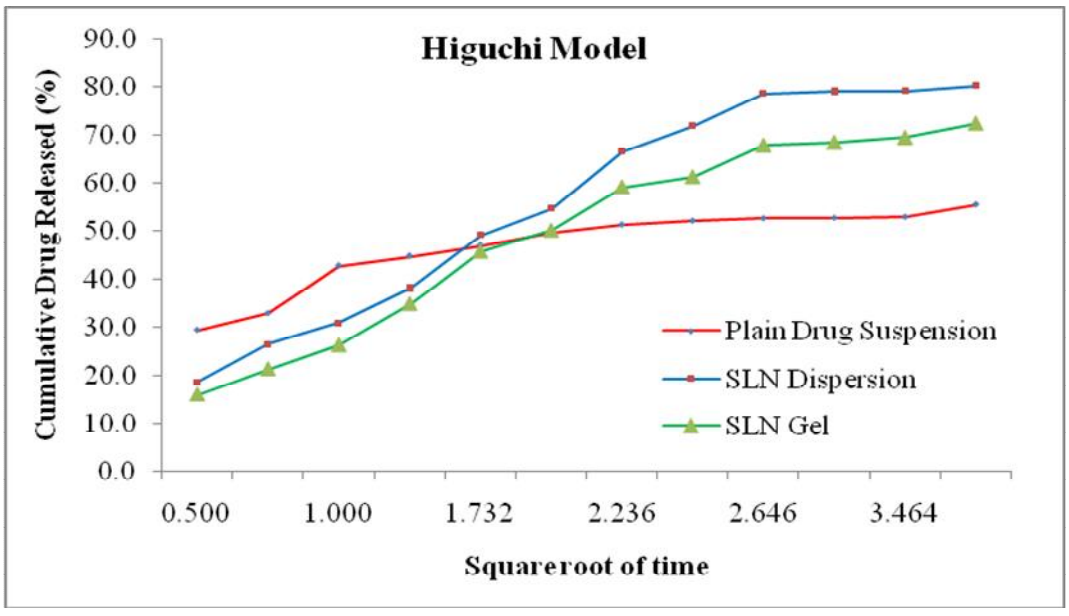

FIGURE 4.31(c): Higuchi Model of release kinetics.

Hixon-crowell cube root model:

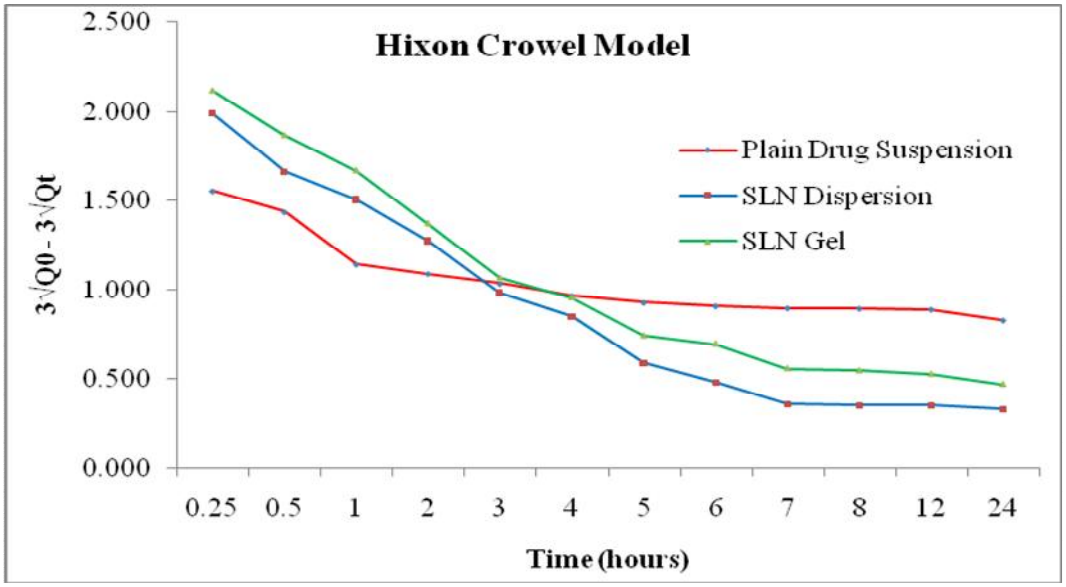

FIGURE 4.31(d): Hixon Crowel Model of release kinetics.

Korsemeyer and peppas model:

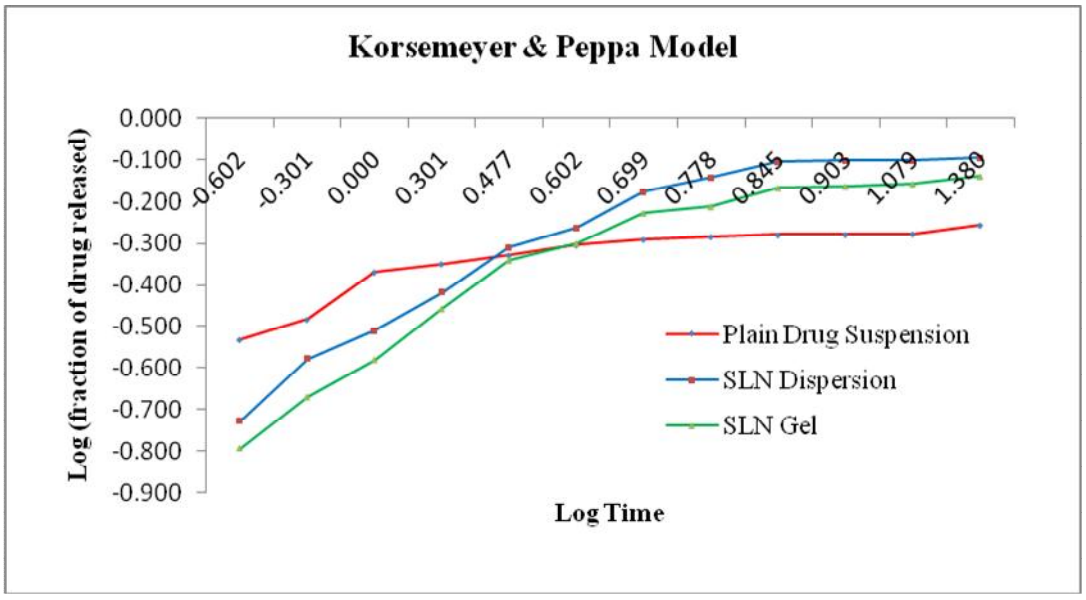

FIGURE 4.31(e): Korsemeyer and Pepppa's Model of release kinetics

The *ex-vivo* release studies data was fitted in to various mathematical models to determine the best-fit model as shown in Table 4.30.

TABLE 4.30 The regression coefficients obtained from model fitting

MODEL	Linear Regression Coefficient (R^2)		
	Plain Drug Suspension	**SLN Dispersion**	**SLN in Gel**
Zero-order	0.8402	**0.9852**	**0.9873**
First-order	0.8529	0.9624	0.9789
Higuchi	0.8137	0.9462	0.9497
Hixon-Crowel	0.7768	0.9161	0.9085
Korsmeyer and Peppas	0.7576 $\Lambda = 0.0211$	0.8911 $\Lambda = 0.0567$	0.8791 $\Lambda = 0.0580$

The release of dug from SLN incoporated formulations best fits in the Zero order release kinetics (R^2 = 0.9936), indicating concentration independent diffusion controlled release [66].

4.8.6 *In-vivo* studies

The concentration of the drug in plasma and brain were determined after intranasal administration of the developed solid lipid nanoparticulate formulation (equivalent to 0.06 mg efavirenz) and were compared with the concentration of the drug achieved in plasma and brain with the oral administration of the marketed formulation (25 mg powder from capsule dispersed in 1 ml water). The ratio of drug concentration in brain to plasma of 15.61% was achieved with the developed formulation in comparison to 0.104% observed with the oral standard indicating the 150 times more brain targeting efficiency of the formulation through intranasal route which may be because of direct nose to brain delivery achieved through integrated olfactory and trigeminal route. The drastic reduction in brain to plasma drug concentration with oral route may be due to first-pass effect, drug degradation in GIT and presence of BBB. The bioavailable fraction of the drug was calculated to be 0.2454 with the

developed formulation while it was found to be 0.0035 with the standard. Relative bioavailabilty was determined to be 70.11 with the developed formulation indicating 70 times better absorption potential of the efavirenz loaded SLN dispersion in comparison to the orally administered drug powder. This may be attributable to systemic absorption of some amount of drug when administered intranasally. This may be higher in comparison to the orally administered drug due to avoidance of first pass metabolism, degradation of drug in GIT, etc. The results were found to be in accordance with the similar investigations with different drugs for brain targeting [48].

4.8.7 Stability Studies

The stability of the formulation was assessed under different storage conditions as per ICH guidelines and the results obtained are as shown in Table 4.31.

TABLE 4.31: Stability study data for the formulation at initial, after 0.5, 1, 2, 3, 6 and 12 months {*Data expressed as mean ± SD (n = 3)}

Temp (^{0}C)/ RH (%)	Time (months)	Appearance	Particle size* (nm)	PDI*	Zeta Potential* (mV)	Drug content (mg/ml)
5°C ± 3°C	0	Transparent with slight bluish	108.5 ± 2.1	0.172 ± 0.003	-21.2 ± 1.9	0.25
	0.5	No significant Change	109.2 ± 1.9	0.175 ± 0.007	-21.1 ± 2.0	0.25
	1	No significant Change	109.9 ± 2.0	0.181 ± 0.009	-20.9 ± 1.5	0.25
	2	No significant Change	110.3 ± 1.8	0.186 ± 0.009	-20.8 ± 1.2	0.25
	3	No significant Change	110.5 ± 2.3	0.190 ± 0.011	-19.7 ± 2.0	0.25
	6	No significant Change	112.3 ± 2.8	0.195 ± 0.015	-18.5 ± 1.8	0.25
	12	No significant change	116.2 ± 2.2	0.201 ± 0.015	-18.9 ± 1.7	0.25

25°C ± 2°C/60% RH ± 5% RH	0	Transparent with slight bluish	108.5 ± 2.1	0.172 ± 0.003	-21.2 ± 1.9	0.25
	0.5	No significant Change	106.5 ± 3.2	0.169 ± 0.004	-20.0 ± 1.8	0.25
	1	No significant Change	109.5 ± 3.5	0.180 ± 0.008	-19.9 ± 2.0	0.25
	2	No significant Change	111.4 ± 3.7	0.197 ± 0.009	-18.2 ±2.2	0.25
	3	No significant Change	112.9 ± 2.9	0.205 ± 0.013	-17.5 ± 1.7	0.25
	6	No significant Change	118.3 ± 2.7	0.209 ± 0.016	-17.0 ± 1.5	0.25
	12	No significant change	125.5 ± 2.7	0.305 ± 0.016	-16.7± 0.01	0.24

The developed formulations were found to be stable for 12 months at 5±3°C and 25 ± 2°C/60 ± 5% RH. No change in the physical appearance of the formulation was observed during the stability studies. No significant change in the Z-average size, PDI and zeta potential were observed during the stability studies when analysed using student's t-test. Thus it can be concluded that efavirenz SLN were stable at long term stability conditions (5±3°C) as well as accelerated conditions (25 ± 2°C/60 ± 5% RH) for 12 months [64, 67, 68].

4.9 References:

1. World Health Organization, (2005). International pharmacopoeia monograph on efavirenz.2005:5-8.
2. USP Medicines Compendium, Monograph. Efavirenz Final Authorized Version 2.0. [Online]. Available: https://mc.usp.org/monographs/efavirenz-2-0. [Accessed 16 November, 2016]
3. Robert M. Silverstein, Francis X. Webster, David J. Kiemle DLB., (2014). *Spectrometric Identification of Organic Compounds*. 8th ed. Wiley Publisher.
4. Kumar YA, Rao NR., (2010). Development of Rapid UV Spectrophotometric Method for the Estimation of Efavirenz in Formulations. *E-Journal Chem*.;7(3):856-860.
5. Kadam AA, Babu CJG, Permal RV, Channabasavaraj K, Mani TT., (2012).

Development and Validation of Method for the Quantitative Estimation of Efavirenz in Bulk and Phrmaceutical Dosage Form. *Am J PharmTech Res*.;2(1):324-330.

6. Seju U, Kumar A, Sawant KK., (2011). Development and evaluation of olanzapine-loaded PLGA nanoparticles for nose-to-brain delivery: In vitro and in vivo studies. *Acta Biomater*.;7(12):4169-4176.
7. Sharma D, Maheshwari D, Philip G, et al., (2014). Formulation and optimization of polymeric nanoparticles for intranasal delivery of Lorazepam using box-behnken design: in vitro and in vivo evaluation. *Biomed Res Int*. 2014;2014:156010.
8. Kamble RN, Mehta P., (2015). Development of simple HPLC method to estimate the blood plasma concentration of Efavirenz in rat after oral administration, Innovare Academic Sciences, *Int. J Pharm & Pharm. Sci.*;7(7):7-10.
9. Heydari R, Rashidipour M, Naleini N., (2014). Determination of efavirenz in plasma by dispersive liquid-liquid microextraction coupled to high-performance liquid chromatography. *Curr Anal Chem*.10(2):280-287.
10. Lakshmi Sailaja , Kishore Kumar K, Ravi Kumar DVR, Mohan Kumar C, Yugandhar NM, Srinubabu G., (2007). Development and Validation of a Liquid Chromatographic Method for Determination of Efavirenz in Human Plasma. *Chromatographia*.;65(5-6):359-361.
11. Saras-Nacenta M, López-Púa Y, Lípez-Cortés LF, Mallolas J, Gatell JM, Carné X., (2001). Determination of efavirenz in human plasma by high-performance liquid chromatography with ultraviolet detection. *J Chromatogr B Biomed Sci Appl*.;763(1-2):53-59.
12. Langmann P, Schirmer D, Väth T, Zilly M, Klinker H, (2001). High-performance liquid chromatographic method for the determination of HIV-1 non-nucleoside reverse transcriptase inhibitor efavirenz in plasma of patients during highly active antiretroviral therapy. *J Chromatogr B Biomed Sci Appl*.;755:151-156.
13. ICH. ICH Topic Q2 (R1) Validation of Analytical Procedures : Text and Methodology. *Int Conf Harmon*. 2005;1994(November 1996):17.

14. Ramachandran G, Kumar a. KH, Swaminathan S, Venkatesan P, Kumaraswami V, Greenblatt DJ., (2006). Simple and rapid liquid chromatography method for determination of efavirenz in plasma. *J Chromatogr B Anal Technol Biomed Life Sci*. ;835(2):131-135.

15. Veldkamp I, van Heeswijk RP, Meenhorst PL, et al., (1999). Quantitative determination of efavirenz (DMP 266), a novel non-nucleoside reverse transcriptase inhibitor, in human plasma using isocratic reversed-phase high-performance liquid chromatography with ultraviolet detection. *J Chromatogr B Biomed Sci Appl*. ;734(1):55-61.

16. Ramaswamy A, Arul Gnana Dhas AS., (2014). Development and validation of analytical method for quantitation of Emtricitabine, Tenofovir, Efavirenz based on HPLC. *Arab J Chem*. 2014.

17. WHO. Safety of Efavirenz. 2010. [Online]. Available: http://www.who.int/hiv/topics/treatment/efavirenz_safety_review.pdf. [Accessed 12 November, 2015]

18. Kappelhoff BS, Rosing H, Huitema AD., Beijnen JH., (2003). Simple and rapid method for the simultaneous determination of the non-nucleoside reverse transcriptase inhibitors efavirenz and nevirapine in human plasma using liquid chromatography. *J Chromatogr B*.;792(2):353-362.

19. Honary S, Zahir F., (2013). Effect of zeta potential on the properties of nano-drug delivery systems - A review (Part 1). *Trop J Pharm Res*.;12(2):255-264.

20. ICH Expert Working Group. Pharmaceutical Development Q8. *ICH Harmon Tripart Guidel*. 2009;8(August):1-28.

21. Fisher SRA, JMP® 8 Design of Experiments Guide, Second Edition. Cary, NC: SAS Institute Inc. ,1965.

22. Journals H, Article R, Parameters P, Kakodkar SSS, Gajare P. Pharmaceutical Quality-by-Design (QbD): Basic Principles. 2015;(1):1-19.

23. Pawar YB, Purohit H, Valicherla GR, et al., (2012). Novel lipid based oral formulation of curcumin: Development and optimization by design of experiments approach. *Int J Pharm*.;436(1-2):617-623.

24. Sood S, Jain K, Gowthamarajan K., (2014). Optimization of curcumin nanoemulsion for intranasal delivery using design of experiment and its toxicity assessment. *Colloids Surfaces B Biointerfaces*.;113:330-337.

25. Xu X, Al-Ghabeish M, Rahman Z, et al., (2015). Formulation and process factors influencing product quality and in vitro performance of ophthalmic ointments. *Int J Pharm*.;493(1-2):412-425.

26. Ćurić A, Keller B-L, Reul R, Möschwitzer J, Fricker G., (2015). Development and lyophilization of itraconazole loaded poly(butylcyanoacrylate) nanospheres as a drug delivery system. *Eur J Pharm Sci*.;78:121-131.

27. Kaur IP, Bhandari R, Bhandari S, Kakkar V., (2008). Potential of solid lipid nanoparticles in brain targeting. *J Control Release*.;127(2):97-109.

28. Kumar S, Randhawa JK., (2013). High melting lipid based approach for drug delivery: Solid lipid nanoparticles. *Mater Sci Eng C*.;33(4):1842-1852.

29. Gupta S, Chavhan S, Sawant KK., (2011). Self-nanoemulsifying drug delivery system for adefovir dipivoxil: Design, characterization, in vitro and ex vivo evaluation. *Colloids Surfaces A Physicochem Eng Asp*.;392(1):145-155.

30. Pouton CW, Porter CJH., (2008). Formulation of lipid-based delivery systems for oral administration: Materials, methods and strategies. *Adv Drug Deliv Rev*. ;60(6):625-637.

31. Venkateswarlu V, Manjunath K., (2004). Preparation, characterization and in vitro release kinetics of clozapine solid lipid nanoparticles. *J Control Release*.;95(3):627-638.

32. Kuo Y, Su F., (2007). Transport of stavudine , delavirdine , and saquinavir across the blood – brain barrier by polybutylcyanoacrylate , and solid lipid nanoparticles.;340:143-152.

33. Attama A, Momoh MA, Builders PF., (2012). Lipid Nanoparticulate Drug Delivery Systems: A Revolution in Dosage Form Design and Development. *Recent Adv Nov Drug Carr Syst*. 2012:107-140.

34. Blasi P, Giovagnoli S, Schoubben A, Ricci M, Rossi C., (2007). Solid lipid nanoparticles for targeted brain drug delivery. *Adv Drug Deliv Rev*.;59(6):454-477.

35. Chemical Products Corporation. (2012). GRAS Notice 000433: Generally Regarded as Safe (GRAS) determination notification for Poloxamer Fatty Acid Formulations; Poloxamer fatty acid esters: 1-36.

36. Corbau R, Mori J, Phillips C, et al., (2010). Lersivirine, a nonnucleoside reverse transcriptase inhibitor with activity against drug-resistant human immunodeficiency virus type 1. *Antimicrob Agents Chemother*.;54(10):4451-4463.

37. Mehnert W, Mäder K., (2012). Solid lipid nanoparticles. *Adv Drug Deliv Rev*. 2012;64:83-101.

38. Park JH, Ban SJ, Ahmed T, et al., (2015). Development of DH-I-180-3 loaded lipid nanoparticle for photodynamic therapy. *Int J Pharm*. 2015;491(1-2):393-401.

39. Michael D. Triplett II BS., (2004). Enabling Solid Lipid Nanoparticle Drug Delivery Technology. Doctor of Philosophy dissertation. The Ohio State University.

40. Mallipeddi R, Rohan LC., (2010). Progress in antiretroviral drug delivery using nanotechnology. *Int J Nanomedicine*.;5(1):533-547.

41. Shegokar R, Singh KK, Müller RH., (2011). Production & stability of stavudine solid lipid nanoparticles - From lab to industrial scale. *Int J Pharm*.;416(2):461-470.

42. Kovacevic A, Savic S, Vuleta G, Müller RH, Keck CM., (2011). Polyhydroxy surfactants for the formulation of lipid nanoparticles (SLN and NLC): Effects on size, physical stability and particle matrix structure. *Int J Pharm*.;406(1-2):163-172.

43. Gupta U, Jain NK., (2010). Non-polymeric nano-carriers in HIV/AIDS drug delivery and targeting. *Adv Drug Deliv Rev*. ;62(4-5):478-490.

44. Füredi P, Kovács K, Ludányi K, Antal I, Klebovich I., (2016). Development and characterization of voriconazole loaded nanoparticles for parenteral delivery. *Int J Pharm*.;510(1):159-163.

45. Das Neves J, Amiji MM, Bahia MF, Sarmento B., (2010). Nanotechnology-based systems for the treatment and prevention of HIV/AIDS. *Adv Drug Deliv Rev*. ;62(4-5):458-477.

46. Severino P, Santana MH a, Souto EB., (2012). Optimizing SLN and NLC by 2 2 full factorial design: Effect of homogenization technique. *Mater Sci Eng*

C.;32(6):1375-1379.

47. Abdel Mouez M, Zaki NM, Mansour S, Geneidi AS., (2014). Bioavailability enhancement of verapamil HCl via intranasal chitosan microspheres. *Eur J Pharm Sci*.;51(1):59-66.
48. Ravi PR, Aditya N, Patil S, Cherian L., (2013). Nasal in-situ gels for delivery of rasagiline mesylate: improvement in bioavailability and brain localization. *Drug Deliv*. ;7544:1-8.
49. Zaki NM, Awad GAS, Mortada ND, Abd ElHady SS., (2006). Rapid-onset intranasal delivery of metoclopramide hydrochloride. Part I. Influence of formulation variables on drug absorption in anesthetized rats. *Int J Pharm*.;327(1-2):89-96.
50. Wong HL, Wu XY, Bendayan R., (2012). Nanotechnological advances for the delivery of CNS therapeutics. *Adv Drug Deliv Rev*.;64(7):686-700.
51. Naik A, Nair H., (2014). Formulation and Evaluation of Thermosensitive Biogels for Nose to Brain Delivery of Doxepin. 2014:1-10.
52. Lun H, Chattopadhyay N, Yu X, Bendayan R., (2010). Nanotechnology applications for improved delivery of antiretroviral drugs to the brain. *Adv Drug Deliv Rev*. ;62(4-5):503-517.
53. Date A a., Shibata A, Goede M, et al., (2012). Development and evaluation of a thermosensitive vaginal gel containing raltegravir+efavirenz loaded nanoparticles for HIV prophylaxis. *Antiviral Res*. 2;96(3):430-436.
54. Wang X, Chi N, Tang X., (2008). Preparation of estradiol chitosan nanoparticles for improving nasal absorption and brain targeting. *Eur J Pharm Biopharm*.;70(3):735-740.
55. Ding J, Na L, Mao S., (2012). Chitosan and its derivatives as the carrier for intranasal drug delivery.;7(October):349-361.
56. Omwoyo WN, Melariri P, Gathirwa JW, et al., (2016). Development, characterization and antimalarial efficacy of dihydroartemisinin loaded solid lipid nanoparticles. *Nanomedicine Nanotechnology, Biol Med*.;12(3):801-809.
57. Blasi P, Giovagnoli S, Schoubben A, et al., (2011). Lipid nanoparticles for brain

targeting I. Formulation optimization. *Int J Pharm*.;419(1-2):287-295.

58. Xia H, Gao X, Gu G, et al., (2011). Low molecular weight protamine-functionalized nanoparticles for drug delivery to the brain after intranasal administration. *Biomaterials*.;32(36):9888-9898.
59. Honary S, Zahir F., (2013). Effect of Zeta Potential on the Properties of Nano-Drug Delivery Systems - A Review (Part 2). *Trop J Pharm Res*.;12(2):265-273.
60. Kumar A, Garg T, Sarma GS, Rath G, Goyal AK., (2015). Optimization of combinational intranasal drug delivery system for the management of migraine by using statistical design. *Eur J Pharm Sci*.;70:140-151.
61. Abbas Z., (2012). Mucoadhesive in situ gels as nasal drug delivery systems : an overview.;7(3):168-180.
62. Kumar TP, Sirisha B, Raju PN, Reddy GN., (2013). Nasal Drug Delivery : A Potential Route for Brain Targetting. *pharma Innov*.;2(1):77-85.
63. Pathak R, Prasad R, Misra M., (2014). Role of mucoadhesive polymers in enhancing delivery of nimodipine microemulsion to brain via intranasal route. *Acta Pharm Sin B*. ;4(2):151-160.
64. Yasir M, Sara UVS., (2014). Solid lipid nanoparticles for nose to brain delivery of haloperidol: in vitro drug release and pharmacokinetics evaluation. Acta Pharmaceutica Sinica B;4(6):454-463.63.
65. Chiappetta DA, Hocht C, Taira C, Sosnik A., (2011). Oral pharmacokinetics of the anti-HIV efavirenz encapsulated within polymeric micelles. *Biomaterials*.;32(9):2379-2387.
66. Singhvi G, Singh M., (2011). In-vitro drug release characterization models. Int. J Pharm. Studies and Res.;2 (1):77-84.
67. Guidance for Industry Q1A(R2) Stability Testing of New Drug Substances and Products. U.S. Department of Health and Human Services, Food and Drug Administration, Center for Drug Evaluation and Research (CDER) Center for Biologics Evaluation and Research (CBER); 2003;(November):1–22.
68. SADC. Registration of Medicines Stability. *SADC Guidel Stab Test*. 2004;(March):1-44.

CHAPTER 5
Summary & Conclusions

5.1 Summary of the work

Infections with Human immune-deficiency virus (HIV) leading to Acquired immune-deficiency syndrome is one of the leading cause of death in the world [1, 2]. Current therapies for HIV infections with antiretroviral drugs is effective in reducing plasma viral levels, but are ineffective in eradicating the virus from sites like CNS which becomes a viral sanctuary site due to the inability of the drugs to reach to these sites. The CNS is the most important HIV reservoir site [3]. This not only results in virological resistance, but also is often associated with the development of various complications such as progressive deterioration in mental function, symptoms of motor abnormalities, mild neurocognitive disorder (MDR), HIV associated dementia (HAD), HIV encephalitis (HIVE) and even death in many cases. Efavirenz (EFV) is a non-nucleoside reverse transcriptase inhibitor (NNRTI) of choice and is recommended as a first line antiretroviral drug used in the high activity antiretroviral therapy (HAART) for the HIV infections [3-5]. EFV has low bioavailability (40-45%) [6] which is reported to be due to low water solubility of the drug, extensive first pass metabolism, metabolism by enzymes, high protein binding, efflux mechanisms, etc [7-9].

Thus, the main aim of the present investigations were to design and develop nanoparticles of EFV with the objectives of providing increased permeability and protection to drug with biocompatible lipid content, avoid first-pass metabolism and efflux-mechanisms, and select the route of administration to deliver EFV to brain/CNS in order to increase the bioavailability of EFV at the reservoir site of HIV. Suitable analytical methods were selected/developed and validated for determining the entrapment efficiency, *in-vitro*, *ex-vivo* drug release profiles and for estimation of EFV in brain and plasma respectively.

Various preliminary experiments were performed for selection of suitable excipients and formulation technique. Various lipids and surfactants were screened primarily on the basis of solubility of the drug in lipid and particle size, PDI, entrapment efficiency achieved with different surfactants in trial batches. The selections were also based on safety profile and approval status of the excipients. The compatibility of the excipients with the drug was assured with FT-IR spectroscopy. Solid lipid nanoparticles were prepared by high pressure homogenization technique using a systematic approach of design of experiments. After the preliminary optimization of stirring time, RPM and temperature, critical process variables involved during the high pressure homogenization (pressure and number of cycles) and formulation variables (amount of drug with respect to lipid and concentration of surfactant) were optimized using 3^2 factorial design with particle size, PDI and entrapment efficiency as responses using Design Expert 9.0.3.1 software (Stat-Ease, Inc., USA). The data were statistically analysed by ANOVA, model equations were generated and contour plots as well as 3D surface plots were constructed for each response. Optimized SLN was evaluated for particle size, polydispersity index, zeta potential and entrapment efficiency. Particles of average size 108.5 nm having PDI of 0.172 were obtained. Entrapment efficiency of 64.9% and zeta potential was found to be -21.2 mV. The formulated solid lipid nanoparticles of EFV were also evaluated for surface morphology using transmission electron microscope and were found to be spherical in shape and non-irritant/harmless with histopathological studies. The optimized SLN were then incorporated in *in-situ* gelling system. Different gelling and mucoadhesive agents were screened based on their gelling properties with SLN dispersion. Poloxamer 188 and poloxamer 407 were selected as thermo-sensitive polymers based on literature [10, 11]. Ratio of poloxamer 188 and poloxamer 407 were optimized (1:2) based on their gelling behaviour at different temperatures. Carbopol 934 P was selected and its concentration was optimized to be 0.4% w/v in the presence of selected thermosensitive polymers. The EFV loaded SLN based gel was evaluated for various parameters like gelation temperature, time, pH, viscosity, transmittance, mucoadhesive strength, spreadability, *in-vitro* and *ex-vivo* release studies. The release of dug was found to best fit in the Zero order release kinetics (R^2 = 0.9873),

indicating concentration independent diffusion controlled release. The *in-vivo* pharmacokinetic studies performed on adult Wistar albino rats by administering the formulation through intranasal route in test group (6 animals) and the marketed formulation (powder from capsules) to the standard group (6 animals). The concentration of EFV in brain and plasma were estimated by the developed and validated HPLC method. The ratio of drug concentration in brain to plasma of 15.61% was achieved with the developed formulation in comparison to 0.104% observed with the oral standard indicating the 150 times more brain targeting efficiency of the formulation through intranasal route. Relative bioavailability was determined to be 70.11 with the developed formulation indicating 70 times better absorption potential of the EFV loaded SLN dispersion in comparison to the orally administered drug powder. The formulations were found to be stable for 12 months at 5±3°C and 25 ± 2°C/60 ± 5% RH as per ICH guidelines. The results revealed increased concentration of the drug in brain, when administered through intranasal route indicating its potential for an attempt towards complete eradication of HIV and cure of HIV-infected patients.

5.2 Achievements with respect to the objectives

Different lipids, surfactants, process, gelling agent, etc. were screened and statistically analyzed for proper selection. By selection of intranasal route of delivery, the first pass metabolism and enzymatic degradation of the drug in GIT was avoided. By the use of poloxamer reported to reduce efflux mechanism, the drug was successfully targeted and released in the brain and thus it could be concluded that the developed formulation has the potential to reach to the latent viral reservoir site for an attempt for complete cure of HIV infections. The analytical method was successfully developed and validated for the estimation of efavirenz in brain and plasma.

5.3 Major contribution and practical implications of the work to society

AIDS is one of the leading causes of death in the world. More than 35 million people

worldwide are living with HIV/AIDS and an estimated 2.1 million individuals worldwide are newly infected with HIV every year as per the statistics obtained from World Health Organization [1, 2]. The society may be likely to witness even further increase in such numbers of people suffering with this fatal disease because of expanding populations and better diagnostics.

Extensive literature review was done to identify the challenges associated with the complete cure of AIDS and approaches which can resolve them. Although multitude researchers have worked on development of solid lipid nanoparticles (SLN) for various drugs, the idea of the development of SLN of anti-HIV drug by systematic approach of design of experiment for optimization of various parameters and to target the drug to brain (reservoir site of HIV) through intranasal route (to avoid various drawbacks associated with oral route) for an attempt towards complete eradication of HIV from its reservoir site was probably yet not investigated by any other researcher. Moreover, the formulations reduces the dose and dosing frequency and are convenient to be administered, it potentially may render the treatment more cost-effective and acceptable to patients. The formulation technique utilized has feasibility for scale-up on industrial scale. Hence, after clinical trials and fulfillment of other regulatory requirements, the developed formulation has good scope for commercialization and may prove to be a boon to the society at large for the complete treatment and eradication of the highly-dreaded disease of AIDS.

5.4 Recommendation for future research

The present investigations on antiretroviral drug delivery system intended to be administered through intranasal route for direct nose to brain delivery involves the use of single antiretroviral agent. It has been reported that use of combination of drugs can lead to more efficacious treatments and reduction of resistance. Hence, further studies with development and evaluation of nanoformulations of combination of drugs should be conducted. The nanoformulation approach for intranasal delivery opens new therapeutic strategies for attacking human immune-deficiency virus and other diseases for improving

treatment success rates. Future research may also involve the identification of exact site of CNS where HIV potentially makes the reservoir and suitable model should be developed to estimate the reach of drug to that particular site and their effectiveness.

5.5 Conclusion

With the present investigations, it may be concluded that solid lipid nanoparticles of a poorly soluble drug efavirenz were successfully developed and optimized using the systematic approach of design of experiments (DoE) by high pressure homogenization technique. Thermosensitive *in-situ* gel was prepared with the optimized SLN dispersion. The intranasal administration of the formulation showed 150 times more brain targeting efficiency and 70 times better absorption potential of the drug from efavirenz loaded SLN formulation in comparison to the orally administered marketed formulation (capsule). Thus, it may be concluded that the developed formulation has better potential to target brain where the HIV viruses are reported to harbor even with low dose of efavirenz, rendering the treatment more cost-effective as well and acceptable to patients because of convenience of application of *in-situ* gelling formulation. Hence, the developed formulation, after necessary investigations of clinical trials, has the promising potential for an attempt to completely eradicate HIV reservoir and cure AIDS.

5.6 References

1. WHO | HIV/AIDS. [Online]. Available: http://www.who.int/gho/hiv/en/. [Accessed 12 November, 2015.
2. Global HIV/AIDS Overview. [Online]. Available : https://www.aids.gov/federal-resources/around-the-world/global-aids-overview/. [Accessed 12 November, 2015]
3. Rao KS, Ghorpade A, Labhasetwar V., (2009). Targeting anti-HIV drugs to the CNS. *Expert Opin Drug Deliv*.;6(8):771-784.

4. Cundy KC, Lynch G, Lee WA.. (1997). Antiviral Research. 1997;35(2):113-122.
5. Hasegawa T, Kawaguchi T., (2002). Delivery of Anti-Viral Nucleoside Analogues to the Central Nervous System. *Curr Med Chem -Anti-Infective Agents*.;1(1):55-63.
6. Corbau R, Mori J, Phillips C, et al., (2010). Lersivirine, a nonnucleoside reverse transcriptase inhibitor with activity against drug-resistant human immunodeficiency virus type 1. *Antimicrob Agents Chemother*.;54(10):4451-4463.
7. Mistry A, Stolnik S, Illum L., (2009). Nanoparticles for direct nose-to-brain delivery of drugs;379:146-157.
8. Kaur IP, Bhandari R, Bhandari S, Kakkar V., (2008). Potential of solid lipid nanoparticles in brain targeting. *J Control Release*.;127(2):97-109.
9. Gupta U, Jain NK., (2010). Non-polymeric nano-carriers in HIV/AIDS drug delivery and targeting. *Adv Drug Deliv Rev*. ;62(4-5):478-490.
10. Naik A, Nair H., (2014). Formulation and Evaluation of Thermosensitive Biogels for Nose to Brain Delivery of Doxepin. *Biomed Res. Int.*;2014.1-10.
11. Wong HL, Wu XY, Bendayan R., (2012). Nanotechnological advances for the delivery of CNS therapeutics. *Adv Drug Deliv Rev*.;64(7):686-700.

Bibliography

- Abbas Z., (2012). Mucoadhesive in situ gels as nasal drug delivery systems : an overview.;7(3):168-180.
- Abdel Mouez M, Zaki NM, Mansour S, Geneidi AS., (2014). Bioavailability enhancement of verapamil HCl via intranasal chitosan microspheres. *Eur J Pharm Sci*.;51(1):59-66.
- Adams G.L. , Boies L.R. HPA.(1989). *Fundamentals of Otolaryngology, A Textbook of Ear, Nose and Throat Diseases*. Philadelphia.
- Alexander Krämer, Mirjam Kretzschmar KK., (2010). *Modern Infectious Disease Epidemiology Concepts, Methods, Mathematical Models, and Public Health*. New York: Springer.
- Arbelaez-Camargo D, Suñé-Negre JM, Roig-Carreras M, et al., (2016). Preformulation and characterization of a lidocaine hydrochloride and dexamethasone sodium phosphate thermo-reversible and bioadhesive long-acting gel for intraperitoneal administration. *Int J Pharm*.;498(1-2):142-152.
- Attama A, Momoh MA, Builders PF. Lipid Nanoparticulate Drug Delivery Systems: A Revolution in Dosage Form Design and Development (2012). *Recent Adv Nov Drug Carr Syst*. 2012:107-140.
- Avachat AM, Parpani SS., (2015). Formulation and development of bicontinuous nanostructured liquid crystalline particles of efavirenz. *Colloids Surfaces B Biointerfaces*.;126:87-97.
- Bhanushali RS, Gatne MM, Gaikwad R V, Bajaj AN, Morde MA., (2015). Nanoemulsion based Intranasal Delivery of Antimigraine Drugs for Nose to Brain Targeting;71(6):707-709.
- Blasi P, Giovagnoli S, Schoubben A, et al., (2011). Lipid nanoparticles for brain targeting I. Formulation optimization. *Int J Pharm*. ;419(1-2):287-295.
- Blasi P, Giovagnoli S, Schoubben A, Ricci M, Rossi C., (2007). Solid lipid nanoparticles for targeted brain drug delivery. *Adv Drug Deliv Rev*.;59(6):454-477.
- Blasi P, Schoubben A, Traina G, et al., (2013). Lipid nanoparticles for brain targeting III. Long-term stability and in vivo toxicity. *Int J Pharm*.;454(1):316-323.
- Bocedi A, Notaril S NP., (2004). Binding of anti- HIV drugs to human serum albumin. *Drug Metab Dispos*.:606-609.
- Bozdağ-Pehlivan S, Subaşi B, Vural I, Ünlü N, Çapan Y., (2011). Evaluation of drug-excipient interaction in the formulation of celecoxib tablets. *Acta Pol Pharm - Drug Res*. ;68(3):423-433.
- Burkoth AK, Anseth KS. A review of photocrosslinked polyanhydrides: in situ forming

degradable networks. *Biomaterials*. 2000;21(23):2395-2404.

- Chan DC, Fass D, Berger JM, Kim PS. , (1997) Core structure of gp41 from the HIV envelope glycoprotein. *Cell*.;89(2):263-273.
- Chemical Products Corporation. (2012). GRAS Notice 000433: Generally Regarded as Safe (GRAS) determination notification for Poloxamer Fatty Acid Formulations; Poloxamer fatty acid esters: 1-36.
- Chen Y, Liu L., (2012). Modern methods for delivery of drugs across the blood-brain barrier. *Adv Drug Deliv Rev*.;64(7):640-665.
- Chiappetta DA, Hocht C, Taira C, Sosnik A., (2011). Oral pharmacokinetics of the anti-HIV efavirenz encapsulated within polymeric micelles. *Biomaterials*.;32(9):2379-2387.
- Corbau R, Mori J, Phillips C, et al., (2010). Lersivirine, a nonnucleoside reverse transcriptase inhibitor with activity against drug-resistant human immunodeficiency virus type 1. *Antimicrob Agents Chemother*.;54(10):4451-4463.
- Cundy KC, Lynch G, Lee WA., (1997). Bioavailability and metabolism of cidofovir following topical administration to rabbits**.** Antiviral Research ;35(2):113-122.
- Curic A, Keller B-L, Reul R, Moschwitzer J, Fricker G., (2015). Development and lyophilization of itraconazole loaded poly(butylcyanoacrylate) nanospheres as a drug delivery system. *Eur J Pharm Sci*.;78:121-131.
- Dale Purves, George J Augustine, David Fitzpatrick, Lawrence C Katz, Anthony-Samuel LaMantia, James O McNamara and SMW, (2001). *Neuroscience*. 2nd ed. Sunderland (MA): Sinauer Associates.
- Das Neves J, Amiji MM, Bahia MF, Sarmento B., (2010). Nanotechnology-based systems for the treatment and prevention of HIV/AIDS. *Adv Drug Deliv Rev*. ;62(4-5):458-477.
- Das Neves J, Sarmento B., (2014). Mucosal delivery of biopharmaceuticals: Biology, challenges and strategies. *Mucosal Deliv Biopharm Biol Challenges Strateg*. 9781461495:1-601.
- Date A a., Shibata A, Goede M, et al., (2012). Development and evaluation of a thermosensitive vaginal gel containing raltegravir+efavirenz loaded nanoparticles for HIV prophylaxis. *Antiviral Res*. 2;96(3):430-436.
- Date A., Destache CJ., (2013). A review of nanotechnological approaches for the prophylaxis of HIV/AIDS. *Biomaterials*.;34(26):6202-6228.
- Delivery AD., (2009). Nanotechnology for Antiretroviral Drug Delivery. *J Am Chem Soc*.:21-23.
- Ding J, Na L, Mao S., (2012). Chitosan and its derivatives as the carrier for intranasal drug delivery.;7(October):349-361.
- Djupesland PG, Mahmoud RA, Messina JC. (2013). Accessing the brain: the nose may know the way. *J Cereb Blood Flow Metab*.;33(5):793-794.

- Dole MN, Patel PA, Sawant SD, Shedpure PS., (2011) Advance applications of fourier transform infrared spectroscopy. *Int J Pharm Sci Rev Res*.;7(2):159-166.
- Drug Bank: Efavirenz. [Online]. Available: http://www.drugbank.ca/drugs/DB00625. [Accessed 12 November, 2015]
- Dumortier G, Grossiord JL, Agnely F, Chaumeil , (2006). Expert Review A Review of Poloxamer 407 Pharmaceutical and Pharmacological Characteristics. 2006;23(12):11095..
- Edition S. Ophthalmic Drug Delivery Systems. *Clin Res*. 966:80-87.
- Eskandari S, Varshosaz J, Minaiyan M, Tabbakhian M., (2011). Brain delivery of valproic acid via intranasal administration of nanostructured lipid carriers: in vivo pharmacodynamic studies using rat electroshock model. *Int J Nanomedicine*. ;6:363-371.
- FDA. FDA approved -HIV-Medicines. 2016. [Online]. Available: https://aidsinfo.nih.gov/education-materials/fact-sheets/21/58/fda-approved-hiv-medicines .[Accessed November 11, 2016].
- FDA. Guidance for Industry Starting Dose in Initial Clinical Trials Guidance for Industry Estimating the Maximum Safe. *FDA*. 2005;(July):27.
- Filiano AJ, Gadani SP, Kipnis J., (2014). Interactions of innate and adaptive immunity in brain development and function. *Brain Res*. 2015;1617:18-27.
- Fisher SRA, JMP® 8 Design of Experiments Guide, Second Edition. Cary, NC: SAS Institute Inc. ,1965.
- Fisher, Bruce; Harvey, Richard P.; Champe PC. (2007). In: *Lippincott's Illustrated Reviews: Microbiology (Lippincott's Illustrated Reviews Series)*:3.
- Foxall RB, Soares RS, Albuquerque AS, Cortesao CS, Victorino RMM, Sousa AE., (2008). Increased frequency of CD25dimCD4+ T-cells in HIV-2 infection, a naturally occurring attenuated form of HIV-1. *Clin Immunol*.;127(2):158-167.
- Füredi P, Kovács K, Ludányi K, Antal I, Klebovich I., (2016). Development and characterization of voriconazole loaded nanoparticles for parenteral delivery. *Int J Pharm*. ;510(1):159-163.
- G.J. T. (1998) *Principles of Human Anatomy*. 8th ed. Mento Park: Benjamin/cummings Science Publishing.
- Gaillard PJ, Visser CC, Appeldoorn CCM, Rip J., (2012). Enhanced brain drug delivery: Safely crossing the blood-brain barrier. *Drug Discov Today Technol*.;9(2):e155-e160.
- Galligioni V, Scagliarini A, Lorenzini L, et al. Nose-to-brain delivery of ribavirin (RBV) for the treatment of viral encephalitis. :4.
- Gelderblom HR. (1996). Structure and Classification of Viruses. In: Baron S, Medical Microbiology. 4th ed. Galveston (TX): University of Texas Medical Branch at Galveston.
- Ginhoux F, Lim S, Hoeffel G, Low D, Huber T. (2013). Origin and differentiation of microglia. *Front Cell Neurosci*.;7(April):45.

- Gizurarson S (2012). Anatomical and histological factors affecting intranasal drug and vaccine delivery. *Curr Drug Deliv*. 2012;9(6):566-582.
- Global HIV/AIDS Overview. [Online]. Available : Global HIV/AIDS Overview. https://www.aids.gov/federal-resources/around-the-world/global-aids-overview/. Accessed November 12, 2015.
- Government of India, Ministry of Health and Family Welfare. *Indian Pharmacopoeia*. The Indian Pharmacopoeia commission; 1996:A-147.
- Guidance for Industry Q1A(R2) Stability Testing of New Drug Substances and Products. U.S. Department of Health and Human Services, Food and Drug Administration, Center for Drug Evaluation and Research (CDER) Center for Biologics Evaluation and Research (CBER); 2003;(November):1–22.
- Gupta S, Chavhan S, Sawant KK., (2011). Self-nanoemulsifying drug delivery system for adefovir dipivoxil: Design, characterization, in vitro and ex vivo evaluation. *Colloids Surfaces A Physicochem Eng Asp*.;392(1):145-155.
- Gupta U, Jain NK., (2010). Non-polymeric nano-carriers in HIV/AIDS drug delivery and targeting. *Adv Drug Deliv Rev*. ;62(4-5):478-490.
- GW K. The First Line of Defense in Brain Pathologies. (1995). *Drug Res (Stuttg)*;45(1):357–360.
- H.P. Rang, M.M.Dale, J.M. Ritter PKM. Pharmacology. In: *Pharmacology*. 5th ed. Churchill Livingstone; 2003:654-665.
- Hasegawa T, Kawaguchi T., (2002). Delivery of Anti-Viral Nucleoside Analogues to the Central Nervous System. *Curr Med Chem -Anti-Infective Agents*.;1(1):55-63.
- Heydari R, Rashidipour M, Naleini N., (2014). Determination of efavirenz in plasma by dispersive liquid-liquid microextraction coupled to high-performance liquid chromatography. *Curr Anal Chem*.10(2):280-287.
- Hilip, LR, Peppas A., (1987). Fickian and anomalous release from swellable devices. *J Control Release*.;5:37-42.
- HIV Drug Interactions., (2011). Efavirenz PK Factsheet. [Online]. Available: http://www.hiv-druginteractions.org/.[Accessed November 12, 2015].
- Honary S, Zahir F., (2013). Effect of zeta potential on the properties of nano-drug delivery systems - A review (Part 1). *Trop J Pharm Res*.;12(2):255-264.
- http://doctors-hospitals-medical-cape-town-south-africa.blaauwberg.net/details.php?id=768. [Accessed 25 June 2016]
- https://www.aids.gov/federal-resources/around-the-world/global-aids-overview/. [Accessed 12 November, 2015]
- Hynes M. Baltimore Classification of Viruses. *Mol Biol Webb*. 2015:1.

- Hynynen K (2007). Focused ultrasound for blood – brain disruption and delivery of therapeutic molecules into the brain.:27-35.
- ICH Expert Working Group. Pharmaceutical Development Q8. *ICH Harmon Tripart Guidel*. 2009;8(August):1-28.
- ICH. ICH Topic Q2 (R1) Validation of Analytical Procedures : Text and Methodology. *Int Conf Harmon*. 2005;1994(November 1996):17.
- Ikeda M, Bhattacharjee AK, Kondoh T, Nagashima T, Tamaki N (2002),. Synergistic effect of cold mannitol and Na(+)/Ca(2+) exchange blocker on blood-brain barrier opening. *Biochem Biophys Res Commun*.;291(3):669-674.
- Infectitious viral diseases. [Online]. Available: usa.gov/search?affiliate=ri.gov&query=viral&sitelimit=health.ri.gov [Accessed 12 November 2015]
- Ingallina C, Rinaldi F, Bogni A, et al., (2016). Niosomal approach to brain delivery: Development, characterization and in vitro toxicological studies. *Int J Pharm*. ;511(2):969-982.
- Jeannot V, Mazzaferro S, Lavaud J, et al., (2016). Targeting CD44 receptor-positive lung tumors using polysaccharide-based nanocarriers: Influence of nanoparticle size and administration route. *Nanomedicine Nanotechnology, Biol Med*. ;12(4):921-932.
- Jogani V V, Shah PJ, Mishra P, Mishra AK, Misra AR., (2007). Nose-to-brain delivery of tacrine:1199-1205.
- Johnson NJ, Hanson LR, Iliff JJ, Ph D, Androulakis IP., (2011). Trigeminal pathways deliver a low molecular weight drug from the nose to the brain and orofacilal structures;7(3):228-237.
- Journals H, Article R, Parameters P, Kakodkar SSS, Gajare P. Pharmaceutical Quality-by-Design (QbD): Basic Principles. 2015;(1):1-19.
- Journals H, Article R, Parameters P, Kakodkar SSS, Gajare P., (2015). Pharmaceutical Quality-by-Design (QbD): Basic Principles;(1):1-19.
- Kadam AA, Babu CJG, Permal RV, Channabasavaraj K, Mani TT., (2012) Development and Validation of Method for the Quantitative Estimation of Efavirenz in Bulk and Phrmaceutical Dosage Form. *Am J PharmTech Res*.;2(1):324-330.
- Kamble RN, Mehta P., (2015). Development of simple HPLC method to estimate the blood plasma concentration of Efavirenz in rat after oral administration, Innovare Academic Sciences, *Int. J Pharm & Pharm. Sci.*;7(7):7-10.
- Kappelhoff BS, Rosing H, Huitema AD., Beijnen JH., (2003). Simple and rapid method for the simultaneous determination of the non-nucleoside reverse transcriptase inhibitors efavirenz and nevirapine in human plasma using liquid chromatography. *J Chromatogr B*.;792(2):353-362.

- Karavasili C, Fatouros DG., (2016). Smart materials: In situ gel-forming systems for nasal delivery. *Drug Discov Today*.; 21(1):157-166.
- Kaur IP, Bhandari R, Bhandari S, Kakkar V., (2008). Potential of solid lipid nanoparticles in brain targeting. *J Control Release*.;127(2):97-109.
- Kawabata Y, Wada K, Nakatani M, Yamada S, Onoue S., (2011). Formulation design for poorly water-soluble drugs based on biopharmaceutics classification system: Basic approaches and practical applications. *Int J Pharm*; 420(1):1-10.
- Kawakami K., (2012). Modification of physicochemical characteristics of active pharmaceutical ingredients and application of supersaturatable dosage forms for improving bioavailability of poorly absorbed drugs. *Adv Drug Deliv Rev*. ;64(6):480-495.
- Kovacevic A, Savic S, Vuleta G, Müller RH, Keck CM., (2011). Polyhydroxy surfactants for the formulation of lipid nanoparticles (SLN and NLC): Effects on size, physical stability and particle matrix structure. *Int J Pharm*.;406(1-2):163-172.
- Kozlovskaya L, Stepensky D., (2013). Quantitative analysis of the brain-targeted delivery of drugs and model compounds using nano-delivery systems. *J Control Release*;171(1):17-23.
- Kreuter J., (2014). Drug delivery to the central nervous system by polymeric nanoparticles: What do we know? *Adv Drug Deliv Rev*.;71:2-14.
- Krol S., (2012). Challenges in drug delivery to the brain: Nature is against us. *J Control Release*. 2012;164(2):145-155.
- Kumar A, Garg T, Sarma GS, Rath G, Goyal AK., (2015). Optimization of combinational intranasal drug delivery system for the management of migraine by using statistical design. *Eur J Pharm Sci*.;70:140-151.
- Kumar M, Misra A, Babbar AK, Mishra AK, Mishra P, Pathak K., (2008) Intranasal nanoemulsion based brain targeting drug delivery system of risperidone. *Int J Pharm*.;358(1-2):285-291.
- Kumar S, Randhawa JK., (2013). High melting lipid based approach for drug delivery: Solid lipid nanoparticles. *Mater Sci Eng C*. ;33(4):1842-1852.
- Kumar TP, Sirisha B, Raju PN, Reddy GN., (2013). Nasal Drug Delivery : A Potential Route for Brain Targetting. *pharma Innov*. 2013;2(1):77-85.
- Kumar YA, Rao NR., (2010). Development of Rapid UV Spectrophotometric Method for the Estimation of Efavirenz in Formulations. *E-Journal Chem*. ;7(3):856-860.
- Kuo Y, Su F., (2007). Transport of stavudine , delavirdine , and saquinavir across the blood – brain barrier by polybutylcyanoacrylate , and solid lipid nanoparticles.;340:143-152.
- Lakshmi Sailaja , Kishore Kumar K, Ravi Kumar DVR, Mohan Kumar C, Yugandhar NM, Srinubabu G., (2007). Development and Validation of a Liquid Chromatographic Method for Determination of Efavirenz in Human Plasma. *Chromatographia*.;65(5-6):359-361.

- Langmann P, Schirmer D, Väth T, Zilly M, Klinker H, (2001). High-performance liquid chromatographic method for the determination of HIV-1 non-nucleoside reverse transcriptase inhibitor efavirenz in plasma of patients during highly active antiretroviral therapy. *J Chromatogr B Biomed Sci Appl*.;755:151-156.
- Lembo D, Cavalli R., (2010). Nanoparticulate delivery systems for antiviral drugs. *Antivir Chem Chemother*.;21(2):53-70.
- Liu L, Guo K, Lu J, et al., (2008). Biologically active core/shell nanoparticles self-assembled from cholesterol-terminated PEG-TAT for drug delivery across the blood-brain barrier. *Biomaterials*;29(10):1509-1517.
- Lochhead JJ, Thorne RG., (2012). Intranasal delivery of biologics to the central nervous system. *Adv Drug Deliv Rev*.;64(7):614-628.
- Lun H, Chattopadhyay N, Yu X, Bendayan R., (2010). Nanotechnology applications for improved delivery of antiretroviral drugs to the brain. *Adv Drug Deliv Rev*. ;62(4-5):503-517.
- Macheras, P., Liadis A., (2006). *Modelling in Biopharmaceutics, Pharmacokinetics and Pharmacodynamics: Homogeneous and Heterogeneous Approaches. Series: Interdisciplinary Applied Mathematics*. Springer, New York.
- Mallipeddi R, Rohan LC., (2010). Progress in antiretroviral drug delivery using nanotechnology. *Int J Nanomedicine*. (1):533-547.
- Marzolini C, Telenti A, Decosterd L a, Greub G, Biollaz J, Buclin T., (2001). Efavirenz plasma levels can predict treatment failure and central nervous system side effects in HIV-1-infected patients. *Aids*.:71-75.
- McGinity JW, Harris MR, Patel K et. al., (1986). *Handbook of Pharmaceutical Excipients*. American Pharmaceutical Association. Washington-DC, USA; 1986.
- Mehnert W, Mäder K., (2012). Solid lipid nanoparticles. *Adv Drug Deliv Rev*. ;64:83-101.
- Michael D. Triplett II BS., (2004). Enabling Solid Lipid Nanoparticle Drug Delivery Technology. Doctor of Philosophy dissertation. The Ohio State University.
- Michael J Pelczar, ECS Chan NRK. *Microbiology*., (1993). 5th ed. Tata Mc Graw Hill Publishing company Ltd.,New Delhi.
- Mishra V, Kesharwani P., (2016). Dendrimer technologies for brain tumor. *Drug Discov Today*.;21(5):766-778.
- Mistry A, Stolnik S, Illum L., (2009). Nanoparticles for direct nose-to-brain delivery of drugs;379:146-157.
- Morsi NM, Ghorab DM, Badie HA., (2012). Bioadhesive Brain Targeted Nasal Delivery of an Ant ischemic Drug.;3(5):1067-1076.
- Morsi N, Ghorab D, Refai H, Teba H., (2016). Ketoroloac tromethamine loaded nanodispersion incorporated into thermosensitive in situ gel for prolonged ocular delivery.

Int J Pharm.;506(1-2):57-67.

- Nagar M, Panwar KS, Chopra VS, Bala I, Trivedi P., (2010). Quality by design: A systematic approach to pharmaceutical development. *Der Pharm Lett*.;2(2):111-130.
- Naik A, Nair H., (2014). Formulation and Evaluation of Thermosensitive Biogels for Nose to Brain Delivery of Doxepin. 2014:1-10.
- Nelson AG, Zhang X, Ganapathi U, et al., (2015). Drug delivery strategies and systems for HIV/AIDS pre-exposure prophylaxis and treatment. *J Control Release*.;219(2015):669-680.
- Nowacek AS, McMillan J, Miller R, Anderson A, Rabinow B, Gendelman HE., (2010). Nanoformulated antiretroviral drug combinations extend drug release and antiretroviral responses in HIV-1-infected macrophages: Implications for NeuroAIDS therapeutics. *J Neuroimmune Pharmacol*.;5(4):592-601.
- Omwoyo WN, Melariri P, Gathirwa JW, et al., (2016). Development, characterization and antimalarial efficacy of dihydroartemisinin loaded solid lipid nanoparticles. *Nanomedicine Nanotechnology, Biol Med*.;12(3):801-809.
- Overview of viral infections. [Online]. Available: http://www.merckmanuals.com/home/infections/viral-infections/overview-of-viral-infections. [Accessed 25 June 2016]
- Pang Z, Lu W, Gao H, et al., (2008). Preparation and brain delivery property of biodegradable polymersomes conjugated with OX26. *J Control Release*. 2008;128(2):120-127.
- Pani NR, Nath LK, Acharya S, Bhuniya B., (2011). Application of DSC, IST, and FTIR study in the compatibility testing of nateglinide with different pharmaceutical excipients. *J Therm Anal Calorim*.;108(1):219-226.
- Park JH, Ban SJ, Ahmed T, et al., (2015). Development of DH-I-180-3 loaded lipid nanoparticle for photodynamic therapy. *Int J Pharm*. 2015;491(1-2):393-401.
- Park K. (2008). Trojan monocytes for improved drug delivery to the brain. *J Control Release*. ;132(2):75.
- Patel S, Chavhan S, Soni H, , Babbar AK, Mathur R MA and SK., (2011). Brain targeting of risperidone-loaded solid lipid nanoparticles by intranasal route. *J Drug Target*.;19(6):468–474.
- Patel T, Zhou J, Piepmeier JM, Saltzman WM (2012). Polymeric nanoparticles for drug delivery to the central nervous system. *Adv Drug Deliv Rev*. 2012;64(7):701-705.
- Pathak R, Prasad R, Misra M., (2014). Role of mucoadhesive polymers in enhancing delivery of nimodipine microemulsion to brain via intranasal route. *Acta Pharm Sin B*. ;4(2):151-160.
- Pawar YB, Purohit H, Valicherla GR, et al., (2012). Novel lipid based oral formulation of curcumin: Development and optimization by design of experiments approach. *Int J*

Pharm.;436(1-2):617-623.

- Pelvig DP, Pakkenberg H, Stark AK, Pakkenberg B. (2008). Neocortical glial cell numbers in human brains. *Neurobiol Aging*.;29(11):1754-1762.
- Perioli L, Ambrogi V, Bernardini C, et al., (2004). Potential prodrugs of non-steroidal anti-inflammatory agents for targeted drug delivery to the CNS. *Eur J Med Chem*. ;39(8):715-727.
- Peroni RN, Di Gennaro SS, Hocht C, et al., (2011). Efavirenz is a substrate and in turn modulates the expression of the efflux transporter ABCG2/BCRP in the gastrointestinal tract of the rat. *Biochem Pharmacol*.;82(9):1227-1233.
- Peter Christoper G V., Vijaya Raghavan C, Siddharth K, Siva Selva Kumar M, Hari Prasad R., (2014). Formulation and optimization of coated PLGA - Zidovudine nanoparticles using factorial design and in vitro in vivo evaluations to determine brain targeting efficiency. *Saudi Pharm J*.;22(2):133-140.
- Pouton CW, Porter CJH., (2008). Formulation of lipid-based delivery systems for oral administration: Materials, methods and strategies. *Adv Drug Deliv Rev*. ;60(6):625-637.
- Qin LJ, Gu YT, Zhang H, Xue YX. (2009). Bradykinin-induced blood-tumor barrier opening is mediated by tumor necrosis factor-α. *Neurosci Lett*. 2009;450(2):172-175.
- Qiu Y, Park K., (2001). Environment-sensitive hydrogels for drug delivery. ;53:321-339.
- Ramachandran G, Kumar a. KH, Swaminathan S, Venkatesan P, Kumaraswami V, Greenblatt DJ., (2006). Simple and rapid liquid chromatography method for determination of efavirenz in plasma. *J Chromatogr B Anal Technol Biomed Life Sci*. ;835(2):131-135.
- Ramaswamy A, Arul Gnana Dhas AS., (2014). Development and validation of analytical method for quantitation of Emtricitabine, Tenofovir, Efavirenz based on HPLC. *Arab J Chem*. 2014.
- Ramaswamy A, Arul Gnana Dhas AS., (2014). Development and validation of analytical method for quantitation of Emtricitabine, Tenofovir, Efavirenz based on HPLC. *Arab J Chem*., 1-7.
- Rao KS, Ghorpade A, Labhasetwar V., (2009). Targeting anti-HIV drugs to the CNS. *Expert Opin Drug Deliv*.;6(8):771-784.
- Rausch DM, Stover ES., (2001). Neuroscience research in AIDS. *Prog Neuro-Psychopharmacology Biol Psychiatry*.;25(1):231-257.
- Ravi PR, Aditya N, Patil S, Cherian L., (2013). Nasal in-situ gels for delivery of rasagiline mesylate: improvement in bioavailability and brain localization. *Drug Deliv*. ;7544:1-8.
- Ren S, Park MJ, Sah H, Lee BJ., (2008). Effect of pharmaceutical excipients on aqueous stability of rabeprazole sodium. *Int J Pharm*.;350(1-2):197-204.
- Retroviruses. [Online]. Available:http://retrovirology.biomedcentral.com/ [Accessed 12 November, 2015]

- Robert M. Silverstein, Francis X. Webster, David J. Kiemle DLB., (2014). *Spectrometric Identification of Organic Compounds*. 8th ed. Wiley Publisher.
- Rohit B, Pal KI., (2013). A Method to Prepare Solid Lipid Nanoparticles with Improved Entrapment Efficiency of Hydrophilic Drugs. *Curr Nanosci*.;9(2):211-220.
- SADC. Registration of Medicines Stability. *SADC Guidel Stab Test*. 2004;(March):1-44.
- Saras-Nacenta M, López-Púa Y, Lípez-Cortés LF, Mallolas J, Gatell JM, Carné X., (2001). Determination of efavirenz in human plasma by high-performance liquid chromatography with ultraviolet detection. *J Chromatogr B Biomed Sci Appl*.;763(1-2):53-59.
- Seju U, Kumar A, Sawant KK., (2011). Development and evaluation of olanzapine-loaded PLGA nanoparticles for nose-to-brain delivery: In vitro and in vivo studies. *Acta Biomater*.;7(12):4169-4176.
- Serralheiro A, Alves G, Fortuna A, Falcao A. (2015). Direct nose-to-brain delivery of lamotrigine following intranasal administration to mice. *Int J Pharm*. ;490(1-2):39-46.
- Severino P, Santana MH a, Souto EB., (2012). Optimizing SLN and NLC by 2 2 full factorial design: Effect of homogenization technique. *Mater Sci Eng C*.;32(6):1375-1379.
- Sharma D, Maheshwari D, Philip G, et al., (2014) Formulation and optimization of polymeric nanoparticles for intranasal delivery of Lorazepam using box-behnken design: in vitro and in vivo evaluation. *Biomed Res Int*.;2014:156010.
- Sharma N, Mishra N., (2014). Importance of Lipid Nanoparticles in the Treatment of Epilepsy: a Focus on Nasal Delivery. *J Pharm Sci Innov*.;3(3):199-207.
- Sharma S, Lohan S, Murthy RSR., (2012). Potential of Chitosan for nose to brain drug delivery, *Int. J. Pharm. Sci. Rev. Res.*;16(1):47-55.
- Shegokar R, Singh KK, Müller RH., (2011). Production & stability of stavudine solid lipid nanoparticles - From lab to industrial scale. *Int J Pharm*. ;416(2):461-470.
- Silva C, Gonzalez-Mira E, Garcia ML, et al., (2011). Preparation, characterization and biocompatibility studies on risperidone-loaded solid lipid nanoparticles (SLN): High pressure homogenization versus ultrasound. *Colloids Surfaces B Biointerfaces*.;86(1):158-165.
- Singh AK SA and MN (2012). Nasal cavity: A promising platform for drug delivery and research approaches from nasal to brain targeting. *J drug del ther*.;2(3):22-33.
- Singhvi G, Singh M., (2011). In-vitro drug release characterization models. Int. J Pharm. Studies and Res.;2 (1):77-84.
- Sood S, Jain K, Gowthamarajan K., (2014). Optimization of curcumin nanoemulsion for intranasal delivery using design of experiment and its toxicity assessment. *Colloids Surfaces B Biointerfaces*.;113:330-337.
- Soto-Ramirez LE, Rodriguez-Diaz R, Harris DR, Hazra R., (2010). HIV drug resistance-associated mutations in antiretroviral na??ve HIV-1-infected Latin American

children. *Adv Virol*.;2010.

- Sozio P, Cerasa LS, Laserra S, et al., (2013). Memantine-sulfur containing antioxidant conjugates as potential prodrugs to improve the treatment of Alzheimer's disease. *Eur J Pharm Sci*.;49(2):187-198.
- Thakur DS, Behera CK, Patidar A, Kumar P, Kumar P, Lal C., (2010). Anti-HIV agents: A step towards future. *Int J Pharm Sci Rev Res*.;3(2):10-18.
- The National Toxicology Program (NTP) Interagency Center for the Evaluation of, Alternative Toxicological Methods (NICEATM). Test Method Protocol for Solubility Determination Phase III. 2003:1-10.
- The United States Pharamcopoeial convention, (2011), Standards A. General Notices and Requirements. USP 34; 6.
- Top 10 Deadliest Diseases in the world. [Online]. Available: https://www.microhealthllc.com/top-10-deadliest-diseases-in-the-world/ [Accessed 25 June 2016]
- USP Medicines Compendium, Monograph. Efavirenz Final Authorized Version 2.0. [Online]. Available: https://mc.usp.org/monographs/efavirenz-2-0. [Accessed 16 November, 2016]
- Van der Meel R, Vehmeijer LJC, Kok RJ, Storm G, van Gaal EVB., (2013). Ligand-targeted particulate nanomedicines undergoing clinical evaluation: Current status. *Adv Drug Deliv Rev*.;65(10):1284-1298.
- Varatharajan L, A TS., (2009). The transport of anti-HIV drugs across blood–CNS interfaces: Summary of current knowledge and recommendations for further research. *Antiviral Res*.;82(2):A99-A109.
- Varatharajan L, A TS., (2009). The transport of anti-HIV drugs across blood–CNS interfaces: Summary of current knowledge and recommendations for further research. *Antiviral Res*.;82(2):A99-A109.
- Veldkamp I, van Heeswijk RP, Meenhorst PL, et al., (1999). Quantitative determination of efavirenz (DMP 266), a novel non-nucleoside reverse transcriptase inhibitor, in human plasma using isocratic reversed-phase high-performance liquid chromatography with ultraviolet detection. *J Chromatogr B Biomed Sci Appl*. ;734(1):55-61.
- Venkateswarlu V, Manjunath K., (2004). Preparation, characterization and in vitro release kinetics of clozapine solid lipid nanoparticles. *J Control Release*.;95(3):627-638.
- Vikram Singh A, Nath LK, Pani NR., (2011). Development and validation of analytical method for the estimation of lamivudine in rabbit plasma. *J Pharm Anal*. ;1(4):251-257.
- Virus vs Retrovirus. [Online]. Available: http://www.differencebetween.com/difference-between-retrovirus-and-vs-virus/. [Accessed 25 June 2016]

- Vykhodtseva N, McDannold N, Hynynen K., (2008). Progress and problems in the application of focused ultrasound for blood-brain barrier disruption. *Ultrasonics*;48(4):279-296.
- Wang X, Chi N, Tang X., (2008). Preparation of estradiol chitosan nanoparticles for improving nasal absorption and brain targeting. *Eur J Pharm Biopharm*.;70(3):735-740.
- WHO | HIV/AIDS. [Online]. Available: http://www.who.int/gho/hiv/en/. [Accessed 12 November, 2015.
- WHO. Safety of Efavirenz. 2010. [Online]. Available: http://www.who.int/hiv/topics/treatment/efavirenz_safety_review.pdf. [Accessed 12 November, 2015]
- William N. Rom SBM., (2007). *Environmental and Occupational Medicine*. 4th ed. Lippincott Williams & Wilkins.
- Woensel M Van, Wauthoz N, Rosière R, et al., (2013). Formulations for Intranasal Delivery of Pharmacological Agents to Combat Brain Disease: A New Opportunity to Tackle GBM:1020-1048.
- Wong HL, Wu XY, Bendayan R. (2012). Nanotechnological advances for the delivery of CNS therapeutics. *Adv Drug Deliv Rev*.;64(7):686-700.
- World Health Organization, (2005). International pharmacopoeia monograph on efavirenz.2005:5-8.
- Xia H, Gao X, Gu G, et al., (2011). Low molecular weight protamine-functionalized nanoparticles for drug delivery to the brain after intranasal administration. *Biomaterials*.;32(36):9888-9898.
- Xu X, Al-Ghabeish M, Rahman Z, et al., (2015). Formulation and process factors influencing product quality and in vitro performance of ophthalmic ointments. *Int J Pharm*.;493(1-2):412-425.
- Yasir M, Sara UVS., (2014). Solid lipid nanoparticles for nose to brain delivery of haloperidol: in vitro drug release and pharmacokinetics evaluation. Acta Pharmaceutica Sinica B;4(6):454-463.
- Zaki NM, Awad GAS, Mortada ND, Abd ElHady SS.(2006) Rapid-onset intranasal delivery of metoclopramide hydrochloride. Part I. Influence of formulation variables on drug absorption in anesthetized rats. *Int J Pharm*. 2006; 327(1-2):89-96.

Appendix A

Approval from CPCSEA & IAEC for pharmacokinetic studies on animals

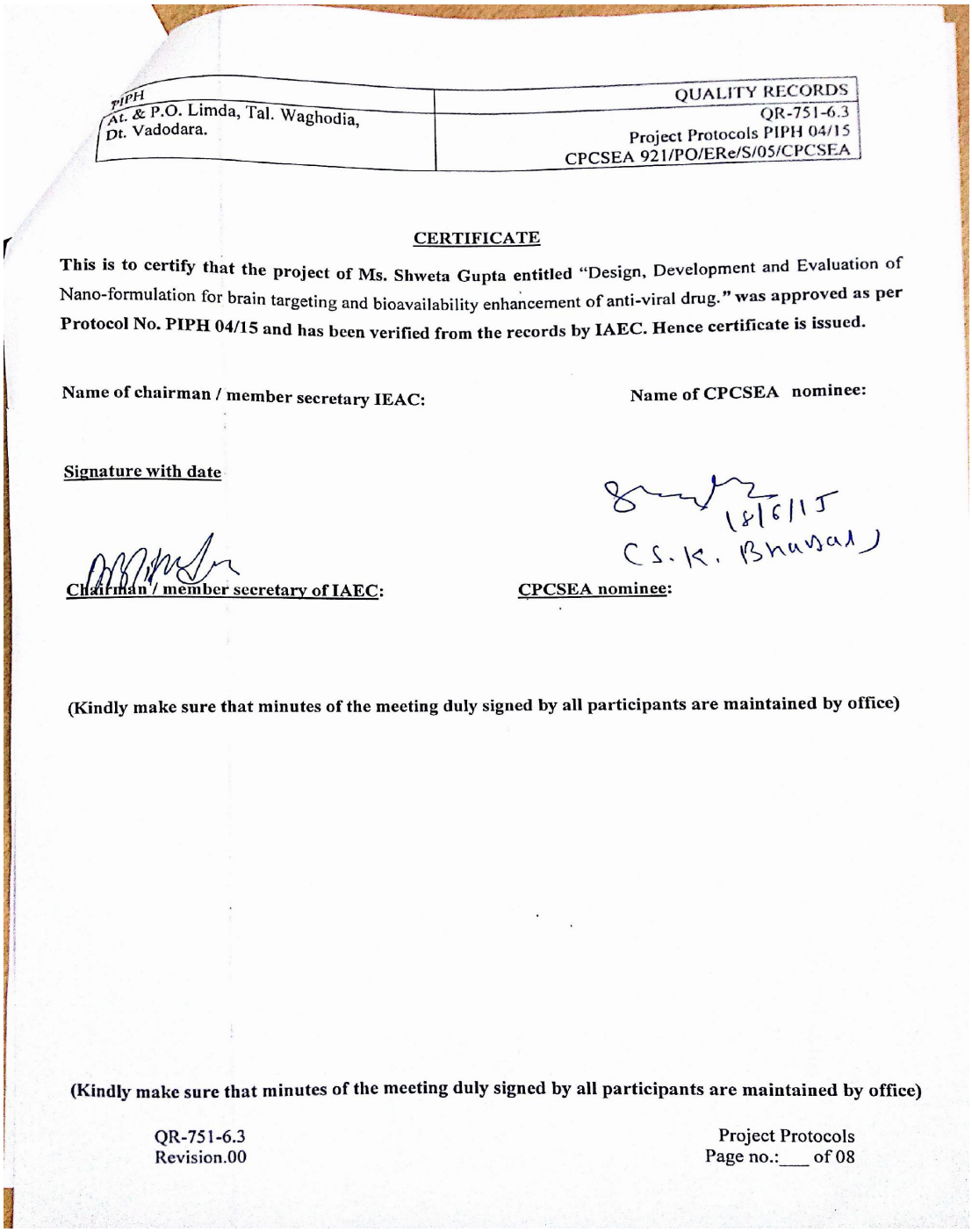

PIPH
At. & P.O. Limda, Tal. Waghodia,
Dt. Vadodara.

QUALITY RECORDS
QR-751-6.3
Project Protocols PIPH 04/15
CPCSEA 921/PO/ERe/S/05/CPCSEA

CERTIFICATE

This is to certify that the project of Ms. Shweta Gupta entitled "Design, Development and Evaluation of Nano-formulation for brain targeting and bioavailability enhancement of anti-viral drug." **was approved as per Protocol No. PIPH 04/15 and has been verified from the records by IAEC. Hence certificate is issued.**

Name of chairman / member secretary IEAC:

Name of CPCSEA nominee:

Signature with date

18/6/15

C.S.K. Bhansali

Chairman / member secretary of IAEC:

CPCSEA nominee:

(Kindly make sure that minutes of the meeting duly signed by all participants are maintained by office)

(Kindly make sure that minutes of the meeting duly signed by all participants are maintained by office)

QR-751-6.3
Revision.00

Project Protocols
Page no.:___ of 08

Appendix B

Certificate from PASM regarding ethical issues

PARUL SEVASHRAM HOSPITAL
(Parul Institute of Medical Sciences & Research)
CENTRAL LABORATORY

PSH / Outward No. 5/11/15/01 Date = 5/11/2015

CERTIFICATE:

This is to certify that the plasma used for the project "Development and validation of analytical method for the estimation of Efavirenz in plasma" by Ms. Shweta Gupta was provided by Parul Arogya Seva Mandal Hospital with due considerations of ethical issues and consent of volunteers.

Mr. Ketan Patel
Central Lab Incharge

PARUL SEVASHRAM HOSPITAL

Dr. Varun G.
Pathologist

P.O. Limda, Ta. Waghodia, Dist. Vadodara. Phone : 02668 - 290900 / 910, Mob.: 98791 85000, 98791 86000
E-mail : parulsevashram@gmail.com / Website : www.parulsevashramhospital.com

Appendix C

Dose Calculation

The dose of drug to be administered to the rats for *in-vivo* studies was calculated based on human equivalent dose (HED) as per guideline by FDA.

Human Dose of EFV : 600 mg

Average adult weight : 60 kg

Hence,

HED = 600 mg / 60 Kg

=10 mg/Kg

As per FDA guidelines for dose calculation,

HED (mg / Kg) = Animal dose (mg / Kg) X 0.16 (for rats)

⇨ Animal dose (mg / Kg) = HED (mg / Kg) / 0.16

= 10/0.16 mg / Kg

= 62.5 mg / Kg

=0.0625 mg/gram

Weight of rat: 400 gram

Oral Rat dose = 0.0625 X 400 = **25 mg**

Nanoparticulate dose :

Amount of drug in 100 ml = 25 mg

0.25 ml formulation was taken

Hence, Amount of drug administered intranasally

= 0.25 X 25/100

= 0.0625 mg

List of Publications/ Patent

Publications from the present research work :

- Gupta S, Kesarla R, Chotai N, Misra, AN, Omri AW, (2017). Systematic approach for the Formulation and Optimization of Solid Lipid Nanoparticles of efavirenz by high pressure homogenization using Design of Experiment (DOE) for brain targeting and enhanced bioavailability, Biomed Research International, Volume 2017 (2017), Article ID 5984014, 18 pages, https://doi.org/10.1155/2017/5984014. (**JCR Impact factor: 2.134, No. of citation:01**)

- Gupta S, Kesarla R, Chotai N, Omri A, (2017). Development and validation of reversed phase HPLC gradient method for the estimation of efavirenz in plasma. PLoS ONE 12(5): e0174777. https://doi.org/10.1371/journal.pone.0174777 (**JCR Impact factor: 3.057**)

Other publications:

- Gupta, S. et al., **2011**. "Self-nanoemulsifying drug delivery system for Adefovir Dipivoxil: Design, characterization, in-vitro and ex-vivo evaluation". Colloids and Surfaces A: Physicochemical and Engineering Aspects, 392(1)5,145-155. [**JCR Impact Factor: 2.760, No. of citations: 80]**.
- Gupta, S. and Rajesh KS. **2013**. "Ophthalmic drug delivery systems with emphasis on in-situ hydrogels". Pharmagene- A genesis journal, 1(2), 79-86.
- Gupta, S. et al., **2013**. "Formulation strategies to improve the bioavailability of poorly absorbed drugs with special emphasis on self emulsifying systems". ISRN Pharmaceutics, Article ID 848043, Volume 2013, Hindawi Publishing Corporation. [**No. of citations: 44]**
- Gupta, S. et al., **2016.** "Formulation, optimization and evaluation of colon targeted delivery system for Isradipine". World Journal of Pharmacy and Pharmaceutical Sciences, 5 (5), 632-649. [SJIF Impact Factor 6.041]

Papers presented

- Gupta, S. et al., 2009. "Controlled release bilayered buccoadhesive tablets of Losartan Potassium: Formulation & Characterization". Presented in IPC 2009, Ahmedabad, Gujarat, India.
- Gupta, S. et al. 2013. "Formulation of Mentholated Hydrogel and its optimization using box-behnken design for treatment of burns and wounds". Presented in AICTE sponsored seminar on "Quality by Design for Better Method Development and Validation" organized by Parul Institute of Pharmacy & Research and Parul Institute of Pharmacy on 18^{th}-19^{th} October, 2013.
- Gupta, S. et al. 2014. "Topical gel containing solid lipid nanoparticles (SLN) with improved efficacy and patient compliance." Presented in VIC-VCCI-Expo 2014.

Patent filed

Title: Topical Gel containing solid lipid nanoparticles

Patent Application No.: 3658/MUM/2014

Application date: 19/11/2014

Publication date : 20/05/2016

Journal No. - 21/2016

Link :http://ipindiaonline.gov.in/patentsearch/PublishedSearch/publishApplicationNumber.aspx?application_number=to+3fHvLM2HBmJoF1uzwGA==